Title
Cortical Plasticity Across TImescales

Author
englund, mackenzie

Publication Date
2022

Peer reviewed|Thesis/dissertation

Cortical Plasticity Across Timescales

By

MACKENZIE ENGLUND
DISSERTATION

Submitted in partial satisfaction of the requirements for the degree of

DOCTOR OF PHILOSOPHY

in

Psychology

in the

OFFICE OF GRADUATE STUDIES

of the

UNIVERSITY OF CALIFORNIA

DAVIS

Approved:

Leah Krubitzer, Chair

Danielle Stolzenberg

Eliza Bliss-Moreau

Committee in Charge

2022

Table of Contents

General Introduction/Abstract

While there is no doubt that all divisions of the brain have co-evolved over time, we choose to study the neocortex – the hallmark of mammalian brain evolution – due to the abundance of observed neocortical phenotypic variability across the nearly 7000 extant mammalian species (Mountcastle 1997, Kaas and Balaram 2015, Burgin et al., 2018). At the systems-level, this variability lies in the parcellation of the neocortex and thus in the information that is processed within and across cortical minicolumns (the fundamental computational units of the six-layered neocortex) (Bastos et al., 2018, Garey 1999). One way to parcellate the cortex is by cortical field, each with unique connectivity and function (Krubitzer 2007). Composed of minicolumns that share a common general function, cortical fields are classically defined by electrophysiological properties, connections, and cytoarchitecture.

Species display variability in neocortical and cortical field organization, specifically in 1) the size of the cortical sheet, 2) how sensory domains are allocated, 3) the relative size of cortical fields, 4) the number of cortical fields, 5) the magnification of behaviorally relevant body parts within cortical fields, and 6) the connections within and across cortical fields (Krubitzer and Prescott 2018). Evolutionary tinkering with peripheral morphology, subcortical connections, and the neocortical developmental program has produced these systems-level changes to the neocortex, fundamentally altering the function of the neocortex and thus the behaviors animals can engage in (Finlay and Uchiyama 2015, Florio et al., 2015). As behavior is the target of selection, only cortical properties and mechanisms that support/co-vary with a certain behavior are selected for (such as network connectivity, neural response properties, or gene expression).

Over short and long timescales, (within and across lifetimes), an individual's behavior can change as the physical and social environments change. Discussed in detail below, the neocortex has a remarkable ability to adapt to changes on long and short timescales. While neocortical plasticity serves as a buffer against environmental variation, some properties of the cortex are resistant to change (such as the existence of six-layers or the general location of

cortical areas), which limits the degree of change that can occur within the lifetime of individual, and places constraints on potential species-level differences (Allman 1999). Using the comparative approach, the Krubitzer lab has studied the differences between within-lifetime and evolutionary changes that are possible to the neocortex.

The following chapters extend this body of work, by providing answers to three specific questions. First, how can experimental manipulations in the laboratory inform us of the types of changes that occur over evolutionary time? The first chapter answers this by providing a review of the types of changes to the neocortex that occur over short and long timescales, and how experimental models of sensory loss provide information on how the developmental program can be altered over the course of evolutionary time to produce phenotypic variation. Second, how does early sensory loss alter the neocortical developmental program, and are there behavioral correlates to these changes in adulthood? To answer this question, chapters 2 and 3 present data on the early loss of vision in short-tailed opossums (Monodelphis *domestica*), extending previous findings from the Krubitzer laboratory on cross-modal plasticity. I first provide a behavioral correlate to the previously observed cross-modal changes, showing that blind animals are better at performing sensorimotor tasks when those tasks rely on the spared senses. Second, I provide a drafted manuscript on how the developmental program is altered by the early loss of vision. Specifically, I show that the loss of vision causes transient corticocortical projections to stabilize in blind animals, allowing for cross-modal plasticity.

Third, how does the developmental program vary between species in early postnatal development? In this line of research, and the last chapter presented in this dissertation, I present a new technique for cross-species comparisons of cortex-wide *in-situ* hybridization. I use this technique to demonstrate some similarities and differences in the cortical developmental program between two rodent species (mice and voles). This last work is currently in revision, and we are adding additional developmental timepoints to address differences in trajectory (versus a single day in development). Taken together, the work

presented in this dissertation makes two important contributions to the field of neuroscience. First, we show how the age of onset of sensory loss impacts cortical plasticity, and that the observed effects are due to a lack of axon pruning in development and not a growth of new connections. Second, cortex-wide gene expression patterns have never been quantitatively compared between species. Altogether, these chapters provide data on the limits of neocortical plasticity within and across species. Importantly, learning how and where evolution has tinkered with the neocortical developmental program over all time to produce species variation informs us of the rules of cortical and brain evolution. I hope that other scientists not only enjoy reading these papers, but also apply these new techniques in their research to answer longstanding questions of cortical development and evolution.

References

1. Mountcastle, V. B. (1997). The columnar organization of the neocortex. *Brain: a journal of neurology*, *120*(4), 701-722.
2. Bastos, A. M., Usrey, W. M., Adams, R. A., Mangun, G. R., Fries, P., & Friston, K. J. (2012). Canonical microcircuits for predictive coding. *Neuron*, *76*(4), 695-711.
3. Kaas, J. H., & Balaram, P. (2015). The types of functional and structural subdivisions of cortical areas. In *Recent Advances on the Modular Organization of the Cortex* (pp. 35-62). Springer, Dordrecht.
4. Burgin, C. J., Colella, J. P., Kahn, P. L., & Upham, N. S. (2018). How many species of mammals are there?. *Journal of Mammalogy*, *99*(1), 1-14.
5. Edelman, G. M., & Gally, J. A. (2001). Degeneracy and complexity in biological systems. *Proceedings of the National Academy of Sciences*, *98*(24), 13763-13768.
6. Allman, J. M. (1999). *Evolving brains* (No. 68). Scientific American Library.
7. Garey, L. J. (Ed.). (1999). *Brodmann's' localisation in the cerebral cortex'*. World Scientific.
8. Krubitzer, L. (2007). The magnificent compromise: cortical field evolution in mammals. *Neuron*, *56*(2), 201-208.
9. Krubitzer, L. A., & Prescott, T. J. (2018). The combinatorial creature: cortical phenotypes within and across lifetimes. *Trends in neurosciences*, *41*(10), 744-762.
10. Florio, M., Albert, M., Taverna, E., Namba, T., Brandl, H., Lewitus, E., ... & Huttner, W. B. (2015). Human-specific gene ARHGAP11B promotes basal progenitor amplification and neocortex expansion. *Science*, *347*(6229), 1465-1470.
11. Finlay, B. L., & Uchiyama, R. (2015). Developmental mechanisms channeling cortical evolution. *Trends in neurosciences*, *38*(2), 69-76.

Chapter 1:

At the time of this dissertation, the following manuscript entitled "**Phenotypic alterations in cortical organization and connectivity across different time scales**," is currently in revision at *Brain, Behavior, and Evolution*, and thus is presented in the format of the journal.

Phenotypic alterations in cortical organization and connectivity across different time scales

Mackenzie Englund [1] and Leah Krubitzer [1, 2]

1. Department of Psychology, University of California Davis
2. Center for Neuroscience, University of California Davis

Key Words: Evolution, Development, Cortex
Word Count: 9040
Number of Figures: 5

Corresponding Author:
Leah Krubitzer
Center for Neuroscience
University of California, Davis
1544 Newton Ct
Davis, CA 95618
Phone: 530 -757-8862
Email: lakrubitzer@ucdavis.edu

Abstract

In the following review, we describe the types of phenotypic changes to the neocortex that occur over the longer time scale of evolution, and over the shorter time scale of an individual lifetime. To understand how phenotypic variability emerges in the neocortex, it is important to consider the cortex as part of an integrated system of the brain, the body, the environment in which the brain and body develops and evolves, and the affordances available within a particular environmental context. Changes in any part of this brain/body/environment network impacts the neocortex. We provide data from comparative studies on a wide variety of mammals that demonstrate that body morphology, the sensory epithelium, and the use of a particular morphological structures have a profound impact on neocortical organization and connections. We then discuss the genetic and epigenetic factors that contribute to the development of the neocortex, as well as the role of spontaneous and sensory driven activity in constructing a nervous system. Although the evolution of the neocortex cannot be studied directly, studies in which developmental processes are experimentally manipulated provide important insights into how phenotypic transformations could occur over the course of evolution and demonstrate that relatively small alterations to the body and/or the environment in which an individual develops can manifest as large changes to the neocortex. Finally, we discuss how these phenotypic alterations to the neocortex impact an important target of selection - behavior.

How does the neocortex evolve from a simple form with few cortical fields, present in our early ancestors, to a complex form with multiple, interconnected cortical fields as evidenced in a number of extant mammals? While it is tempting to answer this question from a purely evolutionary perspective, it is important to keep in mind that there are many timescales over which phenotypic change can emerge. One is the long evolutionary time scale in which alterations in the phenotype occur over thousands to millions of years. Another is over much shorter time scales such as generations, years, days and even seconds; the shortest occurring at the synaptic level with potentiation and protein synthesis. Indeed, we have previously argued that phenotypic changes occurring over shorter timescales can masquerade as evolutionary transformations if the context in which an animal develops is static for long periods of time (Krubitzer and Stolzenberg, 2014). Evolutionary transformations are due to changes in DNA sequence or patterns of stable epigenetic marks that occur over millions of years, resulting in altered brain or body morphology and function (such as the wing vs forelimb). Phenotypic modifications occurring over shorter time scales are due to multiple factors inexorably tied to the context in which the brain and body develop, and result in small-scale changes to the brain and body (e.g. bone density, muscle growth, number of synapses). Both the evolutionary and developmental timescales heavily influence the number, size and connectivity of cortical fields, while very short timescales have less of an impact on large-scale features of cortical organization. During development, the *in-utero* environment and the stage at which an animal is born determines the extent to which sensory input can impact the cortical phenotype (Figure 1). In addition, the overall environmental context including temperature, toxins present, sensory stimuli and available affordances also impact the brain and the body. Therefore, to understand how phenotypic change occurs in any part of the brain we must consider the brain and body as parts of a single interacting entity, *the organism,* behaving in and being influenced by the environment in which it resides and develops.

The body and the environment alter the brain over long and short timescales

To appreciate how the body and the environment impact the cortical phenotype over longer timescales we can examine a variety of species with different sensory, morphological and neocortical specializations that live and behave in unique environmental contexts with different affordances. Some of the best examples are found in species with extreme specializations, occupying different niches (e.g. aquatic, arboreal, burrowing), such as the duck-billed platypus (Krubitzer et al., 1995), the star nosed mole (Catania and Kaas, 1996) and the blind mole rat (R et al., 1992). For instance, the platypus has a unique bill lined with rows of mechanosensory and electrosensory receptors (Pettigrew, 1999). When engaging in important, ethologically relevant behaviors such as feeding, navigating and mating, it closes its eyes, ears and nose; receiving all information about the world almost exclusively through the receptors on its bill (Manger and Pettigrew, 1995). When somatosensory cortex is examined using electrophysiological recording techniques, it is found to be dominated by the representation of the bill. In fact, almost 90% of primary somatosensory cortex (S1) is devoted to processing inputs from the bill, and about 60% percent of the entire cortical sheet is dominated by the representation of the bill. Similar types of cortical magnification are observed in other mammals. For example, in S1, there is an enlarged representation of nose rays in the star nosed mole, who forages for small invertebrates using its exquisitely sensitive tactile “nose” (Catania and Kaas, 1995). An enlarged representation of the incisors characterizes the representation of S1 in naked mole rats who live in underground highways and use their incisors to dig extensive tunnel networks, carry objects and young, chew, and investigate their surroundings by tapping their incisors against objects of interest (Catania and Remple, 2002). These types of changes, where the structure and function of the neocortex mirror the body, behavior, and niche of the organism, have been observed to a greater or lesser extent in every mammal examined for all sensory systems (Krubitzer, 2007), and in part, are the product of evolutionary changes to

peripheral morphology and sensory epithelia (e.g. evolving from a snout to a bill with electroreceptors).

The magnification associated with peripheral morphological specializations is not limited to the cortex but is also observed in the dorsal thalamus. For example, in the platypus, the dorsal thalamus is dominated by the ventral posterior nucleus (Ashwell, 2012; Mikula et al., 2008); so much so that it is difficult to identify other major relay nuclei (LGN, MG). Similarly, in the blind mole rat, the lateral geniculate nucleus (LGN) is extremely small and undifferentiated (Rehkämper et al., 1994), while the ventral posterior nucleus is enlarged. Conversely, in species that rely heavily on vision, like the arboreal grey squirrel, the LGN and pulvinar occupy a large portion of the dorsal thalamus, an uncommon feature of the thalamus compared to commonly studied terrestrial, whisking rodent models (Baldwin et al., 2011; Robson and Hall, 1977; Wong and Kaas, 2008). Interestingly, the relative magnification of the pulvinar complex has independently evolved in other mammals that rely heavily on vision such as primates and carnivores, which both exhibit a relatively larger pulvinar complex volume-to-brain-weight ratio compared to rodents (Chalfin et al., 2007). Clearly, an animal's ability to navigate in and explore its environment is a driving force of selection. Thus, evolution has tinkered with both the body plan that allows mammals to interact and move in the environment, and with sensory receptor array type and structure, which determines the type and magnitude of sensory stimuli that is captured and transduced; in turn both factors impact brain organization.

These evolutionary changes to the brain and body co-vary with species adaptations suited for environments that persist over long timescales (i.e. the more stable aspects of an organism's environment, such as the platypus hunting in muddy water, or a star nosed mole catching small prey in a subterranean environment). Over shorter timescales (one or a few generations) similar, but less dramatic, changes to the brain can occur. For example, alterations in cortical field size, magnification of behaviorally relevant sensory surfaces, or alterations in representations of muscle synergies in motor cortex can emerge in dynamic physical and social

environments with no structural changes to the body. In humans for example, rapid migration of populations, changes in food sources, or alterations in manual behaviors such as using keyboards and texting can rapidly influence features of the cortex noted above. These changes are observed across sensory and motor systems and across species. For example, rats who spent the first month of life in an enriched environment show an earlier expansion of the forelimb representation in motor cortex compared to rats reared in standard laboratory conditions (Young et al., 2012). In humans born without arms and who use their feet in a dexterous fashion, motor, somatosensory, and posterior parietal cortex re-organizes to reflect the use of their major effector (the feet) (Liu et al., 2020). In auditory cortex, Pantev and colleagues 1998, found that in skilled musicians (regardless of the instrument they play) there was enlarged representations for piano tones**,** but not pure tones, compared to individuals who had never played an instrument, (Pantev et al., 1998). Numerous examples of this type of plasticity have been demonstrated in the visual system in different species. For example, wild-caught rats have a greater density of neurons in area 17 compared to laboratory rats of the same strain - although whether this effect is confined to a given cortical layer or spans all layers is unknown (Campi et al., 2011). In opossums reared in vertically striped cages, neurons in V1 are preferentially tuned to striped stimuli (Dooley et al., 2016). These examples demonstrate that activity-driven plasticity allows the neocortex to alter the function of sensory and motor areas to match short time-scale environments (see below). The social environment, which is a complex extension of the sensory environment, also has a strong influence on the rate and outcome of developmental processes throughout the nervous system, but a full discussion of this is beyond the scope of this review (see Bales et al., 2019 for review on 'social' touch during development). Lastly, since plasticity itself is a trait that is selected for (e.g. meta-plasticity), we should note that species may have varying levels of cortical plasticity due to species-specific intracellular mechanisms and synaptic transmission/modulation (e.g. species-specific

developmental trajectories of NMDAR subunit NR2A/NR2B ratios) (Erzurumlu and Gaspar 2012, Cho et al., 2009)

Functional changes that emerge over short time scales are often, if not always, accompanied by alterations in anatomical connections. Thus, despite the constraints imposed on evolving and developing brains and bodies (Krubitzer and Prescott, 2018), aspects of cortical organization and connectivity can change very rapidly over the course of a lifetime. While extraordinary diversity in brain organization and behavior can occur over shorter timescales, it is important to note that there are limits to this plasticity; the presence and relative location of a number of cortical fields is maintained as are patterns of cortical and subcortical connections. Furthermore, while some aspects of body morphology can be influenced by environmental factors (e.g. gravitational stress on bone density and diet on orofacial morphology), to a large extent the body plan of a particular mammal and the limits imposed by joint configuration, highly constrains the types of cortical changes that can occur over shorter timescales (see below).

What factors contribute to phenotypic transformations over different time scales?

Of course, over the longer evolutionary timescale, changes to DNA sequence and species-specific patterns of epigenetic markers are the main drivers of phenotypic change. Changes to gene sequences occur via point or chromosomal mutations along with variation in copy number. On the other hand, long-timescale (evolutionary; species-specific) epigenetics changes alter gene expression without changing DNA sequence through distinct histone acetylation or DNA methylation patterns (e.g some genes are methylated in some species but not in others; Shulha et al., 2012). Over millions of years, stable epigenetic and genetic changes, which alter the quantity and/or function of gene product, result in diverse species-specific patterns, sequences, and phenotypes. For example, genetic changes which alter cell cycle kinetics during proliferative periods are responsible for the orders of magnitudes of difference in brain and body size between species (Cárdenas et al., 2018; Liu et al., 2017;

Smaers et al., 2021; Suzuki et al., 2018; Tomasello et al., 2021). Furthermore, changes to genetic sequence and epigenetic markers can alter the graded expression of transcription factors during cortical development (e.g. Emx2, Pax6, Coup-TF1,Sp8), which in turn alters the number and gross organization of cortical fields, and connections (Cholfin and Rubenstein, 2008; Fukuchi-Shimogori and Grove, 2001; Sur and Rubenstein, 2005). This is also true for genes that are involved in the construction of the body. Homeobox genes (*Hox*) are a large family of highly conserved genes involved in the development of the body and limbs (Petit et al., 2017). As with transcription factors in the neocortex, changing the spatial and temporal patterning of *Hox* genes can alter forelimb development profoundly, as revealed in comparative studies of limb development in bats versus mice (Cretekos et al., 2008; Petit et al., 2017). Changes in limb morphology, in turn, alter the types of movements animals are capable of and the way in which sensory receptor arrays interface with the environment, which then manifest as differences in cortical magnification (i.e. the size of the forelimb representation in S1 of a bat versus a mouse), in cortical and subcortical connections, and functional changes in neural circuits.

Importantly, genetic changes that have a direct broad scale effect on the size of the brain, particularly the neocortex, also can impact the organization and connectivity of cortical fields. For instance, Florio and colleagues discovered that the human-specific ARHGAP11B gene, the result of a duplication followed by a point mutation occurring near the time of the human-chimpanzee split, contributed to the expansion of the cortical sheet by increasing the number of basal progenitors (Florio et al., 2015). Recently, Hyde and colleagues used a lentiviral vector to express the human ARHGAP11B variant in marmoset monkeys. Extending Florio's findings, this recent study found that expressing the human ARHGAP11B gene in marmoset fetus brains resulted in an increase in the number of outer subventricular zone (oSVZ) progenitors, an increased number of upper layer neurons, and an expanded cortical sheet (Heide et al., 2020). Together, these studies show how a long timescale event, in this

case a duplication and point mutation, causes a cascade of events across neurodevelopment (increasing progenitors in the oSVZ increases layer 2/3 neurons and affects subsequent developmental events) (Figure 1).

While the specific changes to connections and cortical field organization caused by expressing the human ARHGAP11B variant in the laboratory have yet to be studied, comparative studies indicate that increasing the relative size of the cortical sheet impacts aspects of cortical organization. For example, while the absolute size of V1 scales with brain size and the size of the retina across mammals, the relative size of V1 to association areas has decreased in humans (Arai and Pierani, 2014; Kaskan et al., 2005). Further, the differential expansion of frontal, posterior parietal, and inferotemporal cortex in humans compared to other primates, suggests that as the neocortex increases in size, there is not a simple scaling up of existing cortical fields (Finlay and Uchiyama, 2015; Hill et al., 2010; Van Essen, 2018; Van Essen and Dierker, 2007). Rather, there appears to be widespread alterations in the organization, number and size of cortical fields, and likely connections as well (for review see Halley and Krubitzer, 2019). Given these examples it is easy to imagine how early and specific changes to DNA sequence, such as with ARHGAP11B, initiates developmental cascades that lead to global alterations to the neocortex. Yet direct changes to the genome are not the only mechanism by which the neocortex can be significantly altered. Epigenetic changes including histone modifications, chromatin remodeling, and posttranslational modifications can also strongly influence cortical neurogenesis (see Adam and Harwell, 2020 for review), which could, in turn, orchestrate a similar cascade of events as that described above.

In addition to genetic and epigenetic alterations to the brain and the body, spontaneous and sensory-driven activity have a broad impact on subcortical and cortical organization and connectivity. For example, Gezelius and colleagues (2017) found differential expression of genes that appear to specify the location and identity of distinct thalamic nuclei around embryonic day 14 in mice (Gezelius et al., 2017). Cells in these putative thalamic sensory nuclei

later exhibit gap-junction-mediated spontaneous calcium waves that propagate among nuclei, altering the patterns of other nuclei's calcium waves and triggering changes in thalamic gene expression, which in turn alters the size of cortical fields (Moreno-Juan et al., 2017). Further, these calcium transients also play an important role in establishing the internal organization of cortical fields via thalamocortical-corticothalamic interactions, since the elimination of the calcium transients disrupts the initial columnar organization of barrel cortex in mice, and causes a delay in the maturation of corticothalamic axons (Antón-Bolaños et al., 2019; Moreno-Juan et al., 2020). Perhaps the most important feature of spontaneous calcium waves is that they are modulated by peripheral input. While this has only been shown for the retina, it is probable that early spontaneous activity from somatosensory and auditory afferents from the skin and cochlea affect thalamic calcium waves in the same way. Regardless, the existence of peripheral control over thalamic and cortical patterning shows that while early morphogens and transcription factors play an initial role in cortical patterning, evolutionary tinkering with the ratio of sensory inputs and associated afferents alone is enough to drastically change subcortical and cortical structure and function. In summary, altering the way genes are expressed in the brain and body during development alters cell type, number, and location. Cells then undergo specific processes in specific locations (such as transient calcium waves in the thalamus), which then affect the development of brain regions (such as patterning of the cortex) (Figure 1). Although epigenetic mechanisms also play a critical role in cortical development by enhancing or repressing the expression of different genes involved in brain and body development, altering where and when genes are expressed and the magnitude of their expression (Albert and Huttner, 2018; Elsen et al., 2018; Kawaguchi, 2019), a full discussion of this is beyond the scope of this review.

As described briefly at the beginning of this review, environmental context during development (sensory driven activity/affordances) also impacts cortical organization, connectivity, and functionality via activity-dependent mechanisms and changes to epigenetic

markers. That is, neocortical structure and function are thought to be altered in a way that reflects the sensory receptor array and how it is used. For instance, decades of research in rats and mice have shown that the timing and type of visual experience onset controls the maturation and function of visual cortex via epigenetic activity-dependent mechanisms (Duffy and Mitchell, 2013; Ishikawa et al., 2014; Nott et al., 2015; Tropea et al., 2006). To give one example, visual experience stimulates histone modifications near the transcription site of micro-RNA 132 (miR-132) in visual cortical neurons, resulting in the upregulation of miR-132 expression (Tognini et al., 2011). Importantly, the level of miR-132 expression regulates a number of developmental processes in primary visual cortex including the maturation of dendritic spines and synaptic transmission, both of which impact the receptive fields of neurons in V1 (Mazziotti et al., 2017). Thus, the miR-132 pathway provides one mechanism by which sensory activity alters neocortical function. Sensory driven activity also generates systems-level changes by altering inhibitory parvalbumin (PV) networks, which play a key role in refining neocortical sensory and motor maps (Lunghi et al., 2015; Reh et al., 2020). Dark rearing, monocular deprivation, whisker trimming, and environmental enrichment (i.e., changes in sensory driven activity within the lifetime of an individual) have all been shown to alter the maturation and function of PV-expressing inhibitory networks. One mechanism by which this may occur involves experience-dependent transsynaptic transfer of gene products from sensory afferents to cortical areas. Discovered by the Hensch lab, visual experience was found to facilitate anterograde cell-to-cell transfer of retina-derived *OTX2* homeoprotein through the lateral geniculate nucleus (LGN) to visual cortex (V1) (Sugiyama et al., 2008). Once aggregated in visual cortex, *OTX2* is taken up by PV cells, where it regulates the visual critical period by affecting extracellular matrix maturation (Rebsam and Mason, 2008; Beurdeley et al., 2012). Thus, either a change in visual experience, a change in the presence, absence, or number of retinal afferents, or an epigenetic or genetic change to the transcription rate of *OTX2*, all effect the accumulation of the protein in visual cortex, thereby changing the duration of the visual

critical period and ultimately the extent to which visual cortex function is shaped by the environment.

On a network level, numerous studies which blocked or weakened inhibitory neuron function, by using local infusion of bicuculine into specific cortical areas, have shown that altering levels of inhibition within cortical fields in turn alters the size of functional representations within those fields (Jacobs and Donoghue, 1991). For instance, Brown and colleagues recently showed that infusing bicuculine into the motor cortex of rats during critical periods of development expanded the forelimb area of the motor map, and altered the types of movements represented in motor cortex (Brown et al., 2020). While we limited our discussion to a few key ways in which sensory experience alters cortical area structure and function during short timescales, there are numerous ways in which sensory driven activity modulates cortical development. These activity-based mechanisms (along with competition and self-organizing principles not discussed here) appear to be conserved across mammals, although species-specific differences in the cortical epigenome during development are not well-studied (Kaschube et al., 2010). At any rate, these changes occur over shorter timescales but can persist for generations if the sensory context is static, or if they are incorporated into the genome or epigenome. For this incorporation to occur, the differences in the DNA sequence or epigenetic marks that support these activity-dependent alterations must first become stable in a population. However, the transgenerational stability of allele frequencies and epigenetic markers is not well-studied in the context of the neocortex due to experimental constraints (only mammals have a neocortex), long generation times (even in mice), and the fact that genetics and epigenetics are constrained by absolute time (e.g. mutation rates). As the field of epigenetics continues to grow, we will gain the knowledge required to determine the transgenerational effects of experience on cortical development, organization, and function. For example, comparative analysis of area-specific (thalamus, cortex) single-cell sequencing experiments in developing, closely related species will solve many of the experimental

difficulties posed by transgenerational studies. The experiments described in the following section outline some of the changes to the brain that can occur over short time scales compared with similar alterations to the brain that occur over longer, evolutionary timescales.

Mirroring Evolutionary Transformations with Developmental Manipulations.

Comparative studies provide important insights into what happens when changes to developmental processes occur over long timescales and elucidate the types of systems level changes that evolution has produced. To study what these specific changes to developmental processes may be, and where in the nervous system they occur, we can "tweak" the nervous system in developing animals and determine if we can produce a phenotype that is consistent with what evolution has produced. Specifically, we experimentally induced a complete loss of input from the eyes to understand what happens to the neocortex when the ratio of incoming sensory inputs is dramatically altered, as is the case with extreme morphological specializations like the platypus and star-nosed mole. To accomplish this, our laboratory has worked on a highly altricial, slowly developing mammal, the short-tailed opossum (*Monodelphis domestica*). These animals have a well-developed visual system with a relatively large V1 compared to mammals with similar sized brains (e.g. mice, voles). We bilaterally enucleated opossums at early stages of development (P4; Figure 2), prior to the onset of spontaneous activity in the retina, and well before ganglion cell axons have reached the diencephalon (P5 - P7) and thalamocortical axons have reached the developing cortex (P7 – P10; (Molnár et al., 1998)).

After animals reached adulthood, we examined the size of cortical fields and thalamic nuclei, the functional organization and connections of the cortex, and sensory mediated behavior. We found that despite the complete removal of all visual inputs, we could still identify a primary visual area (V1) by its architecture, although it was extremely small (Kahn and Krubitzer, 2002). Functional mapping using electrophysiological recording techniques revealed that what would

normally be V1 was co-opted by the somatosensory and auditory systems (Kahn and Krubitzer, 2002; Karlen et al., 2006). Interestingly, neurons in this reorganized V1 responded almost exclusively to stimulation of the snout, face, vibrissae and head. More recent studies in bilaterally enucleated opossums reveal functional changes response properties of neurons in the primary somatosensory area (S1) as well. For example, neurons in S1 have smaller receptive fields and greater discriminability compared to sighted animals (Ramamurthy and Krubitzer, 2018). Together, these alterations in the size and functional organization are reminiscent of what evolution has produced in the platypus and blind mole rat (Figure 3). Specifically, like the platypus, bilaterally enucleated opossums have a huge swath of cortex that represents a behaviorally relevant sensory surface (the whiskers; Figure 3C). The reduced size of V1 that is co-opted by the spared sensory systems in bilaterally enucleated opossums is also reminiscent of blind mole rats, in which V1 is reduced in size and has been co-opted by the auditory system (Bronchti et al., 1989).

As observed in comparative studies, our experimental studies show that alterations in the size and function of a structure are not limited to the cortex but are observed in the dorsal thalamus. To quantify these observations, we measured the volume of principal sensory nuclei in the thalamus: the dorsal lateral geniculate (LGNd: visual) and ventral posterior nucleus (VP: somatosensory), of early blind and sighted opossums by measuring the surface area of each nucleus across coronally sectioned tissue stained for either cytochrome oxidase, acetylcholinesterase, or NISSL substance. This investigation first confirmed previous work from our laboratory that the size of LGNd is dramatically decreased in early blind opossums both in absolute and relative size when scaled by brain weight (Karlen and Krubitzer, 2009). On the other hand, in agreement with recent work in embryonically-enucleated mice, we found no difference in the absolute volume of VP between early blind and sighted opossums (Figure 4A). However, when scaled by brain weight, thalamic and brainstem volume, or by the size of

another nucleus (Mediodorsal; MD), VP was significantly larger in early blind opossums compared to sighted controls (Figure 4B). Interestingly, for individuals whose VP and S1 were measured, we found a similar scaling relationship for the volume of VP and the surface area of S1 for both early blind and sighted opossums (Figure 4C). Likewise, LGNd and V1 scaled similarly in blind and sighted opossums (Figure 4D). This was intriguing, as recent work has shown that higher order cortical areas scale in size with primary cortical fields, suggesting that thalamic nuclei, primary and higher order cortical fields all share a specific scaling relationship (Zembrzycki et al., 2015). Viewed through an evolutionary lens, our thalamic and cortical measurement data in short-tailed opossums shows that we can mimic evolutionary phenotypes by tweaking particular neural structures at particular developmental stages. In this case, we altered the ratio of sensory inputs experimentally. However, evolution has done this over the long timescale by altering peripheral morphology and receptor arrays (e.g. duck billed platypus, star-nosed mole and blind mole rat). Importantly, our experimental manipulation demonstrates that dramatic phenotypic changes to the cortex and thalamus are possible by simply altering incoming sensory input during early development, although this is unlikely to be the sole driver of phenotypic change to the cortex and thalamus.

In addition to alterations in cortical field/thalamic nuclei size and functional organization, there are significant alterations in cortical and thalamocortical connections of both the targeted system and the spared sensory systems. V1 in bilaterally enucleated opossums still received input from cortical fields and thalamic nuclei associated with visual processing, as in sighted animals, but the density of those inputs was decreased. This retention of visual pathways in the absence of functional vision is also observed in naturally evolved mammals, such as the blind mole rat (Cooper et al., 1993). In addition to retained connections, V1 in early blind animals had a variety of aberrant connections from cortical and thalamic nuclei of the spared sensory systems. For example, V1 received input from somatosensory (S1), auditory (A1) cortex, and frontal cortex (Dooley and Krubitzer, 2019; Karlen et al., 2006). V1 also received input from

thalamic nuclei associated with somatosensory (ventral posterior nucleus) and auditory processing (medial geniculate nucleus). These same changes in subcortical inputs to V1 have also been reported in anophthalmic mice (Chabot et al., 2008; Charbonneau et al., 2012). Interestingly, the cortical connections of spared sensory systems were also altered in that S1 received projections from auditory cortex, multimodal cortex and architectonically defined visual areas. While the corticocortical connections of V1 in the blind mole rat have yet to be directly studied, 2-Deoxyglucose and subcortical tracing experiments have shown that auditory activation of visual cortex appears to be mediated by projections from the inferior colliculus to the dLGN (Bronchti et al., 2002; Doron and Wollberg, 1994). Interestingly, in anopthalmic mice and early enucleated hamsters, the lateral geniculate nucleus also receives input from the inferior colliculus, a structure associated with auditory processing (Bronchti et al., 2002; Izraeli et al., 2002; Piché et al., 2004). The true similarities and differences in thalamic and cortical connections between experimentally and evolutionarily produced phenotypes will need to be elucidated with anatomical tracing experiments in blind mole rats.

Taken together, our experimental manipulations (tweaks) in developing animals are consistent with the types of changes naturally produced over longer time scales. This leads to two conclusions. First, altering the ratio of sensory input through genetically mediated changes to sensory organs (e.g. eyes, cochlea, skin) that have occurred over the long time scale of evolution could induce massive changes to the neocortex and dorsal thalamus without direct genetic alterations to these structures. Second, large alterations could occur over short timescales if the sensory inputs and environmental context are altered (e.g. movement towards nocturnality, cave dwelling, burrowing). The conditions under which these short timescale alterations could occur have been previously discussed (Krubitzer and Seelke, 2012).

What about behavior?

While genes are heritable and are passed on through generations, and have a causal effect linked to characteristics of development and the ultimate phenotype that emerges, genes are not the direct targets of selection. Rather, genes co-vary with the targets of selection. It is the behavior an animal generates, its morphological phenotype and even its extended phenotype that are the targets of selection (Krubitzer and Seelke, 2012). Thus, our laboratory embarked on a series of experiments in which we examined behavior mediated by the spared sensory systems in bilaterally enucleated animals. First, we trained early blind and sighted opossums to perform a two-alternative force choice texture discrimination task and found that early blind animals outperformed sighted animals in discrimination accuracy (i.e. blind animals were more sensitive to small differences in textures) (Ramamurthy et al., 2021) (Figure 5A/B). Second, we used a variable ladder rung paradigm to study un-trained, naturalistic navigation in early blind and sighted opossums (Figure 5C). We found that early blind opossums outperformed sighted animals and had increased limb placement accuracy compared to sighted controls, while showing similarities in kinematics and crossing time (Englund et al., 2020) (Figure 5D). Moreover, in both of these studies, whisker trimming decreased accuracy and altered the strategies animals employed to complete the tasks. In the discrimination task, whisker-trimmed opossums closely contacted the walls of the apparatus to gain sensory information. In the navigation task animals compensated for the lack of whiskers by holding their snout closer to the rungs, and tapping the rungs significantly more times to gain sensory information. Also in the ladder rung task, whisker trimming affected early blind opossums to a greater extent than sighted animals, and forced smaller forelimb trajectories during crossing and a more cautious approach to navigating the ladder (Figure 5E/5F). These studies, along with those conducted in other animal models and congenitally blind humans show that the loss of one sense leads to enhanced performance on tasks involving the spared senses (Ricciardi et al., 2014). These

enhanced tactile behaviors are reminiscent of other mammals with specialized tactile behaviors such as the blind mole rat, mouse, and rat. Thus, experimentally or naturally altering the ratio of sensory inputs allows for specialized behavior, which can then be selected on by the environment.

Conclusions:

Above, we presented data from our own and other laboratories showing how manipulations made to the developing nervous system can mirror evolutionary-produced phenotypes in brain and behavior. By making these manipulations and comparing how they alter development and ultimately the adult phenotype, we can learn where and when evolution has tinkered with the developmental program to create species-level variation. Yet the extent to which these developmental tweaks recapitulate evolutionary processes is still unknown. However, it is clear from both comparative and developmental studies that there is no single factor that contributes to phenotypic change. Rather, there are multiple mechanisms that operate at multiple levels of organization (e.g. sensory epithelium, body morphology, dorsal thalamus, neocortex) that can produce similar phenotypic outcomes, and the environmental context in which an animal develops can impact these mechanisms and in turn the cortical phenotype. Any animal is a combination of these different factors that contribute to the phenotype of the brain, the body and behavior, and this “combinatorial creature” can emerge over the longer time scale of evolution and the shorter timescale of an individual lifetime (Krubitzer and Prescott, 2018).

Funding:

National Institute of Neurological Disorders and Stroke grant F 31 NS115242-01 (ME)

McDonnell Foundation grant 220020516 (LK)

Author contributions:

Conceptualization: ME, LK

Investigation: ME, LK

Funding acquisition: LK

Supervision: LK

Writing: ME, LK

Competing interests:

Authors declare that they have no competing interests

References

Adam, M. A., & Harwell, C. C. (2020). Epigenetic regulation of cortical neurogenesis; orchestrating fate switches at the right time and place. Current Opinion in Neurobiology, 63, 146-153.

Albert, M., Huttner, W.B., 2018. Epigenetic and Transcriptional Pre-patterning—An Emerging Theme in Cortical Neurogenesis. Front. Neurosci. 12. https://doi.org/10.3389/fnins.2018.00359

Antón-Bolaños, N., Sempere-Ferràndez, A., Guillamón-Vivancos, T., Martini, F.J., Pérez-Saiz, L., Gezelius, H., Filipchuk, A., Valdeolmillos, M., López-Bendito, G., 2019. Prenatal activity from thalamic neurons governs the emergence of functional cortical maps in mice. Science 364, 987–990. https://doi.org/10.1126/science.aav7617

Arai, Y., Pierani, A., 2014. Development and evolution of cortical fields. Neuroscience Research 86, 66–76. https://doi.org/10.1016/j.neures.2014.06.005

Ashwell, K.W.S., 2012. Development of the dorsal and ventral thalamus in platypus (Ornithorhynchus anatinus) and short-beaked echidna (Tachyglossus aculeatus). Brain Struct Funct 217, 577–589. https://doi.org/10.1007/s00429-011-0364-3

Baldwin, M.K.L., Wong, P., Reed, J.L., Kaas, J.H., 2011. Superior colliculus connections with visual thalamus in gray squirrels (Sciurus carolinensis): Evidence for four subdivisions within the pulvinar complex. Journal of Comparative Neurology 519, 1071–1094. https://doi.org/10.1002/cne.22552

Bales, K. L., Witczak, L. R., Simmons, T. C., Savidge, L. E., Rothwell, E. S., Rogers, F. D., ... &

Del Razo, R. A. (2018). Social touch during development: Long-term effects on brain and behavior. Neuroscience & Biobehavioral Reviews, 95, 202-219.
Beurdeley, M., Spatazza, J., Lee, H. H., Sugiyama, S., Bernard, C., Di Nardo, A. A., ... & Prochiantz, A. (2012). Otx2 binding to perineuronal nets persistently regulates plasticity in the mature visual cortex. Journal of Neuroscience, 32(27), 9429-9437.
Bronchti, G., Heil, P., Sadka, R., Hess, A., Scheich, H., Wollberg, Z., 2002. Auditory activation of 'visual' cortical areas in the blind mole rat (Spalax ehrenbergi). European Journal of Neuroscience 16, 311–329. https://doi.org/10.1046/j.1460-9568.2002.02063.x
Bronchti, G., Heil, P., Scheich, H., Wollberg, Z., 1989. Auditory pathway and auditory activation of primary visual targets in the blind mole rat (Spalax ehrenbergi): I. 2-deoxyglucose study of subcortical centers. Journal of Comparative Neurology 284, 253–274. https://doi.org/10.1002/cne.902840209
Brown, A.R., Coughlin, G.M., Teskey, G.C., 2020. Seizures Alter Cortical Representations for Complex Movements. Neuroscience 449, 134–146. https://doi.org/10.1016/j.neuroscience.2020.09.002
Campi, K.L., Collins, C.E., Todd, W.D., Kaas, J., Krubitzer, L., 2011. Comparison of Area 17 Cellular Composition in Laboratory and Wild-Caught Rats Including Diurnal and Nocturnal Species. Brain Behav Evol 77, 116–130. https://doi.org/10.1159/000324862
Cárdenas, A., Villalba, A., de Juan Romero, C., Picó, E., Kyrousi, C., Tzika, A.C., Tessier-Lavigne, M., Ma, L., Drukker, M., Cappello, S., Borrell, V., 2018. Evolution of Cortical Neurogenesis in Amniotes Controlled by Robo Signaling Levels. Cell 174, 590-606.e21. https://doi.org/10.1016/j.cell.2018.06.007
Catania, K.C., Kaas, J.H., 1996. The Unusual Nose and Brain of the Star-Nosed Mole: A star in the brain. BioScience 46, 578–586. https://doi.org/10.2307/1312987
Catania, K.C., Kaas, J.H., 1995. Organization of the somatosensory cortex of the star-nosed mole. Journal of Comparative Neurology 351, 549–567. https://doi.org/10.1002/cne.903510406
Catania, K.C., Remple, M.S., 2002. Somatosensory cortex dominated by the representation of teeth in the naked mole-rat brain. PNAS 99, 5692–5697. https://doi.org/10.1073/pnas.072097999
Chabot, N., Charbonneau, V., Laramée, M.-E., Tremblay, R., Boire, D., Bronchti, G., 2008. Subcortical auditory input to the primary visual cortex in anophthalmic mice. Neuroscience Letters 433, 129–134. https://doi.org/10.1016/j.neulet.2008.01.003
Chalfin, B.P., Cheung, D.T., Muniz, J.A.P.C., Silveira, L.C. de L., Finlay, B.L., 2007. Scaling of neuron number and volume of the pulvinar complex in new world primates: Comparisons with humans, other primates, and mammals. Journal of Comparative Neurology 504, 265–274. https://doi.org/10.1002/cne.21406
Charbonneau, V., Laramée, M.-E., Boucher, V., Bronchti, G., Boire, D., 2012. Cortical and subcortical projections to primary visual cortex in anophthalmic, enucleated and sighted mice. European Journal of Neuroscience 36, 2949–2963. https://doi.org/10.1111/j.1460-9568.2012.08215.x
Cho, K. K., Khibnik, L., Philpot, B. D., & Bear, M. F. (2009). The ratio of NR2A/B NMDA receptor subunits determines the qualities of ocular dominance plasticity in visual cortex. Proceedings of the National Academy of Science*s*, *106*(13), 5377-5382.
Cholfin, J.A., Rubenstein, J.L.R., 2008. Frontal cortex subdivision patterning is coordinately regulated by Fgf8, Fgf17, and Emx2. Journal of Comparative Neurology 509, 144–155. https://doi.org/10.1002/cne.21709
Cooper, H.M., Herbin, M., Nevo, E., 1993. Visual system of a naturally microphthalmic mammal: The blind mole rat, Spalax ehrenbergi. Journal of Comparative Neurology 328, 313–350. https://doi.org/10.1002/cne.903280302

Cretekos, C.J., Wang, Y., Green, E.D., Martin, J.F., Rasweiler, J.J., Behringer, R.R., 2008. Regulatory divergence modifies limb length between mammals. Genes Dev 22, 141–151. https://doi.org/10.1101/gad.1620408
Dooley, J.C., Krubitzer, L.A., 2019. Alterations in cortical and thalamic connections of somatosensory cortex following early loss of vision. J Comp Neurol 527, 1675–1688. https://doi.org/10.1002/cne.24582
Doron, N., Wollberg, Z., 1994. Cross-modal neuroplasticity in the blind mole rat Spalax Ehrenbergi: a WGA-HRP tracing study. NeuroReport 5, 2697–2702.
Duffy, K.R., Mitchell, D.E., 2013. Darkness Alters Maturation of Visual Cortex and Promotes Fast Recovery from Monocular Deprivation. Current Biology 23, 382–386. https://doi.org/10.1016/j.cub.2013.01.017
Elsen, G.E., Bedogni, F., Hodge, R.D., Bammler, T.K., MacDonald, J.W., Lindtner, S., Rubenstein, J.L.R., Hevner, R.F., 2018. The Epigenetic Factor Landscape of Developing Neocortex Is Regulated by Transcription Factors Pax6→ Tbr2→ Tbr1. Front. Neurosci. 12. https://doi.org/10.3389/fnins.2018.00571
Englund, M., Faridjoo, S., Iyer, C.S., Krubitzer, L., 2020. Available Sensory Input Determines Motor Performance and Strategy in Early Blind and Sighted Short-Tailed Opossums. iScience 23, 101527. https://doi.org/10.1016/j.isci.2020.101527
Erzurumlu, R. S., & Gaspar, P. (2012). Development and critical period plasticity of the barrel cortex. European Journal of Neuroscience, *35*(10), 1540-1553.
Finlay, B. L., & Uchiyama, R. (2015). Developmental mechanisms channeling cortical evolution. Trends in neurosciences, 38(2), 69-76.
Florio, M., Albert, M., Taverna, E., Namba, T., Brandl, H., Lewitus, E., Haffner, C., Sykes, A., Wong, F.K., Peters, J., Guhr, E., Klemroth, S., Prüfer, K., Kelso, J., Naumann, R., Nüsslein, I., Dahl, A., Lachmann, R., Pääbo, S., Huttner, W.B., 2015. Human-specific gene ARHGAP11B promotes basal progenitor amplification and neocortex expansion. Science 347, 1465–1470. https://doi.org/10.1126/science.aaa1975
Fukuchi-Shimogori, T., Grove, E.A., 2001. Neocortex Patterning by the Secreted Signaling Molecule FGF8. Science 294, 1071–1074. https://doi.org/10.1126/science.1064252
Gezelius, H., Moreno-Juan, V., Mezzera, C., Thakurela, S., Rodríguez-Malmierca, L.M., Pistolic, J., Benes, V., Tiwari, V.K., López-Bendito, G., 2017. Genetic Labeling of Nuclei-Specific Thalamocortical Neurons Reveals Putative Sensory-Modality Specific Genes. Cerebral Cortex 27, 5054–5069. https://doi.org/10.1093/cercor/bhw290
Halley, A.C., Krubitzer, L., 2019. Not all cortical expansions are the same: the coevolution of the neocortex and the dorsal thalamus in mammals. Current Opinion in Neurobiology, Neuronal Identity 56, 78–86. https://doi.org/10.1016/j.conb.2018.12.003
Heide, M., Haffner, C., Murayama, A., Kurotaki, Y., Shinohara, H., Okano, H., ... & Huttner, W. B. (2020). Human-specific ARHGAP11B increases size and folding of primate neocortex in the fetal marmoset. *Science*, *369*(6503), 546-550.
Hill, J., Inder, T., Neil, J., Dierker, D., Harwell, J., Essen, D.V., 2010. Similar patterns of cortical expansion during human development and evolution. PNAS 107, 13135–13140. https://doi.org/10.1073/pnas.1001229107
Ishikawa, A.W., Komatsu, Y., Yoshimura, Y., 2014. Experience-Dependent Emergence of Fine-Scale Networks in Visual Cortex. J. Neurosci. 34, 12576–12586. https://doi.org/10.1523/JNEUROSCI.1346-14.2014
Izraeli, R., Koay, G., Lamish, M., Heicklen-Klein, A.J., Heffner, H.E., Heffner, R.S., Wollberg, Z., 2002. Cross-modal neuroplasticity in neonatally enucleated hamsters: structure, electrophysiology and behaviour. European Journal of Neuroscience 15, 693–712. https://doi.org/10.1046/j.1460-9568.2002.01902.x
Jacobs, K.M., Donoghue, J.P., 1991. Reshaping the cortical motor map by unmasking latent intracortical connections. Science 251, 944–947. https://doi.org/10.1126/science.2000496

Kahn, D.M., Krubitzer, L., 2002. Massive cross-modal cortical plasticity and the emergence of a new cortical area in developmentally blind mammals. Proc Natl Acad Sci U S A 99, 11429–11434. https://doi.org/10.1073/pnas.162342799
Karlen, S.J., Kahn, D.M., Krubitzer, L., 2006. Early blindness results in abnormal corticocortical and thalamocortical connections. Neuroscience 142, 843–858. https://doi.org/10.1016/j.neuroscience.2006.06.055
Karlen, S.J., Krubitzer, L., 2009. Effects of Bilateral Enucleation on the Size of Visual and Nonvisual Areas of the Brain. Cerebral Cortex 19, 1360–1371. https://doi.org/10.1093/cercor/bhn176
Kaschube, M., Schnabel, M., Löwel, S., Coppola, D.M., White, L.E., Wolf, F., 2010. Universality in the Evolution of Orientation Columns in the Visual Cortex. Science 330, 1113–1116. https://doi.org/10.1126/science.1194869
Kaskan, P. M., Franco, E. C. S., Yamada, E. S., de Lima Silveira, L. C., Darlington, R. B., & Finlay, B. L. (2005). Peripheral variability and central constancy in mammalian visual system evolution. Proceedings of the Royal Society B: Biological Sciences, 272(1558), 91-100.
Kawaguchi, A., 2019. Temporal patterning of neocortical progenitor cells: How do they know the right time? Neuroscience Research, Timing and shaping mechanisms of neural development 138, 3–11. https://doi.org/10.1016/j.neures.2018.09.004
Krubitzer, L., 2007. The Magnificent Compromise: Cortical Field Evolution in Mammals. Neuron 56, 201–208. https://doi.org/10.1016/j.neuron.2007.10.002
Krubitzer, L., Manger, P., Pettigrew, J., Calford, M., 1995. Organization of somatosensory cortex in monotremes: In search of the prototypical plan. Journal of Comparative Neurology 351, 261–306. https://doi.org/10.1002/cne.903510206
Krubitzer, L., Stolzenberg, D.S., 2014. The evolutionary masquerade: genetic and epigenetic contributions to the neocortex. Current Opinion in Neurobiology, Neural maps 24, 157–165. https://doi.org/10.1016/j.conb.2013.11.010
Krubitzer, L.A., Prescott, T.J., 2018. The Combinatorial Creature: Cortical Phenotypes within and across Lifetimes. Trends in Neurosciences, Special Issue: Time in the Brain 41, 744–762. https://doi.org/10.1016/j.tins.2018.08.002
Krubitzer, L.A., Seelke, A.M.H., 2012. Cortical evolution in mammals: The bane and beauty of phenotypic variability. PNAS 109, 10647–10654. https://doi.org/10.1073/pnas.1201891109
Liu, J., Liu, W., Yang, L., Wu, Q., Zhang, H., Fang, A., Li, L., Xu, X., Sun, L., Zhang, J., Tang, F., Wang, X., 2017. The Primate-Specific Gene TMEM14B Marks Outer Radial Glia Cells and Promotes Cortical Expansion and Folding. Cell Stem Cell 21, 635-649.e8. https://doi.org/10.1016/j.stem.2017.08.013
Liu, Y., Vannuscorps, G., Caramazza, A., Striem-Amit, E., 2020. Evidence for an effector-independent action system from people born without hands. PNAS 117, 28433–28441. https://doi.org/10.1073/pnas.2017789117
Lunghi, C., Emir, U.E., Morrone, M.C., Bridge, H., 2015. Short-Term Monocular Deprivation Alters GABA in the Adult Human Visual Cortex. Current Biology 25, 1496–1501. https://doi.org/10.1016/j.cub.2015.04.021
Manger, P.R., Pettigrew, J.D., 1995. Electroreception and the feeding behaviour of platypus (Ornithorhynchus anatinus: Monotremata: Mammalia). Philosophical Transactions of the Royal Society of London. Series B: Biological Sciences 347, 359–381. https://doi.org/10.1098/rstb.1995.0030
Mazziotti, R., Baroncelli, L., Ceglia, N., Chelini, G., Sala, G.D., Magnan, C., Napoli, D., Putignano, E., Silingardi, D., Tola, J., Tognini, P., Arthur, J.S.C., Baldi, P., Pizzorusso, T., 2017. Mir-132/212 is required for maturation of binocular matching of orientation preference and depth perception. Nature Communications 8, 15488. https://doi.org/10.1038/ncomms15488

Mikula, S., Manger, P., Jones, E., 2008. The thalamus of the monotremes: Cyto- and myeloarchitecture and chemical neuroanatomy. Philosophical transactions of the Royal Society of London. Series B, Biological sciences 363, 2415–40. https://doi.org/10.1098/rstb.2007.2133
Molnár, Z., Knott, G.W., Blakemore, C., Saunders, N.R., 1998. Development of thalamocortical projections in the South American gray short-tailed opossum (Monodelphis domestica). Journal of Comparative Neurology 398, 491–514. https://doi.org/10.1002/(SICI)1096-9861(19980907)398:4<491::AID-CNE3>3.0.CO;2-Y
Moreno-Juan, V., Filipchuk, A., Antón-Bolaños, N., Mezzera, C., Gezelius, H., Andrés, B., Rodríguez-Malmierca, L., Susín, R., Schaad, O., Iwasato, T., Schüle, R., Rutlin, M., Nelson, S., Ducret, S., Valdeolmillos, M., Rijli, F.M., López-Bendito, G., 2017. Prenatal thalamic waves regulate cortical area size prior to sensory processing. Nature Communications 8, 14172. https://doi.org/10.1038/ncomms14172
Moreno-Juan, V., Martini, F.J., Pérez-Saiz, L., Herrero-Navarro, Á., Valdeolmillos, M., López-Bendito, G., 2020. Thalamic spontaneous activity coordinates the timing of corticothalamic innervation in the visual system. bioRxiv 2020.11.13.382366. https://doi.org/10.1101/2020.11.13.382366
Nott, A., Cho, S., Seo, J., Tsai, L.-H., 2015. HDAC2 expression in parvalbumin interneurons regulates synaptic plasticity in the mouse visual cortex. Neuroepigenetics 1, 34–40. https://doi.org/10.1016/j.nepig.2014.10.005
Pantev, C., Oostenveld, R., Engelien, A., Ross, B., Roberts, L.E., Hoke, M., 1998. Increased auditory cortical representation in musicians. Nature 392, 811–814. https://doi.org/10.1038/33918
Petit, F., Sears, K.E., Ahituv, N., 2017. Limb development: a paradigm of gene regulation. Nature Reviews Genetics 18, 245–258. https://doi.org/10.1038/nrg.2016.167
Pettigrew, J.D., 1999. Electroreception in monotremes. Journal of Experimental Biology 202, 1447–1454. https://doi.org/10.1242/jeb.202.10.1447
Piché, M., Robert, S., Miceli, D., Bronchti, G., 2004. Environmental enrichment enhances auditory takeover of the occipital cortex in anophthalmic mice. European Journal of Neuroscience 20, 3463–3472. https://doi.org/10.1111/j.1460-9568.2004.03823.x
R, N., G, R., E, N., 1992. Electrophysiological mapping of body representation in the cortex of the blind mole rat. Neuroreport 3, 505–508. https://doi.org/10.1097/00001756-199206000-00012
Ramamurthy, D.L., Dodson, H.K., Krubitzer, L.A., 2021. Developmental plasticity of texture discrimination following early vision loss in the marsupial Monodelphis domestica. Journal of Experimental Biology 224. https://doi.org/10.1242/jeb.236646
Ramamurthy, D.L., Krubitzer, L.A., 2018. Neural Coding of Whisker-Mediated Touch in Primary Somatosensory Cortex Is Altered Following Early Blindness. J. Neurosci. 38, 6172–6189. https://doi.org/10.1523/JNEUROSCI.0066-18.2018
Reh, R.K., Dias, B.G., Nelson, C.A., Kaufer, D., Werker, J.F., Kolb, B., Levine, J.D., Hensch, T.K., 2020. Critical period regulation across multiple timescales. Proc Natl Acad Sci U S A 117, 23242–23251. https://doi.org/10.1073/pnas.1820836117
Rebsam, A., & Mason, C. A. (2008). Otx2's incredible journey. Cell, *134*(3), 386-387.
Rehkämper, G., Necker, R., Nevo, E., 1994. Functional anatomy of the thalamus in the blind mole rat Spalax ehrenbergi: An architectonic and electrophysiologically controlled tracing study. Journal of Comparative Neurology 347, 570–584. https://doi.org/10.1002/cne.903470408
Ricciardi, E., Bonino, D., Pellegrini, S., Pietrini, P., 2014. Mind the blind brain to understand the sighted one! Is there a supramodal cortical functional architecture? Neuroscience & Biobehavioral Reviews, Multisensory integration, sensory substitution and visual rehabilitation 41, 64–77. https://doi.org/10.1016/j.neubiorev.2013.10.006
Robson, J.A., Hall, W.C., 1977. The organization of the pulvinar in the grey squirrel (Sciurus carolinensis). I. Cytoarchitecture and connections. Journal of Comparative Neurology 173, 355–388. https://doi.org/10.1002/cne.901730210

Shulha, H. P., Crisci, J. L., Reshetov, D., Tushir, J. S., Cheung, I., Bharadwaj, R., ... & Akbarian, S. (2012). Human-specific histone methylation signatures at transcription start sites in prefrontal neurons. PLoS biology, *10*(11), e1001427.
Smaers, J.B., Rothman, R.S., Hudson, D.R., Balanoff, A.M., Beatty, B., Dechmann, D.K.N., de Vries, D., Dunn, J.C., Fleagle, J.G., Gilbert, C.C., Goswami, A., Iwaniuk, A.N., Jungers, W.L., Kerney, M., Ksepka, D.T., Manger, P.R., Mongle, C.S., Rohlf, F.J., Smith, N.A., Soligo, C., Weisbecker, V., Safi, K., 2021. The evolution of mammalian brain size. Sci. Adv. 7, eabe2101. https://doi.org/10.1126/sciadv.abe2101
Sugiyama, S., Di Nardo, A. A., Aizawa, S., Matsuo, I., Volovitch, M., Prochiantz, A., & Hensch, T. K. (2008). Experience-dependent transfer of Otx2 homeoprotein into the visual cortex activates postnatal plasticity. Cell, 134(3), 508-520.
Sur, M., Rubenstein, J.L.R., 2005. Patterning and Plasticity of the Cerebral Cortex. Science 310, 805–810. https://doi.org/10.1126/science.1112070
Suzuki, I.K., Gacquer, D., Van Heurck, R., Kumar, D., Wojno, M., Bilheu, A., Herpoel, A., Lambert, N., Cheron, J., Polleux, F., Detours, V., Vanderhaeghen, P., 2018. Human-Specific NOTCH2NL Genes Expand Cortical Neurogenesis through Delta/Notch Regulation. Cell 173, 1370-1384.e16. https://doi.org/10.1016/j.cell.2018.03.067
Tognini, P., Putignano, E., Coatti, A., Pizzorusso, T., 2011. Experience-dependent expression of miR-132 regulates ocular dominance plasticity. Nature Neuroscience 14, 1237–1239. https://doi.org/10.1038/nn.2920
Tomasello, U., Klingler, E., Niquille, M., Mule, N., Vevey, L. de, Prados, J., Santinha, A.J., Platt, R., Borrell, V., Jabaudon, D., Dayer, A., 2021. MiR-137 and miR-122, two outer subventricular zone-enriched non-coding RNAs, regulate basal progenitor expansion and neuronal differentiation. bioRxiv 2021.04.01.438039. https://doi.org/10.1101/2021.04.01.438039
Tropea, D., Kreiman, G., Lyckman, A., Mukherjee, S., Yu, H., Horng, S., Sur, M., 2006. Gene expression changes and molecular pathways mediating activity-dependent plasticity in visual cortex. Nature Neuroscience 9, 660–668. https://doi.org/10.1038/nn1689
Van Essen, D.C., 2018. Scaling of human brain size. Science 360, 1184–1185. https://doi.org/10.1126/science.aat8948
Van Essen, D.C., Dierker, D.L., 2007. Surface-Based and Probabilistic Atlases of Primate Cerebral Cortex. Neuron 56, 209–225. https://doi.org/10.1016/j.neuron.2007.10.015
Wong, P., Kaas, J.H., 2008. Architectonic Subdivisions of Neocortex in the Gray Squirrel (Sciurus carolinensis). The Anatomical Record 291, 1301–1333. https://doi.org/10.1002/ar.20758
Young, N.A., Vuong, J., Teskey, G.C., 2012. Development of motor maps in rats and their modulation by experience. Journal of Neurophysiology 108, 1309–1317. https://doi.org/10.1152/jn.01045.2011
Zembrzycki, A., Stocker, A.M., Leingärtner, A., Sahara, S., Chou, S.-J., Kalatsky, V., May, S.R., Stryker, M.P., O'Leary, D.D., 2015. Genetic mechanisms control the linear scaling between related cortical primary and higher order sensory areas. eLife 4, e11416. https://doi.org/10.7554/eLife.11416

FIGURES:

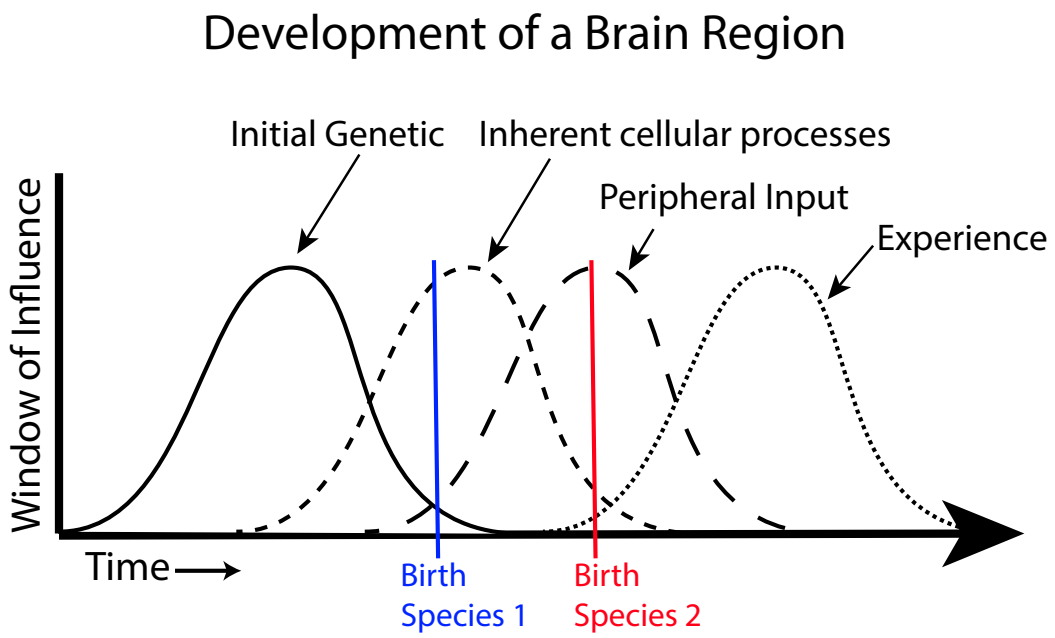

Figure 1. The developmental cascade. Example of the development of a single hypothetical brain region illustrating how different developmental processes cascade in time (X-Axis), beginning with initial genetic processes such as cell-type specification and proliferation. Each process has a window of influence (Y-Axis) where intrinsic (genetic) or extrinsic (environmental/epigenetic) factors can impact brain development. For example, an alteration in genes which regulate cell cycle kinetics during neurogenesis could result in larger progenitor pools and affect the overall size of a brain region, such as the neocortex. Moreover, differences in the developmental stage at which a species is born (blue and red vertical lines) would determine the extent to which the environment and sensory driven activity impacts development.

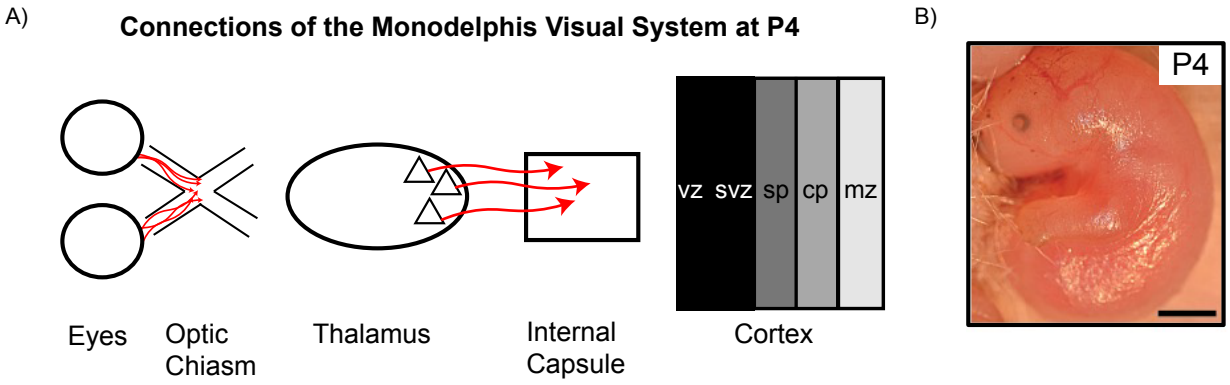

Figure 2. Altering the ratio of sensory inputs in short-tailed opossums via bilateral enucleation. (A) Diagram showing the state of the nervous system at the time of enucleation. Red arrows indicate axonal projections and their location at postnatal day 4 (P4). (B) Image of P4 opossum. Scale bar is 1mm. Abbreviations: VZ; ventricular zone, SVZ; subventricular zone; SP; subplate, CP; cortical plate.

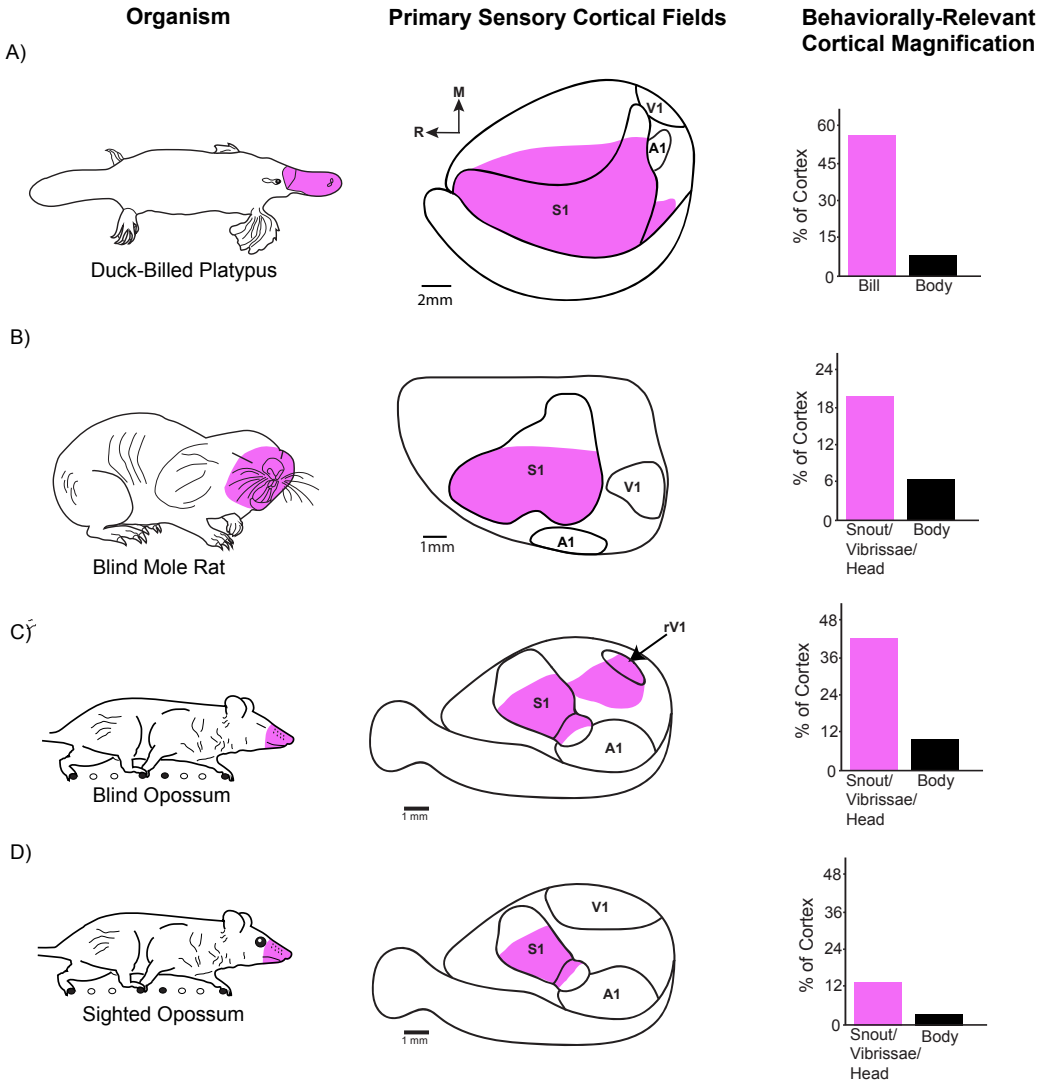

Figure 3. Experimental manipulations can generate cortical phenotypes that resemble those produced naturally in evolution. (A) Image of the duck-billed platypus (left) and flattened cortex showing the approximate size and location of primary sensory cortical fields (middle). A disproportionately large portion of the cortex is occupied by somatosensory cortex. A large portion of the cortex is devoted to processing the bill (pink). Bar graph (right) shows the percentage of cortex (Y-axis) occupied by the bill and body representation (X-axis), illustrating cortical magnification of the behaviorally relevant sensory organ. (B) Image of blind mole rat

(left) and illustration of flattened cortex (middle) showing that S1 occupies a large proportion of the entire cortex and contains and enlarged representation of the snout vibrissae and head (pink). V1 in these animals has be co-opted by the auditory system. Bar graph (right) shows the percentage of cortex devoted to processing inputs from the snout head, and vibrissae. (C) Image of an early blind opossum (left) and corresponding illustration of flattened cortex showing architectonically defined primary sensory fields. Like the platypus and blind mole rat, a large proportion of cortex is devoted to processing the snout, vibrissae and head, compared to sighted animals (pink). Like the blind mole rat, V1 in blind opossums has been co-opted by another sensory system (the somatosensory system). The bar graph to the right shows the percentage of cortex that represents the head, vibrissae and snout. (D) Image of a sighted opossum (left) and flattened cortex with the location of V1, S1, and A1 (middle). Compared to early blind opossums, sighted animals have much less neocortex devoted to processing inputs from the snout, head, and vibrissae (bar graph; right). Illustrations and bar graphs were constructed with data from Krubitzer et al., 1995, Karlen et al., 2006, Kahn and Krubitzer 2002, Necker et al., 1992. Abbreviations: Primary Somatosensory Cortex: S1, Primary Visual Cortex: V1, Primary Auditory Cortex, A1.

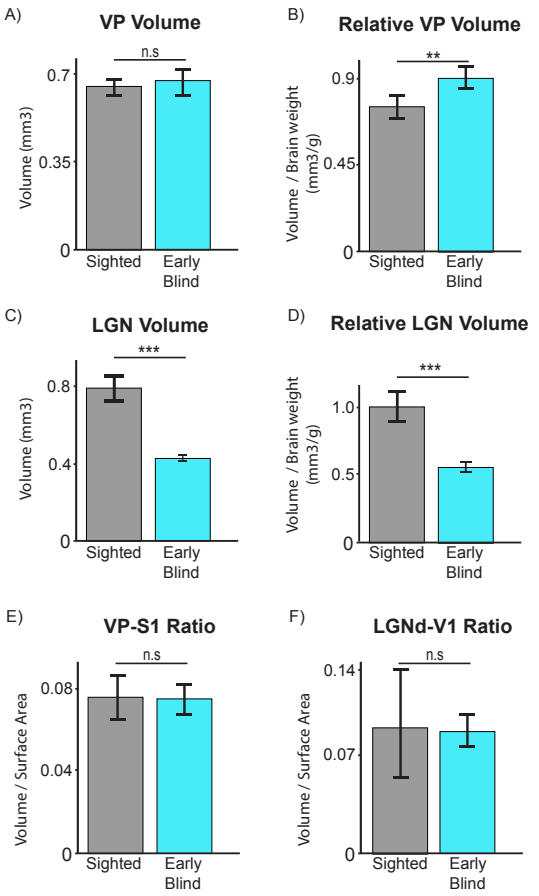

Figure 4. Measurements of thalamic nuclei in early blind and sighted opossums. Bar graphs show that early blind opossums (blue) have a similar VP volume compared to sighted controls (gray) when measured in absolute size (A) ($p(14) = .505$), but have a relatively larger VP volume when scaled by brain weight (B) ($p(14) = .01$). (C/D) Early blind opossums exhibit a reduction in the size of LGN when measured in absolute ($p(24) < .001$) or relative terms ($p(24) < .001$). (E) Bar graphs showing that the size of VP scales with the size of S1 equally in early blind and sighted animals ($p(8) = .922$). (F) Similarly, LGN volume scales with the area size of V1 in both groups ($p(8) = .893$). These results suggest a tight scaling relationship between the volume of thalamic nuclei and the size of cortical fields. Bar graphs are shown as mean with 95%

confidence intervals. Abbreviations: VP; ventral posterior nucleus, LGN; lateral geniculate nucleus, S1; primary somatosensory cortex, V1; primary visual cortex.

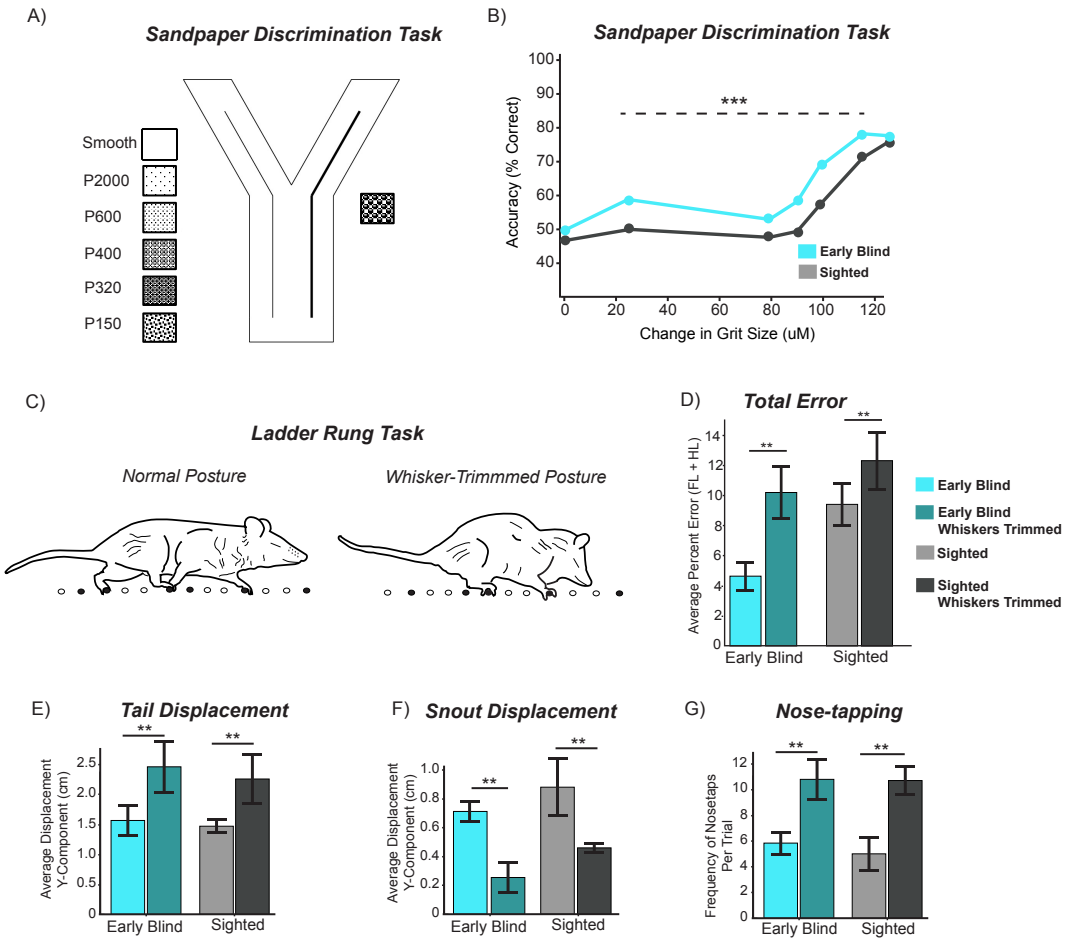

Figure 5. Altering the ratio of sensory inputs alters behavior. (A) Illustration of the two-choice Y-Maze task. Opossums were trained to discriminate between different grits of sandpaper and rewarded for correct decisions. (B) Line graphs showing accuracy in determining changes in grit size. Early blind opossums (blue) can discriminate between finer changes in texture than sighted opossums (gray), (two-way ANOVA: $p < .001$). (C) Illustrations of opossums on the ladder rung task. When the whiskers are present, animals show a standard posture, with a raised snout and long strides (left). When the whiskers are trimmed both early blind and sighted opossums show a hunched posture (right). (D) Bar graph showing total error on the ladder task

before and after whisker trimming. Darker colors denote whisker-trimming scores. A main effect was found for the presence of whiskers on performance ($p = .004$) and for early blind opossums performing better than sighted controls ($p = .007$). (E-G) Bar graphs showing aspects of body posture during ladder crossing, indicating that both animals adopted changes in strategy when the whiskers were trimmed (E: $p = .042$, F: $p = .004$, G: $p = .002$). Bar graphs are shown as mean with bootstrapped 95% confidence intervals. Figures reprinted with permission (Ramamurthy et al; 2021, Englund et al; 2020).

Chapter 2.

The following chapter was published as a research article in *iScience*. Thus, supplementary videos and information can be found online at

https://www.sciencedirect.com/science/article/pii/S2589004220307197

Citation:

Englund, M., Faridjoo, S., Iyer, C. S., & Krubitzer, L. (2020). Available sensory input determines motor performance and strategy in early blind and sighted short-tailed opossums. *Iscience*, *23*(9), 101527.

Available sensory input determines motor performance and strategy in early blind and sighted short-tailed opossums.

Mackenzie Englund[1], Samaan Faridjoo[2], Chris Iyer[3], and Leah Krubitzer[1,4]

1. Department of Psychology, University of California, Davis. 135 Young Hall, 1 Shields Ave., Davis, CA 95616, USA

2. Department of Molecular and Cellular Biology, University of California, Davis. 149 Briggs Hall, 1 Shields Ave., Davis, CA 95616, USA

3. Symbolic Systems Program, Stanford University, 460 Margaret Jacks Hall, 450 Serra Mall, Stanford, Ca 94305, USA

4. Center for Neuroscience, University of California, Davis. 1544 Newton Ct., Davis, CA 95618, USA

Corresponding Author (Lead Contact):
Leah Krubitzer
University of California, Davis
Center for Neuroscience
1544 Newton Court Davis, CA 95618
Phone: (530) 757-8868
Fax: (530) 757-8827
Email: lakrubitzer@ucdavis.edu

SUMMARY

The early loss of vision results in a reorganized neocortex, affecting areas of the brain which process both the spared and lost senses, and leads to heightened abilities on discrimination tasks involving the spared senses. Here, we used performance measures and machine learning algorithms that quantify behavioral strategy, to determine if and how early vision loss alters adaptive sensorimotor behavior. We tested opossums on a motor task involving somatosensation and found that early blind animals had increased limb placement accuracy compared to sighted controls, while showing similarities in crossing strategy. However, increased reliance on tactile inputs in early blind animals resulted in greater deficits in limb placement and behavioral flexibility when the whiskers were trimmed. These data show that compensatory-cross modal plasticity extends beyond sensory discrimination tasks to motor tasks involving the spared senses, and highlights the importance of whiskers in guiding forelimb control.

Keywords:

Cross-modal plasticity, sensorimotor behavior, vision loss, whisking

INTRODUCTION

Navigation through complex space requires a tight coupling between incoming sensory input and motor output (Abbruzzese and Berardelli, 2003; Ferezou et al., 2007). The ability of an animal to make precise, sensory-guided movements while actively exploring the environment depends on the sensory information available, the structure of the peripheral epithelia, the morphology of the body, and the neural circuits involved in integrating sensory information from different modalities. Because evolution has produced species who rely on some senses over others, it is important to look at animals that have different body morphologies and that rely on

different combinations of sensory input, to appreciate general principles of nervous system structure and function that allow mammals to adapt movement strategies in a constantly changing environment. For example, cats and humans use vision to guide complex locomotion (Drew and Marigold, 2015; McVea et al., 2009); bats rely on echolocation to navigate three-dimensional space (Moss and Surlykke, 2010); and many rodents employ tactile inputs relayed through the whiskers to navigate terrestrial and arboreal habitats (Grant et al., 2009; Mitchinson et al., 2011). While different species often rely heavily on one sense, there is accumulating evidence that the developing neocortex is not as strictly constrained by its evolutionary history as previously thought, since the loss of sensory input early in development leads to a massive restructuring of the neocortex based on the remaining sensory inputs (Bell et al., 2019; Cecchetti et al., 2016; Kupers and Ptito, 2014; Renier et al., 2014).

Studies of early vision loss in animal models and humans demonstrate that the neocortex is capable of remarkable functional and anatomical plasticity, and this plasticity appears to support important sensory-mediated behaviors. For example, if visual input is lost in developing mice, rats, and hamsters, neurons in visual cortex (V1) respond to deflections of the whiskers and to auditory stimuli such as tones and clicks (Izraeli et al., 2002; Piché et al., 2007; Toldi et al., 1990). Cortico-cortical connections are also altered by the early loss of vision, as rats enucleated at birth show increased variability and divergence of intra- and interhemispheric connections between V1 and extrastriate cortex (Bock and Olavarria, 2011; Laing et al., 2012). In mice, the early loss of vision alters cortico-cortical connections prior to would-be eye opening, such that projections from S1 to V1 are more broadly distributed in blind mice compared to sighted controls (Dye et al., 2012; Kozanian et al., 2015).

Work from our laboratory in short-tailed opossums (*Monodelphis domestica*) has demonstrated that removing all visual input prior to the onset of spontaneous activity from the retina results in massive cross-modal changes in the functional organization and connections of what would have been visual cortex (Kahn and Krubitzer, 2002; Karlen and Krubitzer, 2009).

Similar to rodents, neurons in the reorganized visual cortex of early blind opossums respond to stimulation of the face and whiskers, and to broadband auditory clicks (Figure 1A, Figure 1B) (Karlen et al., 2006). The spared sensory systems are also affected. There are alterations in cortical and subcortical connections of primary somatosensory cortex (S1) (Figure 1C) (Dooley and Krubitzer, 2019; Karlen et al., 2006)and a spatial sharpening of receptive fields and improved population decoding for whisker-stimulus position for neurons in S1 (Figure 1D) (Ramamurthy and Krubitzer, 2018), indicating that individual neurons in S1 in EB opossums have better discriminability.

Given the overwhelming evidence from our laboratory and others, that early vision loss results in drastic cross-modal changes to sensory and association cortical areas, it is surprising that only a few studies have investigated the behavioral outcomes that result from these neural changes, and none have quantified how kinematics, strategy, and performance during navigation are altered in tandem (Rauschecker, 1995; Renier et al., 2014). One study in rats found that early blind animals perform a maze-running task more quickly, and have alterations in the receptive-field size of neurons in barrel cortex (Toldi et al., 1994), while a finger-maze study in blind humans found no difference in performance compared to sighted participants (Gagnon et al., 2012). Other studies have found that blind individuals can create mental maps of space more efficiently than sighted controls (for review see Schinazi et al., 2016). This limited body of research leaves the sensorimotor behavioral correlates to cross-modal changes in the brain largely unknown.

The goal of the present investigation was to assess differences in both performance and strategy between early blind and sighted opossums on a naturalistic sensorimotor task that requires coordination of the limbs, and postural control of the body and head to navigate across a relatively complex substrate (ladder rung apparatus). We sought to determine the extent to which animals rely on the remaining available sensory information by removing sensory input from the whiskers. To accomplish this, we utilized recently developed, marker-less tracking

algorithms to analyze performance, locomotor patterns, and movement strategies captured on video in short-tailed opossums bilaterally enucleated at postnatal day 4 - prior to the onset of spontaneous retinal activity and the formation of thalamic and cortical visual pathways. As *Monodelphis* is among mammals that use the whiskers for active sensing (whisking), we used a sensorimotor task known to involve somatosensation: the variable ladder-rung walking task (Metz and Whishaw, 2009; Mitchinson et al., 2011). This task is sensitive to minute differences in motor control of the limbs, and has been used to assess motor deficits in peripheral and neurologic disease models (Antonow-Schlorke et al., 2013; Metz and Whishaw, 2002; Schönfeld et al., 2017).

RESULTS

In the following results, we compared both performance and movement strategy in early blind (EB) and sighted control (SC) animals while performing the ladder rung task. Statistics are reported as Adjusted R-Squared (R^2adj), and the F-Statistic is presented with degrees of freedom of the model, F(N). Delta (Δ) indicates the difference between pre whisker-trim and post whisker-trim means within early blind (ΔEB) and sighted opossums (ΔSC).

Early blind opossums outperform sighted controls in variable ladder rung walking, but show similarities in crossing strategy

To determine differences in ladder rung walking performance between early blind and sighted opossums, foot faults on nine variable ladder rung patterns were scored by two independent observers. Using a linear model testing for interactions between experimental group and lighting condition, we found a significant main effect for sightedness on total error, with early blind opossums committing fewer errors than sighted controls (R^2adj = 0.32, F(8) = 6.62, p = 0.007) (Figure 2A). Under the same model, we found no significant effect of lighting (p =0.718), with animals in both experimental groups performing similarly in the light and dark

(Figure S1C). Further, there was no effect of biological sex on performance ($p = 0.086$). We found no differences in performance across different variable patterns, nor in the order in which rung patterns were completed (light or dark first) ($R^2adj = 0.09$, $F(3) = 8.00$, $p = 0.367$, $p = 0.207$) (Figure S1A). Because there was no significant effect for lighting, a reduced model was used to test the individual contributions of forelimb and hindlimb error to total error rate.

Additionally, as opossums completed at least 3 standard patterns on all 7 days prior to walking variable patterns, we analyzed performance on standard patterns across testing days. Group differences were significant on day 1 (habituation day, no variable patterns), with EB opossums performing worse than SC opossums ($p = 0.01$). However, on all testing days (days 2 – 7), there was no significant difference between EB and SC performance on standard patterns ($p_{2\text{-}7} > 0.40$). However, whisker trimming did significantly decrease performance on standard patterns ($p < 0.001$).

On variable patterns, early blind opossums committed significantly less forelimb errors than sighted animals ($R^2adj = 0.32$, $F(4) = 11.81$, $p = 0.004$) (Figure 2B). Additionally, early blind opossums committed significantly less hindlimb errors than sighted animals ($R^2adj = 0.10$, $F(4) = 3.71$, $p = 0.008$) (Figure 2B). Thus, in the absence of vision, early blind opossums outperformed their sighted counterparts, making significantly fewer errors during rung walking whether fore- and hindlimbs were considered separately or together.

To investigate the crossing strategies and kinematics that may underlie differences in performance, we quantified crossing time and nose tapping behavior, and used DeepLabCut marker-less tracking in a randomly-chosen subset of animals ($n = 8$) to track the position of the snout, limbs, and tail, as animals crossed the ladder (Video S1). We found no significant effect of crossing time on performance ($R^2adj = 0.35$, $F(4) = 10.71$, $p = 0.23$), and no significant difference in crossing time between early blind (7.85 ± 0.72s) and sighted animals (6.64 ± 0.9s) ($R^2adj = 0.24$, $F(4) = 7.67$, $p = 0.27$) (Figure 2C). There was also no significant difference in the average frequency of nose taps per-trial between blind and sighted animals ($R^2adj = 0.34$, $F(4)$

= 7.57, p = 0.63) (Figure 2D), or the average height at which animals held their snout during correct placements (R^2adj = 0.60, F(4) = 6.46, p = 0.84) (Figure 2E). These results show that animals in both groups take similar amounts of time to cross the ladder and implement some of the same strategies while doing so, but early blind animals show increased performance.

Next, we quantified average forelimb trajectories during correct placements in both groups (n = 155 forelimb motions). Average peak height did not differ between groups (R^2adj = 0.24, F(4) = 7.67, p = 0.27) (Figure 2F). However, during forelimb motion, early blind animals were relatively quicker to lift their forelimb compared to sighted control animals (R^2adj = 0.72, F(4) = 1646.0, p < 0.001) (Figure 2F; Green Rectangle). This was quantified as the average height of the limb during the second quartile of a forelimb motion (52 – 104ms). Surprisingly, average forelimb peak height significantly predicted average forelimb error, with higher peaks indicating better performance (R^2adj = 0.78, F(4) = 13.06, p = 0.028). While one might expect larger movements to be correlated with more errors, peak height may be an indicator of an animal's confidence in its estimation of where the next rung is located. In the X-direction (step length), both early blind and sighted opossums exhibit similar forelimb kinematics (i.e. similar step lengths), possibly constrained by the finite spacing of the rungs (Figure 2G). Thus, apart from differences in when the forelimb was lifted off of a rung, there was no overall difference in the behavioral strategy shown by the metrics that we used. However, it should be noted that differences in the kinematics of other body parts that we did not quantify, particularly in how the position of the whiskers relates to the position of the forelimbs, may also contribute to differences in performance.

Whisker trimming causes deficits in performance in forelimb but not hindlimb placement. Performance deficits and limb trajectories are altered to greater extents in early blind animals.

Work from our laboratory has recently shown that neurons in the whisker representation of S1 have smaller receptive fields and increased selectivity (i.e. greater discriminability) (Ramamurthy and Krubitzer, 2018). Thus, we examined the role of the whiskers during variable ladder rung walking. To accomplish this, we trimmed the mystacial, submandibular, and genal vibrissae, and re-tested animals on variable patterns over the course of two additional testing days. We found a significant main effect for whisker trimming on overall performance in early blind and sighted animals (R^2adj = 0.31, F(4) = 11.62, $p < 0.001$, ΔEB = +5.57% error, ΔSC = +2.90% error) (Figure 3A; Figure S3A). While absolute increases in error were ~6% and 3% for EB and SC opossums respectively, relative increases in error were 50% and 33% (comparing pre- and post-trim means), showing the extreme detriment of whisker trimming to rung walking performance. Moreover, increases in error due to whisker trimming are driven by increases in forelimb error (R^2adj = 0.32, F(4) = 11.81, $p < 0.001$, ΔEB = +8.81% error, ΔSC = +5.92% error) but not hindlimb error (R^2adj = 0.10, F(4) = 3.71, p = 0.40, ΔEB = +1.09% error, ΔSC = +0.65% error) (Figure 3B). Whisker trimming caused a two-fold increase in total error in early blind opossums, increasing their error rate to similar levels to those observed in sighted animals with whiskers, highlighting their heavy reliance on this spared sensory system. We found that overall, average forelimb error significantly predicted average hindlimb error (R^2adj = 0.32, $p < 0.001$ for animals with whiskers, and R^2adj = 0.10, p = 0.03 for whisker trimmed animals) (Figure 3C), illustrating the relationship between forelimb and hindlimb movement in precision quadrupedal locomotion, as animals that were accurate forelimb placers were also accurate hindlimb placers.

Next, to assess how the absence of tactile sensory information provided by the whiskers altered limb placement, we compared forelimb and hindlimb trajectories during correct forelimb placements before and after whisker-trimming using data derived from DeepLabCut marker-less tracking. We found that whisker trimming differentially altered the trajectories of forelimb motion in early blind and sighted animals, such that sighted animals exhibited little reduction in peak height while whisker-trimmed early blind animals show a significant reduction in forelimb peak

height during correct placement (R^2adj = 0.40, F(4) = 3.46, p = 0.02, ΔEB = -0.27 cm, ΔSC = -0.1 cm) (Figure 3D; Figure 3E; Figure S1D). The 2.5-fold differential reduction in average forelimb peak height between groups demonstrates the greater effect of whisker trimming on early blind opossums' sensorimotor coordination. The X-component (step length) of forelimb trajectories during correct placements was also altered due to whisker trimming, resulting in shorter steps for both groups (ΔEB = -0.8 cm, ΔSC = -1.69 cm) (Figure 3F; Figure 3G). Likewise, hindlimb trajectories in both groups became shallower after whisker trimming (Figure 3H; Figure 3I). Interestingly, the average reduction in hindlimb peak height matched the reduction in forelimb peak height in EB opossums exactly (ΔEB = -0.27 cm). Again, a less extreme reduction in hindlimb peak height was observed in sighted controls after whisker trimming (ΔSC = -0.23 cm) (Figure S1D). Together, this data shows the importance of whiskers for forelimb placement, and further, the importance of forelimb placement in guiding hindlimb placement. In sum, removing a heavily relied upon sense, especially in early blind animals, results in changes to performance and locomotor trajectories.

Whisker trimming alters forelimb dynamics by causing variable motions and different movement types.

Since whisker trimming resulted in changes to forelimb trajectories, we sought to determine the underlying sources of these changes. Observation from video and trajectory plots indicates that variance in forelimb movements may increase after whisker trimming. Therefore, we assessed the variance of the Y-Component (step height) of forelimb trajectories between early blind and sighted opossums, with and without whiskers. As expected, the lowest variance in all groups was at the beginning, peak, and end of a forelimb movement (Figure 4A). While this is most likely due to the fact that peaks were aligned for analysis and that ladder rungs were at fixed intervals, restrictions on the musculoskeletal system and muscle synergies also

contribute to highly stereotyped movements during locomotion. Variance of forelimb movements was not correlated with the number of strikes analyzed (R^2adj = 0.01, F(1) = 1.12, p = 0.31). However, by animal, higher variance of correct forelimb placements was found to significantly predict average hindlimb error, again indicating that animals may be less certain of an upcoming rung's position (R^2adj = 0.30, F(1) = 7.47, p = 0.02).

We then binned our analyses into a pre-peak retraction (frames 20 - 50), and a post peak extension (frames 50 - 80) phase. We excluded the first and last 20 frames of motion from this analysis to ensure frames where the forelimb was potentially resting on a rung were excluded. The retraction phase is noted to be the swing portion of the forelimb movement (Jacobs et al., 2014). This part of the movement begins on a ladder rung. The elbow then moves from full extension to full flexion at the peak of the motion. The extension phase is noted to be the swing-to-stance portion of the limb movement, where the elbow goes from flexion to extension, ending with the forepaw being placed on an upcoming rung. While there was no difference in the overall variance between early blind (0.063 ± 0.007cm) and sighted (0.060 ± 0.005cm) opossums (R^2adj = 0.22, F(3) = 11.51, p = 0.23), whisker trimming significantly increased variance in both groups during the retraction phase of a forelimb movement (R^2adj = 0.22, F(3) = 11.51, p < 0.001, ΔEB = +0.046, ΔSC = +0.036) (Figure 4B). Conversely, whisker trimming did not significantly affect variance in the extension (placement) phase of forelimb movement (R^2adj = 0.042, F(3) = 2.69, p = 0.21, ΔEB = -0.011, ΔSC = -0.015) (Figure 4A – Figure 4D), showing that whiskers are critical for quick and accurate detection of future forelimb placement locations, but that the guidance of the motion is not affected once the opossum has already detected a rung.

Next, to characterize stereotypical movement types between groups, we used K-Means clustering to classify forelimb step height waveforms into stereotypical movements. *A priori,* we sorted waveforms by sightedness and whisker presence to detect differences within groups, and used the elbow point method and highest silhouette coefficient (SCoef) to determine the number

of clusters used for each experimental condition. For sighted animals, both methods converged on three clusters ($SCoef_3$ = 0.24) (Figure 4E; Figure S2). For early blind animals, the elbow method estimated 3 clusters (Figure S2), while the silhouette method estimated 2 ($SCoef_2$ = 0.23, $SCoef_3$ = 0.21). Thus, both 2 and 3 clusters were considered for analysis. Interestingly, forelimb movements of both early blind and sighted animals clustered into similar movement types regardless of whether they were clustered into 2 or 3 stereotypical movements (Figure S2). The only observed difference was in the retraction phase of a single movement type of early blind animals (Figure 4E). For both early blind and sighted opossums, the extension phase involved either a quick, medium, or slow placement trajectory.

In whisker-trimmed animals, forelimb movements clustered definitively into two similar types regardless of blind or sighted condition: one movement where the forelimb was lifted off the rung immediately, but took a slow linear trajectory to its peak height, and one quick nonlinear movement with a shallow peak (EB: $SCoef_2$ = 0.23, $SCoef_3$ = 0.19) (SC: $SCoef_2$ = 0.31, $SCoef_3$ = 0.17) (Figure 4E). Thus, stereotypical movement types were not influenced by the presence or absence of vision, but instead by the presence or absence of whiskers. Additionally, movements were most notably changed in the retraction phase, showing increased variability and altered waveform shape, illustrating the importance of whiskers in detecting the upcoming rung.

Opossums adapt to whisker trimming by altering body posture and strategy.

Finally, to examine the alternate strategies used by opossums after whisker trimming, we quantified aspects of body posture during correct forelimb placements. First, we quantified the distance in the X direction (stride length) between the right forelimb and right hindlimb, as well as between the right forelimb and snout, during correct motions. Animals with whiskers, regardless of blind or sighted condition, show standard locomotor postures, with limbs oscillating between long (> 5 cm) and short distances (~ 1 cm), reminiscent of the quadrupedal

gait cycle (Figure 5A, Figure 5B solid lines) (Video S2/Video S4). However, whisker-trimmed opossums show flattened trajectories, which never reach large amplitudes (Figure 5A, Figure 5B dotted lines). Instead, these condensed limb distances illustrate the hunched, conservative approach that blind and sighted animals employed when crossing the ladder without whiskers (Video S3/Video S5).

Additionally, animals without whiskers held their snout closer to the rungs on average (R^2adj = 0.59, F(4) = 6.46, p = 0.004, ΔEB = -0.46 cm, ΔSC = -0.42 cm) (Figure 5C), and exhibited significantly more nose tapping behavior (R^2adj = 0.34, F(4) = 6.46, p = 0.002, ΔEB = +3.89 taps, ΔSC = +4.56 taps) (Figure 5D), possibly in order to gain tactile and/or olfactory information. Whisker trimming was also accompanied by an increase in average tail height during correct placements (R^2adj = 0.51, F(4) = 4.95, p = 0.042, ΔEB = +0.90 cm, ΔSC = +0.78 cm) (Figure 5E), and a dramatic increase in crossing time (R^2adj = 0.24, F(4) = 7.672, p = 0.001, ΔEB = +4.86s, ΔSC = +3.40s) (Figure 5F; Figure S3B-F).

To further examine how sighted and blind animals adapted to whisker trimming, we analyzed crossing time in both lighting conditions. Proving an effective control, we found that whisker trimming increased crossing time for early blind animals irrespective of lighting condition (p_{light} = 0.022, p_{dark} = 0.015, ΔEB_{light} = +4.00s, ΔEB_{dark} = +5.86s) (Figure 5F). However, whisker trimming only increased crossing time for sighted controls in the dark, suggesting that whisker-trimmed sighted animals employ the use of visual cues when visual information is available (p_{light} = 0.45, p_{dark} < 0.001, ΔSC_{light} = +1.27s, ΔSC_{dark} = +5.44s) (Figure 5F). These metrics indicate that early blind and sighted animals adopt a conservative strategy to ladder crossing when tactile sensory input from the whiskers is removed, and that sighted animals recruit vision in the absence of whiskers.

Discussion

We quantified the extent to which early vision loss impacts movement strategy and performance on a sensorimotor task involving the spared senses. Our results indicate that early blind (EB) animals have superior performance on the ladder rung task, in part due to increased precision of sensory-guided forelimb placement. Whisker-trimming nullified this advantage, demonstrating that EB animals relied more heavily on input from the whiskers to complete the task than sighted animals (SC). Following whisker trimming, both EB and SC animals adopted similar crossing strategies during the dark condition, but SC animals showed no increase in crossing time in the light condition (while EB animals did), suggesting that sighted animals utilized vision when tactile input from the whiskers was unavailable. We first discuss the increased performance of early blind animals on the ladder rung task and compare this with studies in humans that demonstrate cross-modal behavioral plasticity following the early loss of vision. We then discuss the importance of active sensing with the whiskers for locomotion and navigational tasks. Finally, we explore the underlying neural mechanisms that may subserve these sensorimotor abilities, and how they have been modified following the early loss of vision.

Cross-Modal behavioral plasticity following early loss of vision

Recent data from our laboratory indicates that EB animals are better at making fine tactile discriminations, but show no differences in whisking behavior compared to SC opossums (Ramamurthy et al., 2018; Ramamurthy and Krubitzer, 2018). In the current study, we found that EB opossums could detect rungs and place their limbs more accurately during ladder rung walking than SC opossums. While few other animal studies have been conducted, research in humans has extensively examined the behavioral effects of the early loss of vision. Mainly, these studies have focused on two types of behavior: sensory acuity and spatial information processing. For example, it has been shown that EB individuals have increased auditory and tactile spatial acuity, reacting to auditory and tactile spatial targets quicker than SC without

changes in performance [52,53,54]. Using a somatosensory spatial discrimination task, Wong and colleagues found that EB individuals have higher tactile acuity on the fingers than SC, but tactile discriminations made with the lips were the same in both groups (Wong et al., 2011). EB individuals also have quicker reaction times and increased accuracy on texture, but not shape discrimination tasks (Gurtubay-Antolin and Rodríguez-Fornells, 2017; Schubert et al., 2017; Wan et al., 2010).

Although blind individuals use input from multiple senses to navigate, most studies of navigation in the early blind focus on the auditory system (Bedny et al., 2011; Gizewski et al., 2003; Schinazi et al., 2016) . Given the prevalence of EB individuals who navigate their daily environment with a cane, it is surprising that more research has not been dedicated studying spatial navigation through tactile input. Moreover, studies which do employ tactile information to study spatial information processing in the blind often used reaction time, and measured spatial acuity based on stimulus detection only (Fiehler and Rösler, 2010; Leo et al., 2012; Ricciardi et al., 2014). That is, participants in these studies only had to detect a spatial stimulus but were not required to reach toward or touch the target, neglecting potential differences in movement strategy and motor performance.

An important contribution of the present study is that we not only look at performance, but also quantify the strategy adopted by our different groups when performing the ladder rung task. In a recent review, Schinazi and colleagues stress the importance of studying the relationship between strategy and performance in uncovering differences in spatial navigation abilities between congenitally blind and sighted humans (Schinazi et al., 2016). In our study, EB opossums had to detect an upcoming rung, accurately place their forelimb on the rung, and maintain a spatial representation of that rung in order to ensure accurate hindlimb placement. We found that EB opossums had greater precision in targeting upcoming rungs with both the fore- and hind limbs while showing minor differences in limb trajectory. This superior performance was presumably due to input from the spared senses, such as the whiskers. When

this spared sensory input was removed by trimming the whiskers, both EB and SC animals adopted similar crossing strategies, but EB animals showed greater deficits in performance and posture.

Information on the location and distance of gaps is usually provided by the whiskers (Arkley et al., 2017); however, both blind and sighted animals adjusted to whisker trimming by using somatic and possibly olfactory input from the nose, shown by a two-fold increase in nose-tapping behavior. Interestingly, a recent study in rats found that whisker-trimmed animals also used nose-tapping to detect the location of the reach slit during a single-pellet reaching task (Parmiani et al., 2018).

Further quantification of body posture showed that animals in both groups adapted to whisker trimming by taking a more cautious approach - illustrated by a truncated stride length and shortened distance between the snout and forelimb, as well as increased crossing time in most conditions. Of note is that whisker trimming did not cause a significant increase in crossing time for sighted opossums in the light condition, while crossing time did increase for SC in the dark condition, indicating that SC animals may have used the visual system to perform this task when the whiskers were removed. In agreement with Shinazi and colleagues, our results show the importance of studying both performance and strategy, as one or the other may be altered depending on the available sensory information. In our case, without tactile information from the whiskers, EB opossums qualitatively resembled a blind human trying to navigate without a cane, and SC opossums resembled a sighted human trying to navigate in the dark.

Whiskers guide forelimb movements in whisking mammals

Active sensing with the whisker system has been shown to be critical for many animals to detect walls and objects, and is thought to directly guide forelimb placement during locomotion (Arkley et al., 2017, 2014; Grant et al., 2013, 2009; Mitchinson et al., 2007). In the current study, we found that whisker trimming resulted in impairments in sensory-guided

stepping during ladder crossing, regardless of whether opossums were blind or sighted. These results add support to the prevailing theory that whisking is fundamental for guiding limb placement. First and foremost, we found that animals without whiskers had increased forelimb error, but not hindlimb error. Second, in agreement with work on precision stepping in cats and rats (Drew and Marigold, 2015; Whitlock, 2014), where spatial information from the forelimb informs the future trajectory of the hindlimb (by encoding the height and location of obstacles), we found that whisker trimming altered the height of both the forelimb and hindlimb. While both groups of animals exhibited a reduction in forelimb and hindlimb peak height due to whisker trimming, this occurred to a greater extent in EB animals. Moreover, hindlimb trajectory, but not performance, was altered by whisker trimming. Third, recent research in rats has shown that whisker trimming results in increased variation in limb kinematics during locomotion on a continuous substrate (Niederschuh et al., 2015). Similarly, we found that whisker trimming resulted in more variable forelimb movements during the retraction, but not extension phase of the trajectory. We believe the retraction phase to be associated with sensing an upcoming rung, as the nose oscillates vertically during correct placements. While we did not find notable differences in the periodicity of nose oscillations (data not shown), future studies that directly examine the relationship between whisking frequency/contact and forelimb placement will shed light on this aspect of locomotor control. Regardless, increased variance in the retraction but not extension phase may indicate increased hesitation when opossums are detecting an upcoming rung's position, but once located, can make a precise placement.

Across metrics, we found that EB animals show a trend for lower variation. While this speaks to the increased precision of whisker-guided forelimb movements in blind opossums, we cannot rule out visual input altering attention in sighted animals. Nevertheless, in the presence or absence of vision, forelimb movement types cluster into similar stereotyped movements. On the other hand, we found that the absence of whiskers forces forelimb placement trajectories to conform to similarly stereotyped movements in blind and sighted opossums. Thus, it was the

loss of whiskers, and not the loss of vision, that impacted the produced stereotyped forelimb movements.

Neural mechanisms that may subserve adaptive cross modal behavioral plasticity

Following the early loss of vision, cortical areas associated with both the lost sense as well as spared sensory systems are profoundly affected. In EB mice, rats, and cats, the connections of primary visual cortex are drastically altered, such that cortico-cortical projections from somatosensory and auditory areas densely project to what would have been visual cortex (Berman, 1991; Dye et al., 2012; Laemle et al., 2006; Négyessy et al., 2000). Studies in our laboratory demonstrate that in enucleated opossums, V1 receives input from somatosensory areas of the cortex and thalamus, and that cortical connections of S1 are altered as well (Dooley and Krubitzer, 2019; Karlen et al., 2006). Similar to studies in animal models, indirect measures of connectivity such as resting state fMRI and DTI in EB humans show that S1 is more densely connected (correlated) with V1, and that posterior parietal cortex exhibits denser projections with sensory areas as well (Klinge et al., 2010; Liu et al., 2007; Ptito et al., 2008, 2005; Shu et al., 2009; Wittenberg et al., 2004).

Functional changes accompany these anatomical changes in early blind animals and humans. Visually deprived mice and rats have altered excitatory synaptic function in V1, and neurons in a large proportion of the reorganized primary visual cortex respond to auditory stimuli (Goel et al., 2006; Piché et al., 2007; Zheng et al., 2014). In early blind *Monodelphis*, all of what would be visual cortex (V1) is co-opted by the somatosensory and auditory system (Kahn and Krubitzer, 2002). While the functional organization of posterior areas in parietal cortex has not been extensively explored in *Monodelphis*, research in rats and cats shows that activity in posterior parietal cortex increases before and during gait modifications (Beloozerova and Sirota, 2003; Whitlock, 2014). Importantly, in blind rats, neurotoxic lesions to posterior parietal cortex cause deficits in spatial memory during maze-running (Pinto-Hamuy et al., 2004). Functional

changes due to early vision loss have been extensively studied in humans. In EB individuals, V1 is activated during somato-motor tasks involving the hands (Gizewski et al., 2003), and during tasks involving memory, spatial processing, and language (Amedi et al., 2003; Bedny et al., 2011; Ricciardi et al., 2014). Visual cortex is also activated by guided hand motions, regardless of whether participants are SC or EB (Fiehler and Rösler, 2010). Further, in congenitally blind humans, posterior parietal cortex retains its role as an encoder of the spatial position of a reach target and shows increased integration of tactile information (through variability of the BOLD signal) in participants completing a tactile spatial discrimination task (Leo et al., 2012; Lingnau et al., 2014).

Taken together, studies in animal models and humans demonstrate that visual cortex is not dysfunctional in the absence of vision, but instead contributes to a number of behaviors including tactile and spatial processing (for review: Ricciardi et al., 2014). These studies also suggest that superior performance on tactile discriminations may be due to changes in the structure and function of somatosensory and posterior parietal cortices. Given previous data from our laboratory in EB opossums showing: 1) a somatosensory-driven reorganization of V1, 2) dense projections from somatosensory cortex to V1 and thalamic motor nuclei, 3) alterations in neural response properties in the whisker representation in S1, and 4) increased connections between S1 and posterior parietal cortex, we posit that these neural changes could support the heightened abilities of EB opossums observed in this study, and also explain the extreme detriments to performance when the whiskers were trimmed. While we have focused on the cortical mechanisms that may account for differences in performance between EB and SC animals, it is possible that subcortical changes as well as alteration in the morphology of the whiskers may contribute to differences in performance, as seen in visually deprived mice and cats who have increased diameters of macro-vibrissae (Rauschecker et al., 1992). It may also be possible that EB animals are more efficient in their acquisition of sensory information through differences in whisker movement. Previous data from our laboratory indicates this is not the

case, as EB and SC *Monodelphis* have similar whisker set-points and whisking frequencies (Ramamurthy and Krubitzer, 2018). Research in functionally blind rats with similar results adds support for EB animals having heightened sensory coding versus heightened sensory acquisition (Arkley et al., 2014). These data have implications for congenitally blind humans, suggesting that sensory substitution devices which rely on tactile input, and behavioral therapies which involve the rapid acquisition of spatial information through tactile input, will be effective in increasing the ability of EB individuals to navigate in a complex environment.

Limitations of the Study

A concern of the present study is that we do not directly show that cross-modal changes in the brain due to the early loss of vision are responsible for the observed heighted performance of EB animals. While we do not claim causation, decades of prior research from our laboratory in the same experimental model, and the rigorous quantification of behavioral strategy, posture, and performance in the present study, support the hypothesis that cross-modal changes to the brain due to the early loss of vision lead to enhanced sensorimotor performance on tasks involving the spared senses. The present study describes the phenomena that allows future work, through targeted inactivation experiments, to probe the individual contributions of cross-modal changes to S1, V1, and PPC to sensorimotor behavior.

Another limitation of this study was that we did not quantify how opossums grasped each rung or how whisker movements preceded forelimb movements. We believe both of these aspects of behavior to be critical for locomotion in whisking mammals but chose to focus on macro-scale aspects of body posture, as neither had been described before. Previous research in blind rats, and recent data from our laboratory in EB opossums, shows that there is no difference in active whisking between blind and sighted animals (Arkley et al., 2014; Ramamurthy and Krubitzer, 2018). However, we note that possible differences in whisking behavior could exist, as this task causes constant changes in head and limb positioning. Future

research on how forelimb trajectories match the frequency of whisking will elucidate how the whiskers guide individual movements.

A third limitation of this study was our use of a 660nm lamp. While this is outside the range of sensitivity for even the longest wavelength cone that *Monodelphis* possesses (**λ** = 500 - 570nm), we cannot completely rule out that rods did not capture any light. In *Monodelphis*, the retinal rod pathway has sensitivity ranges between 400-600nm, and closely resembles that of placental mammals (Bowmaker and Dartnall, 1980; Hunt et al., 2009; Lutz et al., 2018). However, peak lamp power at 660nm does not mean there is no detectable illumination outside of the detectable range for *Monodelphis*, and therefore it is likely that opossums did receive some form of visual input from this low energy light – yet performance data from pilot experiments (see Transparent Methods) found no difference in total error whether the lamp was on or off. Testing the illuminance of the red lamp at the ladder apparatus also revealed extremely low-energy light. Therefore, we find it unlikely that form-vision via rods contributed to sighted animals' ability to cross the apparatus in the dark. While well-studied in primates, future studies in rodents which quantify how eye movements are related to forelimb control will elucidate if active vision guides forelimb control in whisking animals, as this is currently thought to rely on olfactory and somatosensory cues alone (Klein et al., 2012).

Resource Availability

Lead contact:

Further information and requests for resources should be directed to and will be fulfilled by the Lead Contact, Leah Krubitzer (lakrubitzer@ucdavis.edu)

Data and Code Availability:

The datasets and code generated during this study are available at:
https://www.github.com/maceng4/Monodelphis_Ladder_Rung

ACKNOWLEDGEMENTS

Thanks to Dr. Andrew Fox and Dr. Eliza Bliss-Moreau for providing consultation on statistical measures and python scripts. Thanks to Cynthia Weller, Heather Dodson, and Carly Jones for assistance with data collection; and to Dr. Andrew Halley, Dr. Deepa Ramamurthy, Dr. Chris Bresee, and Carlos Pineda for manuscript comments. This research was supported by the McDonnell Foundation (Grant 220020516 to L.A.K).

AUTHOR CONTRIBUTIONS

Conceptualization, M.E, L.A.K. Methodology, M.E; Investigation, M.E, S.F, C.I, and L.A.K.; Writing and Editing, M.E, L.A.K; Funding Acquisition, L.A.K; Supervision, L.A.K.

DECLARATION OF INTERESTS

No competing interests declared.

REFERENCES

Abbruzzese, G., Berardelli, A., 2003. Sensorimotor integration in movement disorders. Movement Disorders 18, 231–240. https://doi.org/10.1002/mds.10327
Amedi, A., Raz, N., Pianka, P., Malach, R., Zohary, E., 2003. Early 'visual' cortex activation correlates with superior verbal memory performance in the blind. Nature Neuroscience 6, 758–766. https://doi.org/10.1038/nn1072
Antonow-Schlorke, I., Ehrhardt, J., Knieling, M., 2013. Modification of the Ladder Rung Walking Task—New Options for Analysis of Skilled Movements. Stroke Res Treat 2013. https://doi.org/10.1155/2013/418627

Arkley, K., Grant, R.A., Mitchinson, B., Prescott, T.J., 2014. Strategy Change in Vibrissal Active Sensing during Rat Locomotion. Current Biology 24, 1507–1512. https://doi.org/10.1016/j.cub.2014.05.036
Arkley, K., Tiktak, G.P., Breakell, V., Prescott, T.J., Grant, R.A., 2017. Whisker touch guides canopy exploration in a nocturnal, arboreal rodent, the Hazel dormouse (Muscardinus avellanarius). J Comp Physiol A 203, 133–142. https://doi.org/10.1007/s00359-017-1146-z
Bedny, M., Pascual-Leone, A., Dodell-Feder, D., Fedorenko, E., Saxe, R., 2011. Language processing in the occipital cortex of congenitally blind adults. PNAS 108, 4429–4434. https://doi.org/10.1073/pnas.1014818108
Bell, L., Wagels, L., Neuschaefer-Rube, C., Fels, J., Gur, R.E., Konrad, K., 2019. The Cross-Modal Effects of Sensory Deprivation on Spatial and Temporal Processes in Vision and Audition: A Systematic Review on Behavioral and Neuroimaging Research since 2000 [WWW Document]. Neural Plasticity. https://doi.org/10.1155/2019/9603469
Beloozerova, I.N., Sirota, M.G., 2003. Integration of Motor and Visual Information in the Parietal Area 5 During Locomotion. Journal of Neurophysiology 90, 961–971. https://doi.org/10.1152/jn.01147.2002
Berman, N.E.J., 1991. Alterations of visual cortical connections in cats following early removal of retinal input. Developmental Brain Research 63, 163–180. https://doi.org/10.1016/0165-3806(91)90076-U
Bock, A.S., Olavarria, J.F., 2011. Neonatal enucleation during a critical period reduces the precision of cortico-cortical projections in visual cortex. Neuroscience Letters 501, 152–156. https://doi.org/10.1016/j.neulet.2011.07.005
Bowmaker, J.K., Dartnall, H.J., 1980. Visual pigments of rods and cones in a human retina. The Journal of Physiology 298, 501–511. https://doi.org/10.1113/jphysiol.1980.sp013097
Cecchetti, L., Kupers, R., Ptito, M., Pietrini, P., Ricciardi, E., 2016. Are Supramodality and Cross-Modal Plasticity the Yin and Yang of Brain Development? From Blindness to Rehabilitation. Front. Syst. Neurosci. 10. https://doi.org/10.3389/fnsys.2016.00089
Collignon, O., De Volder, A.G., 2009. Further evidence that congenitally blind participants react faster to auditory and tactile spatial targets. Can J Exp Psychol 63, 287–293. https://doi.org/10.1037/a0015415
Collignon, O., Voss, P., Lassonde, M., Lepore, F., 2009. Cross-modal plasticity for the spatial processing of sounds in visually deprived subjects. Exp Brain Res 192, 343–358. https://doi.org/10.1007/s00221-008-1553-z
Dooley, J.C., Krubitzer, L.A., 2019. Alterations in cortical and thalamic connections of somatosensory cortex following early loss of vision. J Comp Neurol 527, 1675–1688. https://doi.org/10.1002/cne.24582
Drew, T., Marigold, D.S., 2015. Taking the next step: cortical contributions to the control of locomotion. Current Opinion in Neurobiology 33, 25–33. https://doi.org/10.1016/j.conb.2015.01.011
Dye, C.A., Abbott, C.W., Huffman, K.J., 2012. Bilateral enucleation alters gene expression and intraneocortical connections in the mouse. Neural Development 7, 5. https://doi.org/10.1186/1749-8104-7-5
Englund, M., Faridjoo, S., Iyer, C., Krubitzer, L.A., 2018. Early loss of vision leads to enhanced performance on tactilely mediated behaviors in the short-tailed opossum (monodelphis domestica). Society for Neuroscience Abstracts.
Ferezou, I., Haiss, F., Gentet, L.J., Aronoff, R., Weber, B., Petersen, C.C.H., 2007. Spatiotemporal Dynamics of Cortical Sensorimotor Integration in Behaving Mice. Neuron 56, 907–923. https://doi.org/10.1016/j.neuron.2007.10.007
Fiehler, K., Rösler, F., 2010. Plasticity of multisensory dorsal stream functions: Evidence from congenitally blind and sighted adults. Restorative Neurology and Neuroscience 28, 193–205. https://doi.org/10.3233/RNN-2010-0500

Gagnon, L., Schneider, F.C., Siebner, H.R., Paulson, O.B., Kupers, R., Ptito, M., 2012. Activation of the hippocampal complex during tactile maze solving in congenitally blind subjects. Neuropsychologia 50, 1663–1671. https://doi.org/10.1016/j.neuropsychologia.2012.03.022
Gizewski, E.R., Gasser, T., de Greiff, A., Boehm, A., Forsting, M., 2003. Cross-modal plasticity for sensory and motor activation patterns in blind subjects. NeuroImage 19, 968–975. https://doi.org/10.1016/S1053-8119(03)00114-9
Goel, A., Jiang, B., Xu, L.W., Song, L., Kirkwood, A., Lee, H.-K., 2006. Cross-modal regulation of synaptic AMPA receptors in primary sensory cortices by visual experience. Nature Neuroscience 9, 1001–1003. https://doi.org/10.1038/nn1725
Grant, R.A., Haidarliu, S., Kennerley, N.J., Prescott, T.J., 2013. The evolution of active vibrissal sensing in mammals: evidence from vibrissal musculature and function in the marsupial opossum Monodelphis domestica. Journal of Experimental Biology 216, 3483–3494. https://doi.org/10.1242/jeb.087452
Grant, R.A., Mitchinson, B., Fox, C.W., Prescott, T.J., 2009. Active Touch Sensing in the Rat: Anticipatory and Regulatory Control of Whisker Movements During Surface Exploration. J Neurophysiol 101, 862–874. https://doi.org/10.1152/jn.90783.2008
Gurtubay-Antolin, A., Rodríguez-Fornells, A., 2017. Neurophysiological evidence for enhanced tactile acuity in early blindness in some but not all haptic tasks. NeuroImage 162, 23–31. https://doi.org/10.1016/j.neuroimage.2017.08.054
Hallgren, K.A., 2012. Computing Inter-Rater Reliability for Observational Data: An Overview and Tutorial. TQMP 8, 23–34. https://doi.org/10.20982/tqmp.08.1.p023
Hunt, D.M., Chan, J., Carvalho, L.S., Hokoc, J.N., Ferguson, M.C., Arrese, C.A., Beazley, L.D., 2009. Cone visual pigments in two species of South American marsupials. Gene 433, 50–55. https://doi.org/10.1016/j.gene.2008.12.006
Izraeli, R., Koay, G., Lamish, M., Heicklen-Klein, A.J., Heffner, H.E., Heffner, R.S., Wollberg, Z., 2002. Cross-modal neuroplasticity in neonatally enucleated hamsters: structure, electrophysiology and behaviour. European Journal of Neuroscience 15, 693–712. https://doi.org/10.1046/j.1460-9568.2002.01902.x
Jacobs, B.Y., Kloefkorn, H.E., Allen, K.D., 2014. Gait Analysis Methods for Rodent Models of Osteoarthritis. Curr Pain Headache Rep 18, 456. https://doi.org/10.1007/s11916-014-0456-x
Kahn, D.M., Krubitzer, L., 2002. Massive cross-modal cortical plasticity and the emergence of a new cortical area in developmentally blind mammals. Proc Natl Acad Sci U S A 99, 11429–11434. https://doi.org/10.1073/pnas.162342799
Karlen, S.J., Kahn, D.M., Krubitzer, L., 2006. Early blindness results in abnormal corticocortical and thalamocortical connections. Neuroscience 142, 843–858. https://doi.org/10.1016/j.neuroscience.2006.06.055
Karlen, S.J., Krubitzer, L., 2009. Effects of Bilateral Enucleation on the Size of Visual and Nonvisual Areas of the Brain. Cerebral Cortex 19, 1360–1371. https://doi.org/10.1093/cercor/bhn176
Klein, A., Sacrey, L.-A.R., Whishaw, I.Q., Dunnett, S.B., 2012. The use of rodent skilled reaching as a translational model for investigating brain damage and disease. Neurosci Biobehav Rev 36, 1030–1042. https://doi.org/10.1016/j.neubiorev.2011.12.010
Klinge, C., Eippert, F., Röder, B., Büchel, C., 2010. Corticocortical connections mediate primary visual cortex responses to auditory stimulation in the blind. J. Neurosci. 30, 12798–12805. https://doi.org/10.1523/JNEUROSCI.2384-10.2010
Kozanian, O.O., Abbott, C.W., Huffman, K.J., 2015. Rapid Changes in Cortical and Subcortical Brain Regions after Early Bilateral Enucleation in the Mouse. PLoS ONE 10, e0140391. https://doi.org/10.1371/journal.pone.0140391
Kupers, R., Ptito, M., 2014. Compensatory plasticity and cross-modal reorganization following early visual deprivation. Neuroscience & Biobehavioral Reviews, Multisensory integration,

sensory substitution and visual rehabilitation 41, 36–52. https://doi.org/10.1016/j.neubiorev.2013.08.001
Laemle, L.K., Strominger, N.L., Carpenter, D.O., 2006. Cross-modal innervation of primary visual cortex by auditory fibers in congenitally anophthalmic mice. Neuroscience Letters 396, 108–112. https://doi.org/10.1016/j.neulet.2005.11.020
Laing, R.J., Bock, A.S., Lasiene, J., Olavarria, J.F., 2012. Role of retinal input on the development of striate–extrastriate patterns of connections in the rat. Journal of Comparative Neurology 520, 3256–3276. https://doi.org/10.1002/cne.23096
Leo, A., Bernardi, G., Handjaras, G., Bonino, D., Ricciardi, E., Pietrini, P., 2012. Increased BOLD Variability in the Parietal Cortex and Enhanced Parieto-Occipital Connectivity during Tactile Perception in Congenitally Blind Individuals. Neural Plasticity 2012, 1–8. https://doi.org/10.1155/2012/720278
Lingnau, A., Strnad, L., He, C., Fabbri, S., Han, Z., Bi, Y., Caramazza, A., 2014. Cross-Modal Plasticity Preserves Functional Specialization in Posterior Parietal Cortex. Cerebral Cortex 24, 541–549. https://doi.org/10.1093/cercor/bhs340
Liu, Y., Yu, C., Liang, M., Li, J., Tian, L., Zhou, Y., Qin, W., Li, K., Jiang, T., 2007. Whole brain functional connectivity in the early blind. Brain 130, 2085–2096. https://doi.org/10.1093/brain/awm121
Lutz, N.D., Lemes, E., Krubitzer, L., Collin, S.P., Haverkamp, S., Peichl, L., 2018. The rod signaling pathway in marsupial retinae. PLOS ONE 13, e0202089. https://doi.org/10.1371/journal.pone.0202089
Mathis, A., Mamidanna, P., Cury, K.M., Abe, T., Murthy, V.N., Mathis, M.W., Bethge, M., 2018. DeepLabCut: markerless pose estimation of user-defined body parts with deep learning. Nat Neurosci 21, 1281–1289. https://doi.org/10.1038/s41593-018-0209-y
McVea, D.A., Taylor, A.J., Pearson, K.G., 2009. Long-Lasting Working Memories of Obstacles Established by Foreleg Stepping in Walking Cats Require Area 5 of the Posterior Parietal Cortex. J. Neurosci. 29, 9396–9404. https://doi.org/10.1523/JNEUROSCI.0746-09.2009
Metz, G.A., Whishaw, I.Q., 2009. The Ladder Rung Walking Task: A Scoring System and its Practical Application. JoVE 1204. https://doi.org/10.3791/1204
Metz, G.A., Whishaw, I.Q., 2002. Cortical and subcortical lesions impair skilled walking in the ladder rung walking test: a new task to evaluate fore- and hindlimb stepping, placing, and co-ordination. Journal of Neuroscience Methods 115, 169–179. https://doi.org/10.1016/S0165-0270(02)00012-2
Mitchinson, B., Grant, R.A., Arkley, K., Rankov, V., Perkon, I., Prescott, T.J., 2011. Active vibrissal sensing in rodents and marsupials. Philos Trans R Soc Lond B Biol Sci 366, 3037–3048. https://doi.org/10.1098/rstb.2011.0156
Mitchinson, B., Martin, C.J., Grant, R.A., Prescott, T.J., 2007. Feedback control in active sensing: rat exploratory whisking is modulated by environmental contact. Proc Biol Sci 274, 1035–1041. https://doi.org/10.1098/rspb.2006.0347
Moss, C.F., Surlykke, A., 2010. Probing the Natural Scene by Echolocation in Bats. Front. Behav. Neurosci. 4. https://doi.org/10.3389/fnbeh.2010.00033
Négyessy, L., Gál, V., Farkas, T., Toldi, J., 2000. Cross-modal plasticity of the corticothalamic circuits in rats enucleated on the first postnatal day. European Journal of Neuroscience 12, 1654–1668. https://doi.org/10.1046/j.1460-9568.2000.00057.x
Niederschuh, S.J., Witte, H., Schmidt, M., 2015. The role of vibrissal sensing in forelimb position control during travelling locomotion in the rat (Rattus norvegicus, Rodentia). Zoology 118, 51–62. https://doi.org/10.1016/j.zool.2014.09.003
Parmiani, P., Lucchetti, C., Franchi, G., 2018. Whisker and Nose Tactile Sense Guide Rat Behavior in a Skilled Reaching Task. Front Behav Neurosci 12. https://doi.org/10.3389/fnbeh.2018.00024

Piché, M., Chabot, N., Bronchti, G., Miceli, D., Lepore, F., Guillemot, J.-P., 2007. Auditory responses in the visual cortex of neonatally enucleated rats. Neuroscience 145, 1144–1156. https://doi.org/10.1016/j.neuroscience.2006.12.050
Pinto-Hamuy, T., Montero, V.M., Torrealba, F., 2004. Neurotoxic lesion of anteromedial/posterior parietal cortex disrupts spatial maze memory in blind rats. Behavioural Brain Research 153, 465–470. https://doi.org/10.1016/j.bbr.2004.01.003
Ptito, M., Moesgaard, S.M., Gjedde, A., Kupers, R., 2005. Cross-modal plasticity revealed by electrotactile stimulation of the tongue in the congenitally blind. Brain 128, 606–614. https://doi.org/10.1093/brain/awh380
Ptito, M., Schneider, F.C.G., Paulson, O.B., Kupers, R., 2008. Alterations of the visual pathways in congenital blindness. Exp Brain Res 187, 41–49. https://doi.org/10.1007/s00221-008-1273-4
Ramamurthy, D.L., Englund, M., Krubitzer, L.A., 2018. Alterations in somatosensory receptive fields following early blindness are shaped by the environment. Society for Neuroscience Abstracts.
Ramamurthy, D.L., Krubitzer, L.A., 2018. Neural Coding of Whisker-Mediated Touch in Primary Somatosensory Cortex Is Altered Following Early Blindness. J. Neurosci. 38, 6172–6189. https://doi.org/10.1523/JNEUROSCI.0066-18.2018
Rauschecker, J.P., 1995. Compensatory plasticity and sensory substitution in the cerebral cortex. Trends in Neurosciences 18, 36–43. https://doi.org/10.1016/0166-2236(95)93948-W
Rauschecker, J.P., Tian, B., Korte, M., Egert, U., 1992. Crossmodal changes in the somatosensory vibrissa/barrel system of visually deprived animals. Proceedings of the National Academy of Sciences 89, 5063–5067. https://doi.org/10.1073/pnas.89.11.5063
Renier, L., De Volder, A.G., Rauschecker, J.P., 2014. Cortical plasticity and preserved function in early blindness. Neuroscience & Biobehavioral Reviews, Multisensory integration, sensory substitution and visual rehabilitation 41, 53–63. https://doi.org/10.1016/j.neubiorev.2013.01.025
Ricciardi, E., Bonino, D., Pellegrini, S., Pietrini, P., 2014. Mind the blind brain to understand the sighted one! Is there a supramodal cortical functional architecture? Neuroscience & Biobehavioral Reviews, Multisensory integration, sensory substitution and visual rehabilitation 41, 64–77. https://doi.org/10.1016/j.neubiorev.2013.10.006
Schinazi, V.R., Thrash, T., Chebat, D.-R., 2016. Spatial navigation by congenitally blind individuals. WIREs Cognitive Science 7, 37–58. https://doi.org/10.1002/wcs.1375
Schönfeld, L.-M., Dooley, D., Jahanshahi, A., Temel, Y., Hendrix, S., 2017. Evaluating rodent motor functions: Which tests to choose? Neuroscience & Biobehavioral Reviews 83, 298–312. https://doi.org/10.1016/j.neubiorev.2017.10.021
Schubert, J.T.W., Badde, S., Röder, B., Heed, T., 2017. Task demands affect spatial reference frame weighting during tactile localization in sighted and congenitally blind adults. PLoS ONE 12, e0189067. https://doi.org/10.1371/journal.pone.0189067
Seelke, A.M.H., Dooley, J.C., Krubitzer, L.A., 2014. Photic preference of the short-tailed opossum (Monodelphis domestica). Neuroscience 269, 273–280. https://doi.org/10.1016/j.neuroscience.2014.03.057
Shu, N., Liu, Y., Li, J., Li, Y., Yu, C., Jiang, T., 2009. Altered Anatomical Network in Early Blindness Revealed by Diffusion Tensor Tractography. PLoS One 4. https://doi.org/10.1371/journal.pone.0007228
Syakur, M.A., Khotimah, B.K., Rochman, E.M.S., Satoto, B.D., 2018. Integration K-Means Clustering Method and Elbow Method For Identification of The Best Customer Profile Cluster. IOP Conf. Ser.: Mater. Sci. Eng. 336, 012017. https://doi.org/10.1088/1757-899X/336/1/012017
Toldi, J., Farkas, T., Völgyi, B., 1994. Neonatal enucleation induces cross-modal changes in the barrel cortex of rat. A behavioural and electrophysiological study. Neuroscience Letters 167, 1–4. https://doi.org/10.1016/0304-3940(94)91014-6

Toldi, J., Feher, O., Joo, F., Antal, A., Wolff, J.R., 1990. Sodium bromide treatment influences the plasticity of somatosensory responses in the rat cortex as induced by enucleation. Neuroscience 37, 675–683. https://doi.org/10.1016/0306-4522(90)90098-O
Wan, C.Y., Wood, A.G., Reutens, D.C., Wilson, S.J., 2010. Congenital blindness leads to enhanced vibrotactile perception. Neuropsychologia 48, 631–635. https://doi.org/10.1016/j.neuropsychologia.2009.10.001
Whitlock, J.R., 2014. Navigating actions through the rodent parietal cortex. Front. Hum. Neurosci. 8. https://doi.org/10.3389/fnhum.2014.00293
Wittenberg, G.F., Werhahn, K.J., Wassermann, E.M., Herscovitch, P., Cohen, L.G., 2004. Functional connectivity between somatosensory and visual cortex in early blind humans. European Journal of Neuroscience 20, 1923–1927. https://doi.org/10.1111/j.1460-9568.2004.03630.x
Wong, M., Gnanakumaran, V., Goldreich, D., 2011. Tactile spatial acuity enhancement in blindness: evidence for experience-dependent mechanisms. J. Neurosci. 31, 7028–7037. https://doi.org/10.1523/JNEUROSCI.6461-10.2011
Zheng, J.-J., Li, S.-J., Zhang, X.-D., Miao, W.-Y., Zhang, D., Yao, H., Yu, X., 2014. Oxytocin mediates early experience–dependent cross-modal plasticity in the sensory cortices. Nature Neuroscience 17, 391–399. https://doi.org/10.1038/nn.3634
Zhou, H.B., Gao, J.T., 2014. Automatic Method for Determining Cluster Number Based on Silhouette Coefficient [WWW Document]. Advanced Materials Research. https://doi.org/10.4028/www.scientific.net/AMR.951.227

FIGURES:

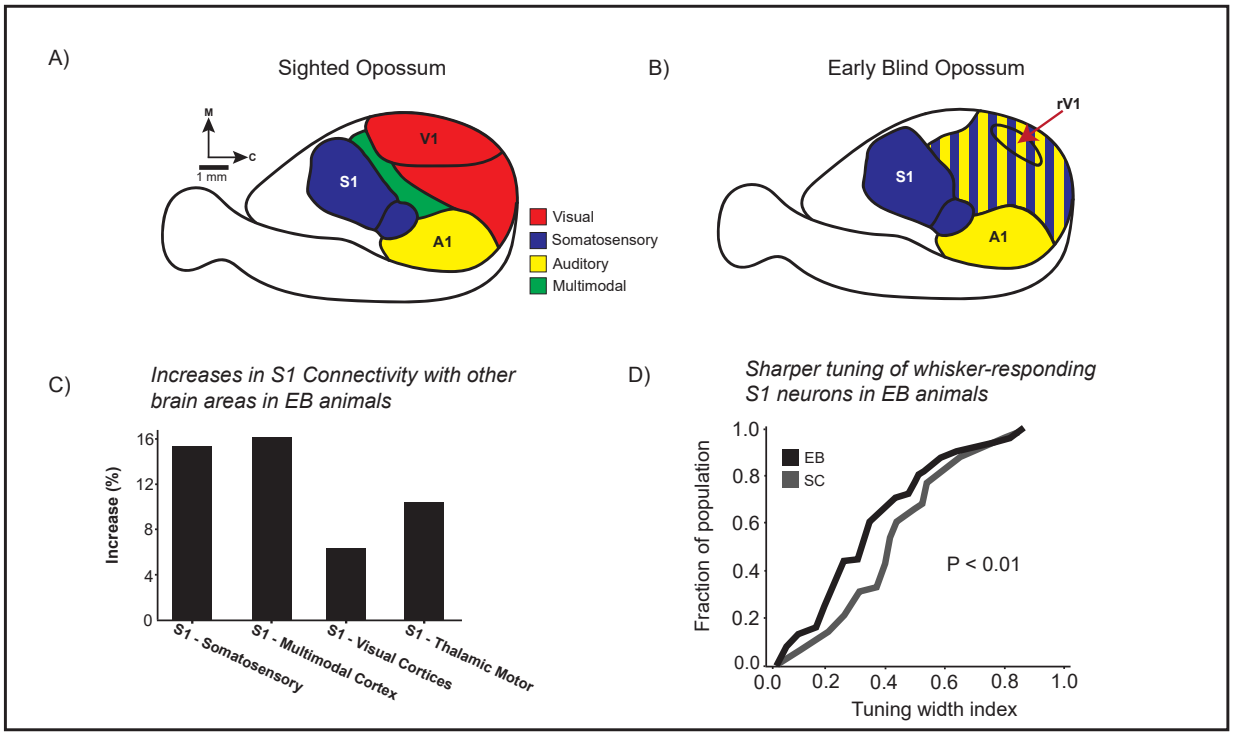

Figure 1. The early loss of vision results in drastic changes to the neocortex. (A) Previous experiments from our laboratory show that a large portion of the Monodelphis neocortex responds to visual (red) and somatosensory (blue) cues. (B) In P4 early blind animals, visual cortex is reorganized by the somatosensory and auditory system (rV1). (C) This is accompanied by an increase in connectivity between S1 and other somatosensory cortices (S1-S2/SR/SC), as well as between S1 and multimodal cortex (S1-MM), visual cortices (S1-V1/CT), and thalamic motor nuclei (S1-VL/VA). (D) Within somatosensory cortex, whisker responding neurons are more sharply tuned in EB (black) compared to SC animals (grey). Abbreviations: primary somatosensory cortex (S1), secondary somatosensory cortex (S2), caudal somatosensory area (SC), rostral somatosensory area (SR), multimodal cortex (MM), primary visual cortex (V1), caudal temporal area (CT), ventral lateral (VL) and ventral anterior (VA)

nuclei of the thalamus. Figures adapted from Kahn and Krubitzer 2006, Dooley and Krubitzer 2018, and Ramamurthy and Krubitzer 2018.

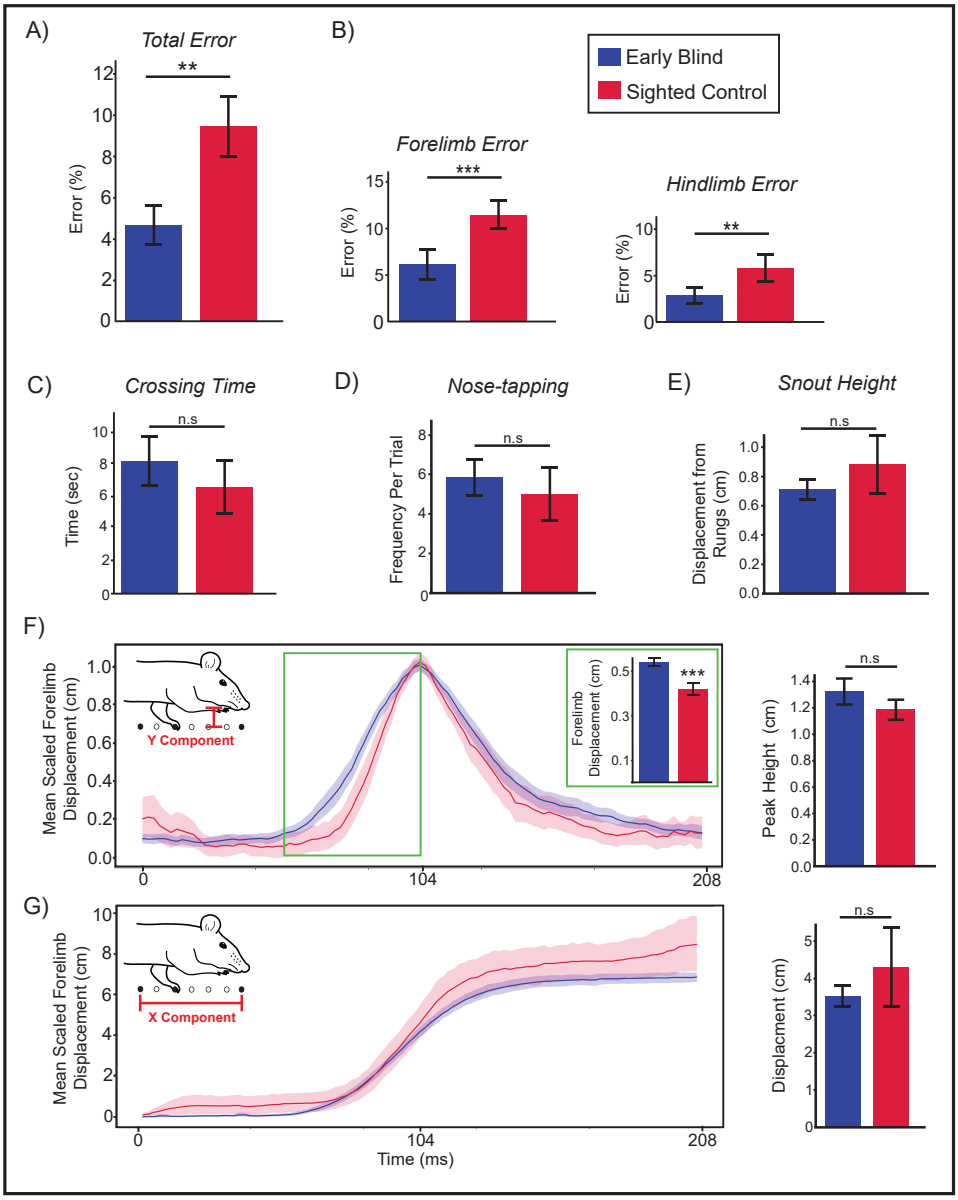

Figure 2. Early blind opossums outperform sighted controls in variable ladder rung walking, but show similarities in crossing strategy. (A) Bar graphs showing that early blind opossums commit significantly less error than sighted opossums ($p = 0.007$). (B) Bar graphs of average forelimb and hindlimb error. On average, early blind animals commit significantly less forelimb ($p = 0.004$) and hindlimb ($p = 0.008$) error than sighted controls. (C) We found no

significant difference in crossing time ($p = 0.27$), (D) average number of nose-taps per trial ($p = 0.626$), or (E) snout height during correct forelimb placements between conditions ($p = 0.806$). (F) Line graphs depicting the average y-component (step height) of forelimb trajectories during correct placements (n = 99 EB; 56 SC) of 8 animals (n = 4 EB; n = 4 SC), scaled by average peak height per animal (inset image, left panel). The green square and inset bar graph denotes the region of non-overlap of 95% confidence intervals, where early blind animals are quicker to lift their right forelimb off of a rung ($p < 0.001$). Bar graph shows quantification of average y-component forelimb trajectory as average peak height (right). Note: bar graph does not include scaling to illustrate there is no statistical difference in peak height between conditions prior to scaling ($p = 0.267$). (G) Line graphs depicting forelimb displacement in the x-direction (stride length). Quantification of average displacement shows no difference in the average x-component of forelimb movement between early blind and sighted opossums ($p = 0.405$) (right). All statistical tests were calculated using linear models (see Transparent Methods: reduced model). (* $p < .05$, ** $p < .01$, *** $p < .001$, n.s = $p > .05$). Bar graphs are presented as between-group averages. Error bars are presented as 95% bootstrapped confidence intervals. See also Figure S1.

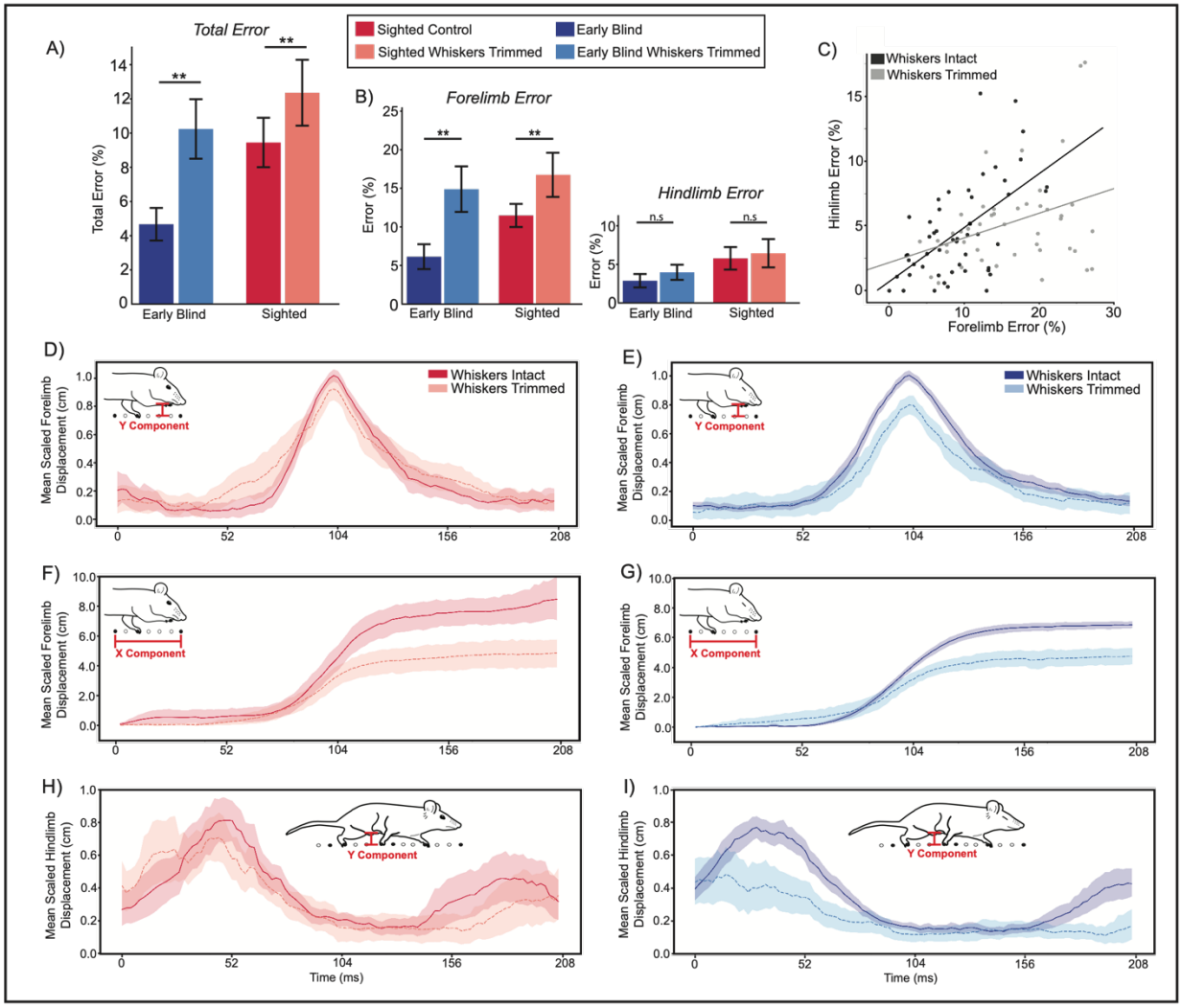

Figure 3. Whisker trimming causes deficits in performance in forelimb but not hindlimb placement. Performance deficits and limb trajectories are altered to greater extents in early blind animals. (A) Bar graph showing average total error before and after whisker trimming in early blind (blue) and sighted (red) opossums. Whisker-trimmed averages are represented by lighter shades (early blind whisker-trimmed: light blue; sighted whisker-trimmed: light red). A main effect was found for the presence of whiskers on performance ($p = 0.004$), with whisker trimming leading to increases in error. (B) Forelimb (left) and hindlimb (right) error

before and after whisker trimming. Collapsing across lighting condition, the reduced model shows a significant main effect for increases in forelimb ($p < 0.001$) but not hindlimb ($p = 0.397$) error due to whisker trimming. (C) Scatter plot with fit lines showing that by animal, average forelimb error significantly predicts average hindlimb error in the presence ($p < 0.001$) or absence ($p = 0.03$) of whiskers. (D, E) Line graphs depict average y-component forelimb trajectories before (solid lines) and after whisker trimming (dashed lines) in sighted (red) and early blind opossums (blue). Whisker trimming reduces step height to a significant extent ($p = 0.019$). (F, G) Line graphs depicting forelimb displacement in the x-direction (stride) before and after whisker trimming. Whisker trimming reduces step width in both conditions. (H, I) Line graphs depict average y-component hindlimb trajectories before and after whisker trimming. Whisker trimming results in shallow hindlimb movements for blind and sighted animals. Overall, trajectories of the limbs are altered to a greater extent in early blind opossums. Line graphs are presented as average trajectories with bootstrapped 95% confidence intervals. Bar graphs are presented as means with error presented as bootstrapped 95% confidence intervals. Where p values are reported, statistical tests were calculated using linear models (see Transparent Methods: reduced model). (* $p < .05$, ** $p < .01$, *** $p < .001$, n.s = $p > .05$). See also Figure S1.

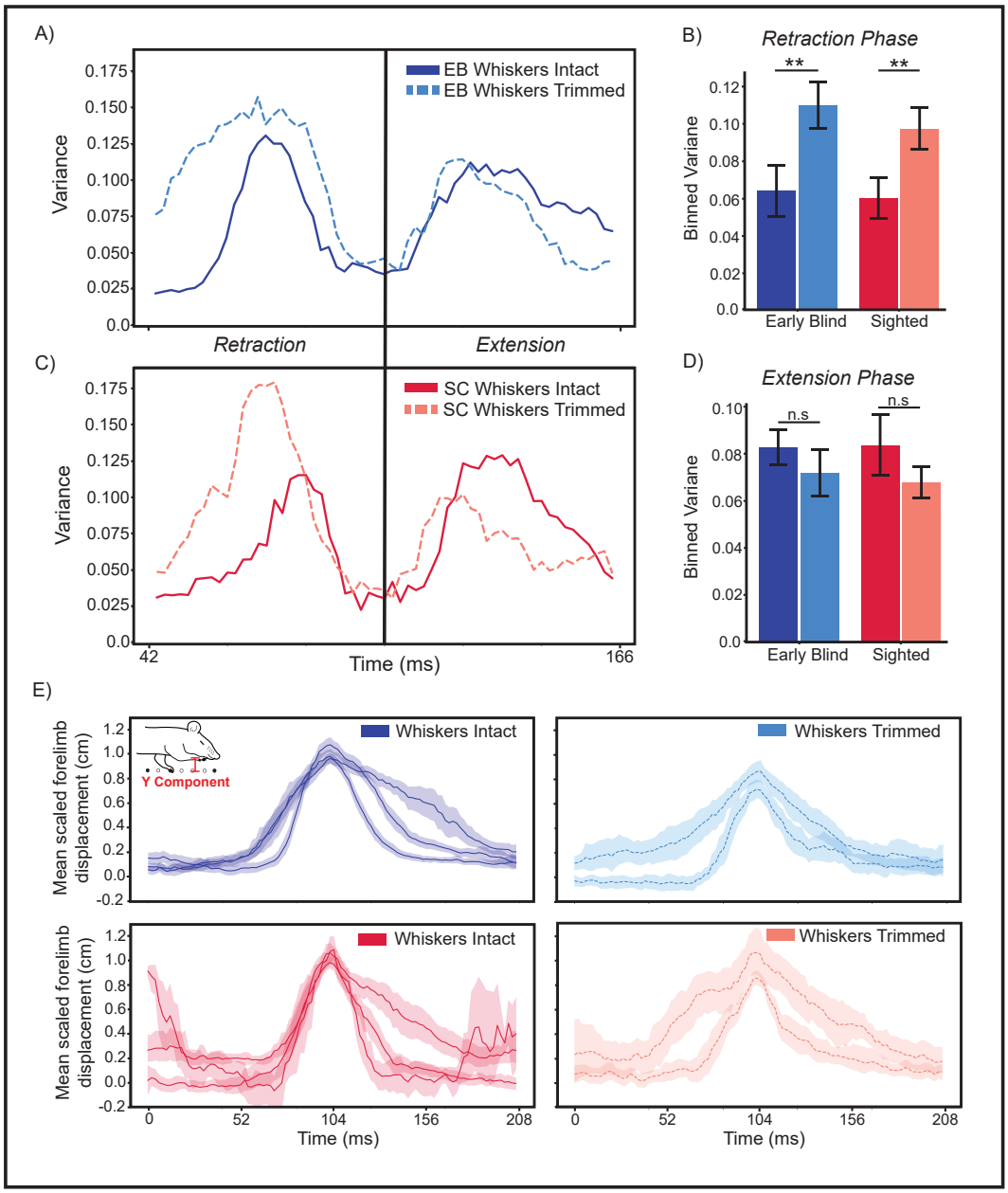

Figure 4. Whisker trimming results in more variable forelimb trajectories and different types of stereotypical movements in both early blind and sighted animals. (A, C) Line graphs with bootstrapped 95% confidence intervals of the average variance of y-component forelimb trajectories across all motions (n = 155) before (solid lines) and after whisker trimming

(dashed lines) in early blind (blue) and sighted (red) opossums. The vertical black line denotes the separation between retraction and extension phases. (B, D) Bar graphs show mean binned variance with 95% confidence intervals during retraction (B) and extension (D) phases. Binned variance is the average variance of the entire retraction or extension phase. Whisker trimming significantly increases variance during the retraction ($p < 0.001$), but not extension ($p = 0.21$) phase of forelimb movement (See Transparent Methods: reduced model). (E) Stereotyped movements of early blind and sighted opossums before and after whisker trimming provided by K-means clustering presented as average line graphs with 95% confidence intervals. The elbow point and silhouette coefficient were used to determine the number of clusters (see Transparent Methods). Stereotypical movements are similar in early blind (top left) and sighted (bottom left) opossums. Whisker trimming alters stereotypical movements in similar ways in early blind (top right) and sighted (bottom right) opossums. Where p values are reported: (* $p < .05$, ** $p < .01$, *** $p < .001$, n.s = $p > .05$). See also Figure S2.

Figure 5. Animals adapt to whisker trimming in similar ways. (A) Average line graphs with 95% confidence intervals of stride (x-component only) between the right forelimb and right hindlimb (left) and the right forelimb and snout (right) in early blind (A) and sighted (B) opossums during correct forelimb strikes. In both groups, whisker trimming reduces stride and decreases the distance between the right forelimb and snout. The flattened whisker-trimmed trajectories illustrate the conservative approach taken by whisker-trimmed opossums, as animals hunch their posture and are less willing to take long strides. Illustrations (right) derived from tracings of animals with (top) and without (bottom) whiskers, representative of typical locomotor postures while ladder crossing. (C,D,E) Bar graphs depict quantified aspects of body posture during ladder crossing. (C) Whisker trimming results in significant decreases in average snout height ($p =0.004$) and (D) more nose tapping behavior ($p =0.002$), (E) while the tail is held higher ($p =0.042$). (F) Bar graph shows the interaction between whiskers and lighting condition

on crossing time. Whisker trimming results in increased crossing time for early blind animals in the light and dark ($p = 0.022$, $p = 0.015$). Whisker trimming only results in increased crossing time for sighted animals in the dark ($p = 0.448$, $p < 0.001$). Bar graphs presented as mean with bootstrapped 95% confidence intervals. Where p values are reported, statistical tests were calculated using linear models and multiple comparisons corrected by the Holm-Sidak methods (see Transparent Methods: reduced model). (* $p < .05$, ** $p < .01$, *** $p < .001$, n.s = $p > .05$). See also Figure S3.

Video S1: **DeepLabCut tracking of an early blind animal with whiskers in the light condition. Related to Transparent Methods.** Down-sampled video shows placement of trackers on the palms of the limbs, tip of the tail, and snout.

Video S2: A sighted (SC) opossum with whiskers during ladder crossing in the light condition. Related to Figures 3 and 5. Note the animal's quick movements and long stride. Video is slowed to 25% speed.

Video S3: A sighted (SC) opossum without whiskers during ladder crossing in the light condition. Related to Figures 3 and 5. Note the animal's hunched posture and cautious approach. Video is slowed to 25% speed.

Video S4: An early blind (EB) opossum with whiskers during ladder crossing in the light condition. Related to Figures 3 and 5. Video is slowed to 25% speed.

Video S5: An early blind (EB) opossum without whiskers during ladder crossing in the light condition. Related to Figures 3 and 5. Video is slowed to 25% speed.

Chapter 3.

The following chapter is a manuscript in preparation for publication.

The stabilization of transient developmental projections leads to cross-modal reorganization of visual cortex in blind short-tailed opossums (Monodelphis *domestica*)

Authors: Mackenzie Englund[1]†, Riley Bottom[3]†, Roberto Perez[3,] Sebastian James[2], Cynthia Weller[1], Stuart P. Wilson[2], Leah A. Krubitzer[1], Kelly J. Huffman[3]*

Affiliations:

[1] Department of Psychology, University of California Davis; 1 Shields Ave, Davis, CA, 95616, US.

[2] Department of Psychology, University of Sheffield; Sheffield S10 2TN, UK.

[3] Department of Psychology, University of California Riverside; 900 University Ave, Riverside, CA, 92521, US.

*Corresponding author.

† These authors contributed equally to this work

Introduction

Everything we know about the physical stimuli that compose our environment is communicated via sensory systems through canonical, neuroanatomical pathways. The precise development of these circuits relies on contributions from internal genetic programs and neuronal activity arising first from spontaneous sources and then from activity generated by external sensory stimulation (Simi & Studer, 2018). The development of distinct cortical areas within the mammalian neocortex is well known to be governed by the synergistic effects of genetic pre-specification and neural activity (Antón-Bolaños et al., 2019; Bishop et al., 2000; Chou et al., 2013; Fukuchi-Shimogori & Grove, 2003; Hubel & Wiesel, 1964; Joshi et al., 2008). Key observations supporting this principle have been described using sensory-specific perturbations within the visual, somatosensory (Van der Loos & Woolsey, 1973) and auditory systems (Zhang et al., 2002), where removal or blockade of early sensory activity resulted in altered size, connectivity, and function across sensory areas of the neocortex (Moreno-Juan et al., 2017).

Yet the mammalian neocortex is also striking for its ability to functionally adapt to changes in sensory inputs. For example, in blind humans, visual cortex is recruited in somatosensory processing (Cohen et al., 1997) - which may underlie the described enhancement of tactile and auditory-mediated behaviors following visual loss (Röder et al., 1999, 2002; Voss et al., 2004). These observations show that adaptive re-organization of sensory cortical areas occurs in individuals afflicted with sensory loss, in a concept termed cross-modal plasticity (Ricciardi et al., 2014).

Cross-modal plasticity has also been described in several animal models (Mezzera & López-Bendito, 2016; Petrus et al., 2014) including in a model of early blindness, the Brazilian short-tailed opossum (*Monodelphis domestica*). These opossums are highly altricial, allowing for postnatal sensory perturbations prior to spontaneous activity and circuit assembly. In a series of studies, pups were subjected to early bilateral enucleation at postnatal day 4 (P4),

prior to retinal ganglion cells and thalamocortical afferents reaching their targets (Molnár et al., 1998; Ramamurthy et al., 2021). Following this early sensory loss, massive cross modal-plasticity was observed in adult opossums, including the re-organization of thalamic and cortical connections to and from primary visual cortex (Karlen et al., 2006), and a reduction in the size of visual areas in the cortex and nuclei in the thalmus (Karlen & Krubitzer, 2009; Englund and Krubitzer, 2021). Importantly, early visual loss was also accompanied by functional reorganization of the cortex, where spared sensory modalities took over areas that normally process visual inputs. Recent behavioral tests showed improved sensorimotor performance and a heavy reliance on tactile sensory inputs in enucleated animals compared to their sighted counterparts (Englund et al., 2020; Ramamurthy et al., 2021), showing the previously described reorganization of the neocortex has significant impacts on behaviors mediated by spared sensory systems.

Despite the remarkable effects of early visual loss, it is still unknown how the developmental program is altered by this early sensory loss to produce these cross-modal changes, as well as how the timing of visual loss impacts these phenomena. To address these gaps in knowledge, we performed bilateral enucleations on *Monodelphis domestica* at both P4 and P12, corresponding to ages before and after thalamocortical (TCA) and retinal ganglion cell (RGC) projections reach their targets respectively, and assessed changes to anatomical connections at the time of eye opening (P36). We also quantified and compared patterns of *Id2* expression, a gene that plays a critical role in cortical development and axonal projections. Using this dual approach (of changes to anatomical connections and gene expression) we were informed of how primary visual cortex is reorganized into a multimodal association area and not an extension or copy of the remaining primary fields. Due to previous electrophysiological experiments finding multimodal responses in rV1 of blind opossums, we hypothesized that both alterations in connections and gene expression would be present, showing complete reorganization of visual cortex into a multimodal area. Without changes in gene expression, we

expected only partial reorganization of visual cortex, suggesting that visual cortex develops largely independent of early visual input. Lastly, we relate these changes to previous findings in adult animals to show how developmental trajectories are altered, allowing for cross-modal plasticity due to the early loss of vision.

METHODS:

Subjects:

A total of 37 short-tailed opossums (16 female; 22 male) derived from 8 litters were used in this study. Animals were randomly designated into 3 experimental groups: 1) sighted control, SC, 2) early blind bilaterally enucleatred at P4 (EB); 3) late blind bilaterally enucleation at P12 (LB) (Figure 1). 18 animals were used for *in situ* hybridization (5 SC, 7 EB, 6 LB), and 16 animals for dye tracing experiments (5 SC, 6 EB, 5 LB). The full experimental timeline is outlined in Figure 1. All animals were obtained through our breeding colony at the University of California Davis. All experimental procedures were approved by UC Davis IACUC and conform to NIH guidelines.

Bilateral Enucleation Surgery:

Bilateral enucleations on *Monodelphis* pups have been conducted in our lab previously and these procedures have been described in detail elsewhere (Kahn & Krubitzer, 2002; Ramamurthy & Krubitzer, 2018). In brief, mothers of experimental litters were anesthetized with Alfaxalone (3 mg/kg, 10 mg/ml IM), while pups were anesthetized by hypothermia via contact with a rubber pouch filled with ice (as *Monodelphis* is fused to the nipple until ~ P14). Under microscope guidance, the skin covering the immature eye was retracted, and the developing retina was removed along with the rest of the optic cup at either P4 (EB) or P12 (LB) timepoints (Figure 2). A flush of sterile saline was applied to rinse the area before obtaining confirmation that all retinal

tissue was removed. The skin was then repositioned over the orbit and sealed with surgical glue. On average, this process takes ~3 minutes per pup. Once enucleation procedures were complete, mothers were allowed to recover in their home cage.

Tissue Collection:

Tissue was collected at postnatal day 36 (P36), 1-3 days after the time of eye-opening and onset of visual experience for *Monodelphis*. At the time of collection, weight and sex were recorded for all animals, while the state of the eyes for sighted opossums was also recorded (open or closed). Only sighted opossums with open eyes at the time of tissue collection were included in our analyses. Animals were euthanized via overdose of Sodium Pentobarbital (> 100 mg/kg, 390 mg/ml) (ISH and Dye Tracing). For *in situ* hybridization (ISH) and dye tracing experiments, animals were perfused with 0.1 M phosphate buffered saline (PBS) followed by 4% paraformaldehyde (PFA) in 0.1 M phosphate buffer. Brains were extracted under microscope guidance and stored in 4% PFA before being shipped to UC Riverside for processing. At the time of extraction, we obtained confirmation that no retinal tissue was present in bilateral enucleated animals via dissection and visual confirmation under microscope guidance.

Dye Tracing

To visualize the development of both intraneocortical and thalamocortical connectivity patterns of primary sensory areas, lipophilic dyes were used in fixed, postmortem hemispheres from all 3 experimental groups. Briefly, Small crystals of DiI (1,1'-Dioctadecyl-3,3,3',3'-tetramethylindocarbocyanine perchlorate) and DiA (4-(4-(dihexadecylamino)styryl)-N-methylpyridinium iodide) were placed into putative primary visual cortex (V1) and putative primary somatosensory cortex (S1), respectively. Proper dye crystal placement locations (DPLs) were designated via estimation from wild type adult electrophysiological and anatomical data delineating cortical area boundaries (Dooley et al., 2015; Karlen et al., 2006). Following 6-8

weeks to allow for dye transport, brains were embedded in gelatin-albumin and sectioned at 100 μm via vibratome (Leica VT1000S, Wetzlar, Germany) in the coronal plane. All sections were counter-stained with 4′,6-diamidino-2-phenylindole (DAPI), mounted onto glass slides and coverslipped with Flouromount-G (Invitrogen, Waltham, MA, USA).

All mounted sections were digitally imaged with a digital high-resolution Zeiss (Oberkochen, Germany) HRm camera attached to a Zeiss Axio Upright Imager A.2 microscope using three filters. The three filters used were as follows: blue for DAPI counterstain, red for DiI, and green for DiA labeling (excitation wavelengths: blue: DAPI—359 nm, red: Cy 3—550 nm, green: GFP—470 nm; emission wavelengths: blue: DAPI—461 nm, red: Cy 3—570 nm, green: GFP—509 nm). All 3 filter-specific images for each section were merged for subsequent visual and quantification analyses.

Dye tracing analyses

First, general patterns of intraneocortical (INCs) and thalamocortical (TC?) connections were assessed visually by trained researchers using anatomically matched sections across all complete cases for each experimental condition. In order to aid visualization of INC patterns, 2D reconstructions were prepared of selected individual cases of SC, EB, and LB P36 dye-injected hemispheres. In these “flattened” neocortical reconstructions, DPLs and labelled cells from section-level data were plotted onto cortical outlines to visualize the anterior-posterior and medial-lateral extents of dye-traced cortical areas. Cortical areas and thalamic nuclei boundaries were determined using DAPI-stains, and image overlays using in-situ hybridized tissue of the opposite hemisphere (see Figure S1).

In order to quantify visually identifiable changes in INC patterning from putative V1 and S1 injection sites, overall projection zones (i.e. regions that contained labelled cells) from the

separate injection sites were calculated as a function of total cortical length in all individual cases in the 3 experimental groups. In addition, the extent of DPL spread at each injection site was quantified for each individual case to ensure the overall size of injection was not a factor in visual and quantified projection zone analyses.

ISH

Brains stored in 4% PFA were prepared for in situ hybridization (ISH) by embedding single hemispheres in gelatin-albumin and sectioning at 100 μm using a vibratome to cut the hemisphere in the coronal plane. Once all sections were collected, previously established protocols for non-radioactive free-floating RNA ISH were used to assess patterns of gene expression in P36 Monodelphis hemispheres in all 3 experimental groups. Details of procedures are described elsewhere (Abbott et al., 2018; Dye et al., 2011). Briefly, digoxigenin-labeled probes for *Id2,* obtained from the Rubenstein lab at UCSF, were hybridized to coronal sections and secondary amplification was achieved via anti-digoxigenin antibodies tagged with alkaline phosphatase. Color signal development was achieved following incubation of sections with NBT/BCIP substrate. After proper signal development was achieved, sections were permeabilized in 50% glycerol, mounted onto glass slides, and coverslipped. All hybridized sections were digitally imaged using a Zeiss SteREO Discovery V.12 dissecting microscope and captured using a digital high-resolution Zeiss Axio camera (HRm) using Axiovision software (version 4.7).

ISH analysis

We used the *Stalefish* software program (Spatial Analysis of Fluorescent and Non-Fluorescent *In-Situ* Hybridization) to analyze all *in-situ* data (Englund et al., 2021). This program uses a semi-automated high-throughput workflow to analyze sectioned tissue which has been hybridized or stained for *in-situ* or histological markers. For each case, we used *Stalefish's*

curve drawing tool to draw Bezier curves along Layers 2/3, 5, and 6 of the neocortex of each coronally-sectioned slice of tissue. The program then reconstructed individual cases on a layer-by-layer basis, creating a Layer 2/3, 5, and 6 map of cortex-wide Id2 expression for each individual. To collect high resolution data, we chose 150 bins for data collection, which spanned medial to lateral. For each slice, data collection began at the most medial aspect of the medial wall (near the subiculum) and continued laterally to the rhinal fissure. To aid in slice alignment during data reconstruction, we used *Stalefish's* landmark mode to place landmarks on each section of tissue at the apex of the medial wall. Next, we placed brains of different individuals (and therefore brains of different sizes/shapes) into a common reference frame using *Stalefish's* transformation function, which applies 3x3 transformation matrices to each case based on triangulated landmarks.

Once brains were in the same coordinate space, enabling point-by-point comparisons, we created average and difference maps by averaging values within conditions (average maps) and subtracting average maps between conditions (difference maps) (Figure S2, S3). Only pixel values which were present in all maps being compared were used for averaging/differencing. 200μM expression profiles were taken by retrieving the pixel value stored in the h5 file of each map and selecting columns of the data-frame which corresponded to the region of interest. Similarly, digital punches were taken using both rows and columns (500μM by 200μM). Thus, simply by selecting indices of the output DataFrames, we were able to select regions of interest (ROIs) for profiles/punches.

Statistical Analysis

Dye tracing quantification: All data were initially assessed and confirmed for normality using the Shapiro-Wilk Test. Ordinary 1-way analyses of variance (ANOVAs) followed by Tukey's post

hoc test were used to establish group differences. Statistical significance was set at $P < 0.05$. Data are presented as mean ± SEM.

Profiles and Punches: Correlations were calculated using Pearson's correlation coefficient: r(n) and $r_{\%}(n)$ are reported with the number of cases used to generate the correlation coefficient. Percent change correlations, $r_{\%}(n)$, were generated by differencing the average profile signal using the percentage change method within Numpy and SciPy Python packages.

Statistical tests for histograms were conducted using linear models, where distance along the cortex was used as an interaction term when appropriate. The general form of these equations used condition (SC/EB/LB) and location as predictors for signal level or percent change. The results of these tests are presented with the adjusted R-squared value (R^2_{adj}) and F-statistic F(*n)*, where *n* is equal to the number of degrees of freedom (cases - 1).

RESULTS:

Alterations in thalamocortical connectivity are dependent on age of enucleation

We undertook comprehensive analysis of thalamocortical (TCA) connectivity at P36 using lipophilic dye tracing following bilateral enucleation at early (P4) and late (P12) stages of visual development. Sighted control (SC) opossums display typical patterns of connections, with the overwhelming majority of labeled cells projecting to S1 in the ventral posterior nucleus (VP; 100% of cases) and cells projecting to V1 in the dorsal lateral geniculate nucleus (dLGN; 100% of cases) and lateral pulvinar (LP; 67% of cases) (Figure 3). However, in addition to typical thalamocortical label, one sighted opossum (out of six) had retrogradely labeled cells from the V1 injections in the ventral anterior and ventral lateral nucleus (Table 1). In contrast, early blind (EB) animals, while still maintaining some level of dLGN-V1 connectivity, despite very early

developmental loss of input from the retina, had aberrant projections to V1 from VP (Figure 3C; 67% of cases). These abnormal thalamocortical connections (VP-V1) closely mirror what has been described in adult opossums who also underwent bilateral enucleation at P4 (Karlen et al., 2006). In to VP projection to V1 in EB opossums, we also found projection from the anterodorsal/ventral (AV/AD; 83% of cases) and ventral anterior/lateral (VA/VL; 67% of cases) nuclei, the lateral pulvinar (LP; 67%), and the medial geniculate (MG; 67%) (Figure 3A/B) nucleus. Thus, V1 in EB opossums exhibited a complex thalamocortical connection profile as early as P36. Dye placements in the putative S1 revealed typical thalamocortical connectivity in EB animals, with the vast majority projections arising from VP (100% of cases). However, S1 also received input from auditory thalamus (MG; 50% of cases) and VA/VL (50% of cases). In sum, opossums who underwent complete loss of retinal input at an age prior to the formation of thalamocortical connections had alterations in thalamocortical inputs to the V1 as well as S1.

Unlike the EB group, LB animals who underwent bilateral enucleation later in development (at a time when rudimentary thalamus to cortex connectivity has been established) normal patterns of thalamic projections to both S1 and V1 were observed. (Figure 3C3). Specifically, S1 received projections from VP (100% of cases) and V1 received projection from LGN (100% of cases) and LP (30% of cases); no VP to V1 or MG to V1 connections were observed in late blind opossums at P36. However, when considering motor and association nuclei, LB opossums showed a similar thalamocortical phenotype to EB opossums; V1 had projections from AV/AD (40% of cases) and VA/VL (80% of cases), and LP (40% of cases) (Figure 3A3-C3). These results show that the time at which vision is lost impacts thalamocortical cross-modal plasticity differentially, the loss of vision prior to TCA innervation results in cross-modal connections from primary thalamic nuclei which receive most of their inputs from the sensory afferents of the spared sensory systems, while the loss of vision after RGC/TCA innervation results only in aberrant projections from thalamic nuclei associated with the motor system.

Alterations in intraneocortical connections are dependent on age of enucleation

Intraneocortical connections (INCs) i.e. cortico-cortical connections within the same hemisphere, were also evaluated using lipophilic dye tracing. Rostral to caudal series of coronal sections following S1 DiA (*S1, Figure 4B1-B3) and V1 DiI (*V1, Figure 4E1-E3) dye crystal injections are presented for all 3 experimental groups in Figure 4. SC animals (Figure 4A2-F2) display typical patterns of early INCs for both S1 and V1. S1 had dense intrinsic connection and connections with the putative motor cortex. V1 had long-range projections from in (F; 33% of cases), motor (M; 33% of cases), and cingulate (Cg; 17% of cases) cortices (Figure 4B2). Interestingly, this does not match the exact pattern of connections observed in adult sighted opossums (discussed below). In contrast to sighted animals, EB opossums show a prominent expansion of the areas labeled from both S1 and V1 dye crystal injections, where projections from S1 extend further caudal, and projections from V1 extend further rostral (Figure 4A1-F1). Additionally, all EB opossums studied showed dense long-range projections to visual cortex from frontal (100%), motor (100%), and cingulate (100%) areas (arrows, Figure 4A1, B1, C1). S1 connectivity is also altered in EB animals where green labeled cells from S1 are present in visual cortex, a phenotype not seen in SC animals (Figure 4D1). Contrary to P36 sighted opossums, the pattern of INCs in P36 early blind opossums matches patterns of connections observed in adults that were bilaterally enucleated at P4 (Karlen et al., 2006). Overall, the patterns of INCs from primary sensory areas revealed cross-modal changes due to very early loss of visual input.

While the pattern of thalamocortical connections differed between LB and EB opossums, the pattern of cortical connections was found to be similar. LB animals showed an intermediate INC phenotype compared to the SC and EB conditions, with red labelled cells from V1 injections observed in frontal (60% of cases), motor (60%), and cingulate (40%) cortices (arrows, Figure 4B3, 4C3). In comparison to EB animals however, the anterior-posterior extent of aberrant INCs

is reduced in the LB group, suggesting that timing may affect the level of cortical reorganization that occurs following sensory input loss.

Overall results from section-level INC analysis are more easily visualized by the representative cases. To accomplish this, we created “flattened” 2D reconstructions from coronal sections by plotting labeled for each slice (Figure 5). Again, EB animals display labeled cells (red dots) from V1 injections in far rostral locations as well as labeled cells (green dots) from S1 in further caudal cortical locations (Figure 5A, B). Although LB cases display clear alterations in projection zones of V1, the extent of this change appears to be reduced compared to EB animals and, unlike the EB group, no change is seen in LB INC patterns of S1 compared to SCs (Figure 5C).

These qualitative changes in cortical connectivity were further confirmed by projection zone quantification for both S1 and V1 injections in SC (n = 5), EB (n = 6), and LB (n = 5) animals, as a function of total cortical length (to control for differences in brain size). 1-way ANOVA revealed a significant effect in S1 projection zones [$F(2,13) = 4.956$, $P = 0.0251$] and *post hoc* tests show only a significant increase in S1 projection zone in EB animals compared to SC ($^{*}P = 0.021$) (Figure 6). These results mirror those seen in the qualitative assessment of the data, where only EB seem to display S1 INC changes. In contrast, in V1 projection zones, which also showed a significant effect [$F(2,13) = 52.13$, $P < 0.0001$], variation as driven by both LB and EB animals, where significant increases in V1 projection zones were found via *post hoc* tests in both EB ($^{****}P < 0.0001$) and LB ($^{**}P = 0.0012$) groups compared to controls. Additionally, quantitative analysis confirmed the reduction in aberrant V1 connectivity in LB opossums compared to EB, as post hoc tests found a significant difference between the groups ($^{***}P = 0.0004$). Thus, our results suggest that differences in connectivity following sensory loss are time-dependent and sensory area-specific (which is likely related to the sensory modality which experienced loss).

Lastly, dye placement location (DPL) spreads were assessed in all cases to control for dye crystal size and non-specific diffusion. No significant differences were present among any groups in both S1 [$F(2,13) = 2.488$, $P = 0.1217$] and V1 [$F(2,13) = 0.5593$, $P = 0.5848$] crystal injections, suggesting that differences in injections do not underlie the observed results. Overall, qualitative and quantitative examination of INC patterns following early and late bilateral enucleation revealed irregular plasticity in connectivity, which appears to be both time and sensory modality dependent.

Early and late blindness differentially affect layer 6 *Id2* Expression

Due to differences in the reorganization of projections to visual cortex in blind opossums, we next assessed changes in gene expression. To accomplish this, we analyzed the expression of *Id2*, a transcriptional regulator dynamically expressed within the developing neocortex associated with early INC patterns (Huffman et al., 2004). The layer-specific expression of *Id2* has been implicated in identifying primary and association cortical areas in neurodevelopment (Englund et al., 2021). *In situ* hybridization of coronally-sectioned hemispheres was performed on serial 100 um thick sections from brains from all three groups. In all cases, *Id2* expression differed by cortical layer and region, similar to what has been observed in mice (Dye et al., 2011a; b) and other mammals (Bottom et al., 2020), with expression localized to cortical layers 2/3 , 5 and 6.

To address differences between conditions in the expression of *Id2,* we utilized the *Stalefish* program to analyze layer-specific cortex-wide expression patterns. As *Id2* is highly expressed in all layers except for layer 4 (Dye et al., 2011), we used the curve drawing tool to analyze layers 2/3, 5, and 6 serial of coronal sections of EB (n=7), LB (n=6), and SC (n=5) opossums. First, we created average maps of each condition by transforming all cases to a common reference frame using *Stalefish's* transformation function, allowing point-by-point averages and comparisons across individual cases (Figure S2). To visualize averaged

expression patterns, we plotted average maps using min-max normalized expression levels. Across conditions, Layer 2/3 maps revealed high expression levels on the most medial and lateral aspects of the neocortex. High lateral expression appeared to partially overlap with putative auditory cortex. Similarly, Layer 5 expression was highest in caudolateral cortex. Conversely, layer 6 expression coincided with the spatial location of primary visual cortex across cases. While this pattern was distinct for EB and SC opossums, LB animals had less clear boundaries between V1 and the rest of the neocortex. Regardless, layer 6 *Id2* expression patterns of EB and SC animals were reminiscent of the adult V1 phenotypes shown in myelin stains (Karlen & Krubitzer, 2006; Ramamurthy & Krubitzer, 2018). To date, the size and location of V1 in adult LB opossums has not been determined.

To quantify differences between conditions, we created difference maps which resulted in regions of interest (ROIs) representing areas of large differences in expression (Figure S3). Thus, using this method we generated ROIs based on computation and not predetermined hypotheses, observing all possible differences before testing specific regions. Similar to what was observed in the average maps, we found no significant areas of difference/interest for layer 2/3 or layer 5 maps. However, both EB and LB layer 6 difference maps (when subtracted from the SC map) revealed a significant ROI near the lateral edge of V1 (Figure 7A/E). Thus, we chose this region for further analysis.

First, we collected 300μM thick expression profiles from layer 6 at a rostral and caudal location for each case. The rostral profile (serving mostly as a control) spanned frontal and somatosensory areas, while the caudal profile encompassed portions of the medial wall, visual, and auditory cortex (Figure 7B, pink and red lines). For rostral profiles, we found that expression level was correlated across conditions, with especially tight coupling between early and late blind opossums ($r_{SC\text{-}EB}$ = .50, $r_{SC\text{-}LB}$ = .49, $r_{EB\text{-}LB}$ = .92, Figure 7C). As a more rigorous measure,

and to better account for magnitude, we used percent change as a differencing method to assess the relatedness of expression profiles between conditions along the medial-lateral axis. Similar to correlations for absolute signal, we found that rostral percent change expression profiles were still correlated along the medial-lateral axis across conditions, although to a lesser degree ($r_{\%SC\text{-}\%EB} = .32$, $r_{\%SC\text{-}\%LB} = .23$, $r_{\%EB\text{-}\%LB} = .57$). These correlational data suggest that the loss of vision at either developmental stage does not alter the *pattern* of rostral layer 6 *Id2* expression. However, correlations inform of the relatedness of change and do not adequately account for differences in overall levels of expression between conditions. Thus, we took a 400μM-square digital micro-punch of rostral somatosensory cortex (similar to tissue punches used in qPCR) to determine quantitative differences in the *level* of layer 6 *Id2* expression at this rostral location (Figure 7F, pink box). Surprisingly, we found that late blind opossums had significantly higher levels of *Id2* expression than either early blind or sighted opossums, and early blind opossums had significantly higher *Id2* expression than sighted controls ($p < .001$, $p < .001$,) (Figure 7G). Therefore, while the loss of vision before the establishment of retinal and thalamic projections results in an increase in *Id2* expression in S1, losing vision after these events appears to cause an even greater increase in layer 6 *Id2*. This represents a potential change in developmental trajectory or compensatory plasticity that occurs in the spared sensory systems.

Next, to elucidate the impact of vision loss on *Id2* expression in caudal areas, including visual and auditory cortex, we selected a 300μM thick expression profile encompassing portions of the medial wall, visual, and auditory cortex (Figure 7B, red line). In contrast to our results for rostral cortex, we found that caudal expression profiles between sighted and blind animals (early or late) exhibited little to no correlation whether considered as absolute signal or percent change ($r_{SC\text{-}EB} = .07$, $r_{\%SC\text{-}\%EB} = .14$, $r_{SC\text{-}LB} = .10$, $r_{\%SC\text{-}\%LB} = .18$). In fact, only absolute signal between EB and LB caudal profiles was significantly correlated ($r_{EB\text{-}LB} = .55$ $r_{\%EB\text{-}\%LB} = .04$) (Figure 7D).

These correlational data, showing that the pattern of *Id2* expression differs in caudal cortex, indicate that the loss of vision impacts gene expression in an area-dependent manner. To confirm the specific impact on the level of *Id2* expression in visual cortex, we selected a digital micro-punch from caudal neocortex, at the spatial location for the lateral portion of V1 (Figure 7F, red box). Our results show a drastic decrease in layer 6 *Id2* expression in early blind opossums ($p < .001$) (Figure 7H). Late blind opossums also showed this reduction, but to a lesser degree ($p < .01$). Lastly, we confirmed our Stalefish analysis results by visually inspecting the layer 6 *Id2* expression in EB, LB, and SC opossums in the *exact* location the caudal punch was taken from (Figure 7I). As pictured, there is an increase in L6 expression across all cases, marking the medial boundary for visual cortex (medial of red boxes in Figure 7I). However, this high level of expression drops immediately in EB opossums on the lateral edge (Figure 7I left, red box), while this level is retained in SC's. However, LB opossums exhibited a striated, and less confined expression of *Id2* in L6 altogether (Figure 7I right). Together, the data from caudal profiles and visual cortex punches suggests an early cross-modal reorganization of lateral visual cortex.

DISCUSSION

The primary goal of this study was to examine how the age of vision loss impacts the development of cortical connectivity and gene expression. By removing visual input through bilateral enucleation at two key developmental stages (before and after retino-thalamic/thalamo-cortical innervation) and assessing changes at eye-opening, we showed how the extent of compensatory and cross-modal plasticity is determined by the age at which vision is lost. Our data show that loss of vision prior to the establishment of retino-geniculate and geniculo-cortical connections results in early and complete cross-modal reorganization of subcortical and cortical connections. On the other hand, removing visual input after these connections have formed results in an intermediate phenotype, where subcortical connections mostly resemble those of sighted animals, and cortical connections resemble those of blind animals. Specifically, V1 in EB opossums receives thalamocortical projections from nuclei associated with the spared sensory systems (MG and VP). Additionally, EB opossums show aberrant thalamocortical connections between areas of the spared senses, such as from auditory thalamus to somatosensory cortex (MG-S1). As late-blind animals do not show these changes in projections from MG and VP, but do show changes in motor nuclei, we conclude that losing vision prior to spontaneous or experience-drive sensory activity results in a cross-modal remodeling of the thalamus and cortex as early as eye opening (P36). The establishment of the reinto-geniculo-cortical pathway and the presence of spontaneous activity in the retina that late blind opossums receive appear to prohibit these primary cross-modal thalamic changes from occurring (likely via activity-dependent competition and an initially normal pruning schedule). Thus, the degree to which cross-modal connections form depends on the developmental stage at which vision is lost: projections from primary sensory thalamic nuclei are altered only when input is lost prior to the establishment of retinal and thalamic pathways, while projections from association/motor nuclei and cortical connections are altered when input is lost at either stage. These changes in projections were accompanied by a drastic reduction in *Id2* expression in layer 6 of visual cortex

in EB compared to SC opossums (with LB opossums showing an intermediate level). The varied levels of Id2 expression between conditions suggests different levels of reorganization between EB and LB opossums, and an association area identity for blind opossums compared to the primary area identity of sighted animals. Below, we discuss these results in the context of the adult phenotype in the same and other species, and the functional implications of the observed anatomical changes.

Comparison with adult phenotypes: long range projections to V1 from rostral cortex are pruned by adulthood in sighted animals but are retained in early blind animals.

For the last two decades, our laboratories have provided extensive data on the anatomical, functional, and behavioral changes to the neocortex that result from early vision loss in Monodelphis *domestica* (Kahn & Krubitzer, 2002; Karlen & Krubitzer, 2009; Ramamurthy & Krubitzer, 2018). These studies focused on quantifying changes to the adult phenotype that were bilaterally enucleated at P4. Our data shows that large-scale changes to thalamocortical (TCA) and intraneocortical (INC) connections are already present at postnatal day 36, immediately after eye opening. The pattern of TCA and INC connections observed in P4 early blind possums at P36 closely resembles the previously observed alterations in adult P4 early blind opossums (Karlen et al., 2006) (Figure 8A). That is, most of the anatomical reorganization due to early blindness appears complete at the time of eye-opening. For example, previous work from the Krubitzer lab in adult opossums found that the visual cortex of blind but not sighted animals receives thalamic input from the ventral posterior and medial geniculate nucleus of the thalamus (Karlen et al., 2006). TCA connections from the spared sensory modalities were also found to be altered in adult EB opossums. Lastly, both our study in P36 animals, and a recent study from our laboratory in adult animals, show MG-S1 projections in early blind but not sighted opossums (Dooley & Krubitzer, 2019).

Similarly, the pattern of TCA connections in sighted opossums at P36 resembled that of adult animals, highlighted by strong dLGN-V1 and LP-V1 connections, and weak but present VA/VL-V1 connections. Future experiments which include pre-eye-opening ages (such as P16-P30) will determine if/how visual experience prunes TCA connections. Furthermore, as anatomical tracing studies have not been conducted in adult late blind opossums, we cannot determine if cross-modal reorganization is complete in LB opossums at P36. This is because early versus late vision loss may alter developmental pruning trajectories differently (i.e axonal pruning is complete in EB opossums at P36 but not in LB opossums). However, projections from primary thalamic nuclei to the cortex in late blind opossums resemble that of sighted controls (VP-S1, dLGN-V1). On the other hand, the pattern of projections from anterior nuclei to visual cortex (AD/AV/LD – V1) in LB opossums resembles that of EB opossums. This agrees with previous work in other species, where sensory loss after TCA innervation and the onset of spontaneous activity was found to alter mostly INC connections (for review see Mezzera and Lopez-Bendito 2016). For example, mice enucleated at birth show a similar pattern of TCA connections to sighted controls for primary thalamic nuclei (dLGN, VP, MGN), but not higher order thalamic nuclei such as LD (Chabot et al., 2007; Charbonneau et al., 2012; Dye et al., 2012). In fact, it is remarkable that across species, the effects of vision loss on cortical reorganization are highly conserved - with changes being more related to the stage at which sensory loss occurs and less related to species (Englund and Krubitzer 2021, Mezzera and Lopez-Bendito 2016). To highlight this conservation of developmental plasticity, preliminary data from our laboratory shows that mice and opossums enucleated immediately after TCA innervation (mice: P0, opossums: P12), show similar changes in L6 *Id2* expression across the neocortex (Figure S4).

To digress, while the TCA phenotype differs between EB and LB opossums, the INC phenotype of both groups, determined by the location of back-labelled cells and the projection zones of dye crystals placed in V1 and S1, showed similar cross-modal reorganization, although

to a greater degree in EB opossums. Importantly, while sighted and blind opossums displayed long-range projections to visual cortex (F-V1, M-V1, Cg-V1) at P36, these connections are not observed in adult sighted opossums. Thus, while EB, LB, and SC opossums all display long range connections at P36, particularly from deep layer frontal cortex to visual cortex (Figure S1), these long-range connections are pruned by adulthood. There are two possibilities for this occurrence. First, axons from FM and surrounding cortex are exuberant early in development but are pruned by visual experience/competition from visual thalamic input (Dütting et al., 1999; Feldheim & O'Leary, 2010; Khalil & Levitt, 2014; Riccomagno & Kolodkin, 2015). Second, and less likely, is that these long-range connections represent a transient process in cortical development, and their existence provides a particular function to development of visual cortex. Transience, especially in gene expression and axon targeting, is a key aspect of neurodevelopment, often serving as a scaffold for later processes (Grant et al., 2012). However, the fact that projections are stabilized by a lack of experience and pruned by experience suggests axon exuberance (discussed in more detail below). However, it should be noted that the lipophilic dyes used in this study do not grant the same degree of specificity as fluorescent tracers used in adult animals, and so it is possible that more area-specific differences exist between all three experimental conditions. Fluorescent tracing experiments in adult LB opossums will address this gap in knowledge. In sum, anatomical results from the current study and previous experiments show that major changes to connections due to vision loss are complete near the time of eye opening, but that the pruning of cortical connections is still underway for sighted animals, who have received little sensory driven visual experience by P36.

Of course, changes in the number and strength of these connections is an ongoing process during the visual critical period. Regardless, our data suggests a strong spontaneous-activity component to cross-modal reorganization as there has not been extensive visual experience at P36. Thus, the absence of retinal afferents alone appears to be enough to generate extensive anatomical changes, and a failure to prune / stabilization of exuberant

connections appears to be the mechanism by which this cross-modal reorganization occurs (e.g., cortical F-V1 connections normally pruned between P36-Adulthood) (Figure 8A). Future studies incorporating intermediate ages and the development of behavior will determine the extent to which early tactile/motor experience may also affect the degree of cross-modal plasticity in the absence of vision. However, previous data from our laboratory suggests that early tactile experience does not play a major role in determining large-scale connections, as EB and SC opossums were found to have equal levels of exploratory behavior when assessed near the time of weaning (Ramamurthy & Krubitzer, 2018). In the next section, we address how these anatomical changes, in combination with the changes in *Id2* expression result in altering the areal identity and potential function of visual cortex in EB opossums.

Evidence that V1 is reorganized into a multimodal association area in early blind opossums.

Studies in congenitally blind humans have shown that V1 is repurposed into an area with many functions (Ricciardi et al., 2014). For instance, using magnetoencephalography (MEG) to measure stimulus-to-brain-activation time, Muller and colleagues recently found that occipital cortex in blind humans is activated by tactile stimulation via a direct thalamocortical circuit (Müller et al., 2019). Furthermore, in EB humans, V1 is activated during tasks which use audition and/or tactile inputs while completing tasks involving sensory discrimination, language processing, and spatial navigation (Bedny et al., 2012; Schinazi et al., 2016). Collectively, these data show that V1 takes on the functional role of a multimodal area which is more characteristic of a parietal association area than a primary cortical area (Gilissen & Arckens, 2021). Furthermore, the age of blindness onset affects cortical networks differently (Li et al., 2013). From our own data in adult EB Monodelphis, we previously showed that V1 is reorganized to process auditory and somatosensory information, with most of rV1 being devoted to the whiskers and snout (Kahn & Krubitzer, 2002; Karlen et al., 2006). As evidenced by the past two decades of research in our laboratory and others, across species the functional reorganization

of V1 due to vision loss is driven by changes in the neuroanatomy (Ewall et al., 2021; Mezzera & López-Bendito, 2016). Above, we show that V1 (or rV1) of EB, LB, and SC opossums receive distinct projections. Given that each experimental condition has a separate connection profile for V1, we surmise that the function of V1 between the three conditions is also separate. Future single-unit electrophysiological studies will determine if this is the case. Obviously, rV1 is a cross-modal area in EB and LB opossums. Strikingly, the TCA and INC connection profile of rV1 in P36 EB opossums resembles that of the adjacent multimodal area (MM) (Dooley et al., 2015). This data suggests that in the complete absence of retinal input, MM expands laterally into what would normally be V1. However, more anatomical data is required to solidify this claim. MM in Monodelphis exhibits many anatomical similarities to posterior parietal cortex (PPC) in humans, primates, cats, and rodents, which plays a critical role in cross-modal plasticity arising from sensory loss (Gilissen & Arckens, 2021).

We conclude this based on the following three lines of evidence. First, our *Id2 in-situ* results show that rV1 takes on the genetic identity of an association and not a primary area. Specifically, *Id2* is expressed in layer 6 of primary sensory areas across species, including visual cortex, and is not expressed in layer 6 of MM (Englund et al., 2021). Therefore, the lack of *Id2* expression in layer 6 of EB animals suggests that rV1 does not have the genetic identity of V1. Critically, corticothalamic axons originating from layer 6 of primary sensory areas are tightly and almost exclusively connected with their respective principal thalamic nuclei, and this connection is hypothesized to correlate with layer 6 gene expression (Antón-Bolaños et al., 2018; Gezelius et al., 2017; Moreno-Juan et al., 2020). However, the lack of layer 6 *Id2* expression only suggests that lateral rV1 in EB opossums does not have the genetic identity of V1 in SC opossums, but does not directly explain *what* this area has been reorganized into. Similarly, the intermediate level of *Id2* observed in LB opossums suggests partial reorganization, or at least that reorganization is still ongoing at P36. Functional studies in MM and rV1/V1 of adult EB, LB and SC will work to determine this.

Second, the TCA connection profile in rV1 of EB opossums resembles the connection profile of MM in sighted opossums (Figure 8B). MM in the adult sighted opossum receives TCA input from LD, VL/VA, VP, dLGN, and LP (Dooley et al., 2015). Likewise, rV1 in the P36 and adult EB opossum receives input from LD, VL/VA, VP, dLGN, and LP (in addition to AD/AV). The role of the AD/AV thalamic projections to rV1 in adult or developing EB opossums has yet be studied, as these nuclei typically project to cingulate, retrosplenial and limbic cortices in other species (Perry & Mitchell, 2019; Wright et al., 2010). In all species studied, these anterior thalamic nuclei play a role in spatial processing, navigation, and memory (Grodd et al., 2020). While the specific TCA connections of MM in adult EB animals is unknown, experiments to resolve this are currently underway in our laboratory. Nonetheless, V1 in P36 or adult sighted opossums does not receive input from AD/AV or VP (Dooley & Krubitzer, 2019; Karlen et al., 2006). Thus, the TCA connection profile of rV1 in EB opossums more closely resembles the sighted control MM than traditional visual cortex. Interestingly, the rV1 TCA connection profile of P36 LB opossums shows an intermediate phenotype, suggesting only partial reorganization. Unfortunately, the adult LB TCA rV1 profile is unknown.

INC connection profiles offer a third line of support that rV1 is anatomically akin to MM in blind opossums. Previous fluorescent tracing studies revealed that rV1 in adult EB opossums receives input from S1, A1, and MM, as well as long-range input from frontal cortex (Karlen et al., 2006). Results from the current study show that the connections from S1 and A1 to V1 are present at P36 in EB and LB opossums, but not sighted opossums. However, long-range projections from frontal to visual cortex are present at P36 regardless of experimental condition (as described in the previous section). Recent data from our laboratory shows that MM receives input from S1, A1, V1, and frontal cortex in both EB and SC adult opossums (Pineda et al., 2021). Thus, the rV1 and MM cortical connection profiles appear similar in adult EB opossums. This is not surprising as these areas are adjacent to one another in the cortex.

While the two studies from our laboratory represent the complete extent of data on the cortical connections of MM in adult opossums, posterior parietal cortex in rodents and primates is well-studied, and known to receive inputs from S1, A1, and V1, as well as long-range connections with motor, cingulate, and frontal cortex – reminiscent of our observations of rV1/MM cortical connections in EB opossums (Reep et al., 1994; Wang et al., 2021; Whitlock, 2017). Altogether, the genetic, TCA, and INC data show that rV1 undergoes an early cross-modal transformation in EB opossums, resulting in the anatomical reallocation of visual cortex into MM, or at least a multimodal association area. On the other hand, rV1 in LB opossums is remodeled mostly by INC connections, albeit there is a moderate reduction in layer 6 *Id2* expression in this experimental group. Comparing data from the current study with adult EB and sighted opossums suggests that the reallocation of V1 into a multimodal region is accomplished via a stabilization of transient TCA and long-range INC projections that are normally pruned in development. Future experiments will determine if this is the case. A possible scenario for how this occurs is described as follows: gene gradients set up initial boundaries for primary cortical fields during neurodevelopment, assisting in the targeting of TCA guidance, but projections are known to overshoot and overlap. As development proceeds with the onset of sensory experience and assistance of top-down cortico-thalamic projections, overlapping areas are refined, resulting in the definitive cortical field boundaries observed in adulthood (Englund et al., 2021; Zembrzycki et al., 2013). Thus, it is easy to imagine how altering the ratio of sensory input alters cortical field boundaries. While previous studies have shown this to be true, as a lack of visual input causes an immense reduction in the size of visual cortex, our data here shows that the failure to prune encroaching adjacent areas is the likely mechanism. While the expansion of one cortical area into another, or representations within cortical areas altering their size is not a novel idea, the distinct inputs from AD/AV-V1 in blind opossums, uncharacteristic of a single nearby cortical area, may shed light on how completely new cortical fields are formed not by intrinsic genetic programs, but by changes to sensory afferents alone (Krubitzer & Kahn, 2003).

That is, TCA projections from nuclei associated with parietal, cingulate, and retrosplenial cortices do not compete for cortical territory with visual cortex (due to the lack of strong drive from the dLGN). Then, nearby areas may compete with one another to expand their individual territories and/or collectively form a novel cortical field. Regardless, data from the current work provides evidence of a likely anatomical reorganization of V1 into a multi-modal region. Future functional, anatomical, and inactivation experiments during behavior, centered on the differences between MM and rV1 in adult blind animals, must be accomplished to definitively show whether these remain distinct areas with separate cross-modal functions, or if there is a direct expansion of MM into the cortical territory of would-be V1.

References

Abbott, C. W., Rohac, D. J., Bottom, R. T., Patadia, S., & Huffman, K. J. (2018). Prenatal Ethanol Exposure and Neocortical Development: A Transgenerational Model of FASD. *Cerebral Cortex (New York, NY)*, *28*(8), 2908–2921. https://doi.org/10.1093/cercor/bhx168

Antón-Bolaños, N., Espinosa, A., & López-Bendito, G. (2018). Developmental interactions between thalamus and cortex: A true love reciprocal story. *Current Opinion in Neurobiology*, *52*, 33–41. https://doi.org/10.1016/j.conb.2018.04.018

Antón-Bolaños, N., Sempere-Ferràndez, A., Guillamón-Vivancos, T., Martini, F. J., Pérez-Saiz, L., Gezelius, H., Filipchuk, A., Valdeolmillos, M., & López-Bendito, G. (2019). Prenatal activity from thalamic neurons governs the emergence of functional cortical maps in mice. *Science*, *364*(6444), 987–990. https://doi.org/10.1126/science.aav7617

Bedny, M., Pascual-Leone, A., Dravida, S., & Saxe, R. (2012). A sensitive period for language in the visual cortex: Distinct patterns of plasticity in congenitally versus late blind adults. *Brain and Language*, *122*(3), 162–170. https://doi.org/10.1016/j.bandl.2011.10.005

Bishop, K. M., Goudreau, G., & O'Leary, D. D. M. (2000). Regulation of Area Identity in the Mammalian Neocortex by Emx2 and Pax6. *Science*, *288*(5464), 344–349. https://doi.org/10.1126/science.288.5464.344

Bottom, R. T., Krubitzer, L. A., & Huffman, K. J. (2020). Early postnatal gene expression in the developing neocortex of prairie voles (Microtus ochrogaster) is related to parental rearing style. *Journal of Comparative Neurology*, *528*(17), 3008–3022. https://doi.org/10.1002/cne.24856

Chabot, N., Robert, S., Tremblay, R., Miceli, D., Boire, D., & Bronchti, G. (2007). Audition differently activates the visual system in neonatally enucleated mice compared with anophthalmic mutants. *European Journal of Neuroscience*, *26*(8), 2334–2348. https://doi.org/10.1111/j.1460-9568.2007.05854.x

Charbonneau, V., Laramée, M.-E., Boucher, V., Bronchti, G., & Boire, D. (2012). Cortical and subcortical projections to primary visual cortex in anophthalmic, enucleated and sighted

mice. *The European Journal of Neuroscience*, *36*(7), 2949–2963. https://doi.org/10.1111/j.1460-9568.2012.08215.x
Chou, S.-J., Babot, Z., Leingärtner, A., Studer, M., Nakagawa, Y., & O'Leary, D. D. M. (2013). Geniculocortical input drives genetic distinctions between primary and higher-order visual areas. *Science (New York, N.Y.)*, *340*(6137), 1239–1242. https://doi.org/10.1126/science.1232806
Cohen, L. G., Celnik, P., Pascual-Leone, A., Corwell, B., Faiz, L., Dambrosia, J., Honda, M., Sadato, N., Gerloff, C., Catala´, M. D., & Hallett, M. (1997). Functional relevance of cross-modal plasticity in blind humans. *Nature*, *389*(6647), 180–183. https://doi.org/10.1038/38278
Dooley, J. C., Franca, J. G., Seelke, A. M. H., Cooke, D. F., & Krubitzer, L. A. (2015). Evolution of mammalian sensorimotor cortex: Thalamic projections to parietal cortical areas in Monodelphis domestica. *Frontiers in Neuroanatomy*, *8*, 163. https://doi.org/10.3389/fnana.2014.00163
Dooley, J. C., & Krubitzer, L. A. (2019). Alterations in cortical and thalamic connections of somatosensory cortex following early loss of vision. *The Journal of Comparative Neurology*, *527*(10), 1675–1688. https://doi.org/10.1002/cne.24582
Dütting, D., Handwerker, C., & Drescher, U. (1999). Topographic Targeting and Pathfinding Errors of Retinal Axons Following Overexpression of EphrinA Ligands on Retinal Ganglion Cell Axons. *Developmental Biology*, *216*(1), 297–311. https://doi.org/10.1006/dbio.1999.9489
Dye, C. A., Abbott, C. W., & Huffman, K. J. (2012). Bilateral enucleation alters gene expression and intraneocortical connections in the mouse. *Neural Development*, *7*, 5. https://doi.org/10.1186/1749-8104-7-5
Dye, C. A., El Shawa, H., & Huffman, K. J. (2011). A Lifespan Analysis of Intraneocortical Connections and Gene Expression in the Mouse I. *Cerebral Cortex (New York, NY)*, *21*(6), 1311–1330. https://doi.org/10.1093/cercor/bhq212
Englund, M., Faridjoo, S., Iyer, C. S., & Krubitzer, L. (2020). Available Sensory Input Determines Motor Performance and Strategy in Early Blind and Sighted Short-Tailed Opossums. *IScience*, *23*(9), 101527. https://doi.org/10.1016/j.isci.2020.101527
Englund, M., James, S. S., Bottom, R., Huffman, K. J., Wilson, S. P., & Krubitzer, L. A. (2021). *Comparing cortex-wide gene expression patterns between species in a common reference frame* (p. 2021.07.28.454203). https://doi.org/10.1101/2021.07.28.454203
Ewall, G., Parkins, S., Lin, A., Jaoui, Y., & Lee, H.-K. (2021). Cortical and Subcortical Circuits for Cross-Modal Plasticity Induced by Loss of Vision. *Frontiers in Neural Circuits*, *15*, 665009. https://doi.org/10.3389/fncir.2021.665009
Feldheim, D. A., & O'Leary, D. D. M. (2010). Visual Map Development: Bidirectional Signaling, Bifunctional Guidance Molecules, and Competition. *Cold Spring Harbor Perspectives in Biology*, *2*(11), a001768. https://doi.org/10.1101/cshperspect.a001768
Fukuchi-Shimogori, T., & Grove, E. A. (2003). Emx2 patterns the neocortex by regulating FGF positional signaling. *Nature Neuroscience*, *6*(8), 825–831. https://doi.org/10.1038/nn1093
Gezelius, H., Moreno-Juan, V., Mezzera, C., Thakurela, S., Rodríguez-Malmierca, L. M., Pistolic, J., Benes, V., Tiwari, V. K., & López-Bendito, G. (2017). Genetic Labeling of Nuclei-Specific Thalamocortical Neurons Reveals Putative Sensory-Modality Specific Genes. *Cerebral Cortex*, *27*(11), 5054–5069. https://doi.org/10.1093/cercor/bhw290
Gilissen, S. R., & Arckens, L. (2021). Posterior parietal cortex contributions to cross-modal brain plasticity upon sensory loss. *Current Opinion in Neurobiology*, *67*, 16–25. https://doi.org/10.1016/j.conb.2020.07.001
Grant, E., Hoerder-Suabedissen, A., & Molnar, Z. (2012). Development of the Corticothalamic Projections. *Frontiers in Neuroscience*, *6*, 53. https://doi.org/10.3389/fnins.2012.00053

Grodd, W., Kumar, V. J., Schüz, A., Lindig, T., & Scheffler, K. (2020). The anterior and medial thalamic nuclei and the human limbic system: Tracing the structural connectivity using diffusion-weighted imaging. *Scientific Reports*, *10*(1), 10957. https://doi.org/10.1038/s41598-020-67770-4

Huang, Z., Liu, J., Jin, J., Chen, Q., Shields, L. B. E., Zhang, Y.-P., Shields, C. B., Zhou, L., Zhou, B., & Yu, P. (2019). Inhibitor of DNA binding 2 promotes axonal growth through upregulation of Neurogenin2. *Experimental Neurology*, *320*, 112966. https://doi.org/10.1016/j.expneurol.2019.112966

Hubel, D. H., & Wiesel, T. N. (1964). Effects of monocular deprivation in kittens. *Naunyn-Schmiedebergs Archiv Für Experimentelle Pathologie Und Pharmakologie*, *248*(6), 492–497. https://doi.org/10.1007/BF00348878

Joshi, P. S., Molyneaux, B. J., Feng, L., Xie, X., Macklis, J. D., & Gan, L. (2008). Bhlhb5 Regulates the Postmitotic Acquisition of Area Identities in Layers II-V of the Developing Neocortex. *Neuron*, *60*(2), 258–272. https://doi.org/10.1016/j.neuron.2008.08.006

Kahn, D. M., & Krubitzer, L. (2002). Massive cross-modal cortical plasticity and the emergence of a new cortical area in developmentally blind mammals. *Proceedings of the National Academy of Sciences*, *99*(17), 11429–11434. https://doi.org/10.1073/pnas.162342799

Karlen, S. J., Kahn, D. M., & Krubitzer, L. (2006). Early blindness results in abnormal corticocortical and thalamocortical connections. *Neuroscience*, *142*(3), 843–858. https://doi.org/10.1016/j.neuroscience.2006.06.055

Karlen, S. J., & Krubitzer, L. (2006). Phenotypic diversity is the cornerstone of evolution: Variation in cortical field size within short-tailed opossums. *The Journal of Comparative Neurology*, *499*(6), 990–999. https://doi.org/10.1002/cne.21156

Karlen, S. J., & Krubitzer, L. (2009). Effects of bilateral enucleation on the size of visual and nonvisual areas of the brain. *Cerebral Cortex (New York, N.Y.: 1991)*, *19*(6), 1360–1371. https://doi.org/10.1093/cercor/bhn176

Khalil, R., & Levitt, J. B. (2014). Developmental remodeling of corticocortical feedback circuits in ferret visual cortex. *Journal of Comparative Neurology*, *522*(14), 3208–3228. https://doi.org/10.1002/cne.23591

Krubitzer, L., & Kahn, D. M. (2003). Nature versus nurture revisited: An old idea with a new twist. *Progress in Neurobiology*, *70*(1), 33–52. https://doi.org/10.1016/S0301-0082(03)00088-1

Lasorella, A., Stegmüller, J., Guardavaccaro, D., Liu, G., Carro, M. S., Rothschild, G., de la Torre-Ubieta, L., Pagano, M., Bonni, A., & Iavarone, A. (2006). Degradation of Id2 by the anaphase-promoting complex couples cell cycle exit and axonal growth. *Nature*, *442*(7101), 471–474. https://doi.org/10.1038/nature04895

Li, J., Liu, Y., Qin, W., Jiang, J., Qiu, Z., Xu, J., Yu, C., & Jiang, T. (2013). Age of Onset of Blindness Affects Brain Anatomical Networks Constructed Using Diffusion Tensor Tractography. *Cerebral Cortex*, *23*(3), 542–551. https://doi.org/10.1093/cercor/bhs034

Mezzera, C., & López-Bendito, G. (2016). Cross-modal plasticity in sensory deprived animal models: From the thalamocortical development point of view. *Journal of Chemical Neuroanatomy*, *75*, 32–40. https://doi.org/10.1016/j.jchemneu.2015.09.005

Molnár, Z., Knott, G. W., Blakemore, C., & Saunders, N. R. (1998). Development of thalamocortical projections in the South American gray short-tailed opossum (Monodelphis domestica). *The Journal of Comparative Neurology*, *398*(4), 491–514.

Moreno-Juan, V., Martini, F. J., Pérez-Saiz, L., Herrero-Navarro, Á., Valdeolmillos, M., & López-Bendito, G. (2020). *Thalamic spontaneous activity coordinates the timing of corticothalamic innervation in the visual system* (p. 2020.11.13.382366). https://doi.org/10.1101/2020.11.13.382366

Müller, F., Niso, G., Samiee, S., Ptito, M., Baillet, S., & Kupers, R. (2019). A thalamocortical pathway for fast rerouting of tactile information to occipital cortex in congenital blindness. *Nature Communications*, *10*(1), 5154. https://doi.org/10.1038/s41467-019-13173-7

Perry, B. A. L., & Mitchell, A. S. (2019). Considering the Evidence for Anterior and Laterodorsal Thalamic Nuclei as Higher Order Relays to Cortex. *Frontiers in Molecular Neuroscience*, *12*, 167. https://doi.org/10.3389/fnmol.2019.00167

Petrus, E., Isaiah, A., Jones, A. P., Li, D., Wang, H., Lee, H.-K., & Kanold, P. O. (2014). Crossmodal induction of thalamocortical potentiation leads to enhanced information processing in the auditory cortex. *Neuron*, *81*(3), 664–673. https://doi.org/10.1016/j.neuron.2013.11.023

Ramamurthy, D. L., Dodson, H. K., & Krubitzer, L. A. (2021). Developmental plasticity of texture discrimination following early vision loss in the marsupial Monodelphis domestica. *Journal of Experimental Biology*, *224*(9). https://doi.org/10.1242/jeb.236646

Ramamurthy, D. L., & Krubitzer, L. A. (2018). Neural Coding of Whisker-Mediated Touch in Primary Somatosensory Cortex Is Altered Following Early Blindness. *The Journal of Neuroscience*, *38*(27), 6172–6189. https://doi.org/10.1523/JNEUROSCI.0066-18.2018

Reep, R. L., Chandler, H. C., King, V., & Corwin, J. V. (1994). Rat posterior parietal cortex: Topography of corticocortical and thalamic connections. *Experimental Brain Research*, *100*(1). https://doi.org/10.1007/BF00227280

Ricciardi, E., Bonino, D., Pellegrini, S., & Pietrini, P. (2014). Mind the blind brain to understand the sighted one! Is there a supramodal cortical functional architecture? *Neuroscience & Biobehavioral Reviews*, *41*, 64–77. https://doi.org/10.1016/j.neubiorev.2013.10.006

Riccomagno, M. M., & Kolodkin, A. L. (2015). Sculpting Neural Circuits by Axon and Dendrite Pruning. *Annual Review of Cell and Developmental Biology*, *31*(1), 779–805. https://doi.org/10.1146/annurev-cellbio-100913-013038

Röder, B., Stock, O., Bien, S., Neville, H., & Rösler, F. (2002). Speech processing activates visual cortex in congenitally blind humans. *European Journal of Neuroscience*, *16*(5), 930–936. https://doi.org/10.1046/j.1460-9568.2002.02147.x

Röder, B., Teder-Sälejärvi, W., Sterr, A., Rösler, F., Hillyard, S. A., & Neville, H. J. (1999). Improved auditory spatial tuning in blind humans. *Nature*, *400*(6740), 162–166. https://doi.org/10.1038/22106

Rubenstein, J. L. R., & Rakic, P. (1999). Genetic Control of Cortical Development. *Cerebral Cortex*, *9*(6), 521–523. https://doi.org/10.1093/cercor/9.6.521

Schinazi, V. R., Thrash, T., & Chebat, D.-R. (2016). Spatial navigation by congenitally blind individuals. *WIREs Cognitive Science*, *7*(1), 37–58. https://doi.org/10.1002/wcs.1375

Simi, A., & Studer, M. (2018). Developmental genetic programs and activity-dependent mechanisms instruct neocortical area mapping. *Current Opinion in Neurobiology*, *53*, 96–102. https://doi.org/10.1016/j.conb.2018.06.007

Van der Loos, H., & Woolsey, T. A. (1973). Somatosensory Cortex: Structural Alterations following Early Injury to Sense Organs. *Science*, *179*(4071), 395–398. https://doi.org/10.1126/science.179.4071.395

Voss, P., Lassonde, M., Gougoux, F., Fortin, M., Guillemot, J.-P., & Lepore, F. (2004). Early- and late-onset blind individuals show supra-normal auditory abilities in far-space. *Current Biology: CB*, *14*(19), 1734–1738. https://doi.org/10.1016/j.cub.2004.09.051

Wang, Q., Liao, C.-C., Stepniewska, I., Gabi, M., & Kaas, J. H. (2021). Cortical connections of the functional domain for climbing or running in posterior parietal cortex of galagos. *Journal of Comparative Neurology*, *529*(10), 2789–2812. https://doi.org/10.1002/cne.25123

Whitlock, J. R. (2017). Posterior parietal cortex. *Current Biology*, *27*(14), R691–R695. https://doi.org/10.1016/j.cub.2017.06.007

Wright, N. F., Erichsen, J. T., Vann, S. D., O'Mara, S. M., & Aggleton, J. P. (2010). Parallel but separate inputs from limbic cortices to the mammillary bodies and anterior thalamic nuclei in the rat. *Journal of Comparative Neurology*, *518*(12), 2334–2354. https://doi.org/10.1002/cne.22336

Zembrzycki, A., Chou, S.-J., Ashery-Padan, R., Stoykova, A., & O'Leary, D. D. M. (2013). Sensory cortex limits cortical maps and drives top-down plasticity in thalamocortical circuits. *Nature Neuroscience*, *16*(8), 1060–1067. https://doi.org/10.1038/nn.3454

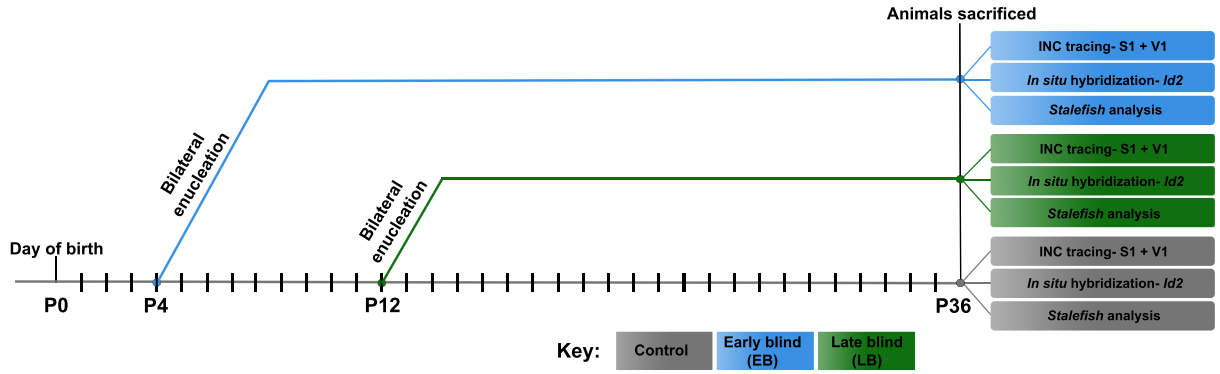

Figure 1. Experimental timeline. 2 experimental enucleated groups and 1 control group of *Monodelphis domestica* were generated for this study. Control animals (blue) did not undergo bilateral enucleation. Early Blind (EB, pink) animals were bilaterally enucleated at postnatal day (P) 4 and Late Blind (LB, purple) animals were enucleated at P12. All groups of animals generated for this study were sacrificed at P36, where their brains were removed for multi-modal endpoints including gene expression assays of *RZRβ* and *Id2*, dye tracing experiments of somatosensory (S1) and visual cortex (V1), and staining for cortical area analyses.

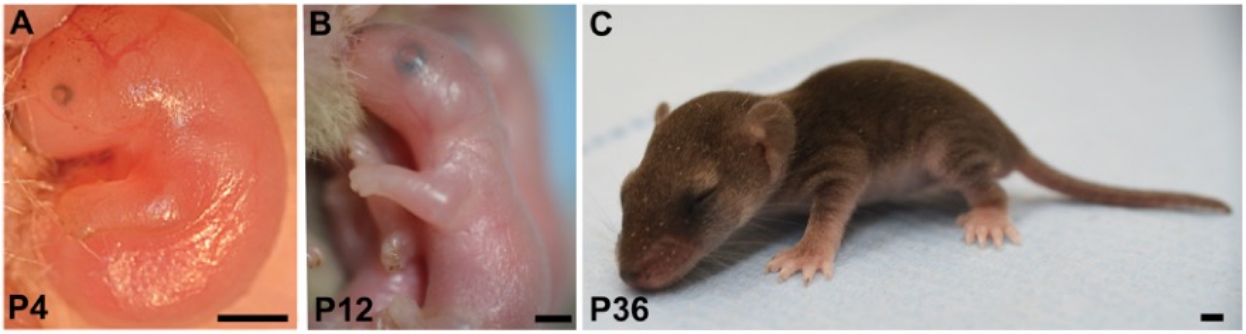

Figure 2. Photographs of *Monodelphis domestica* at ages enucleated and analyzed within current study. A, Opossum at P4, at age of Early Blind enucleation. **B,** Opossum at P12, at age of Late Blind enucleation. **C,** P36 Opossum at age of endpoint analysis. Scalebars 1mm (A),1mm (B) ,3mm (C).

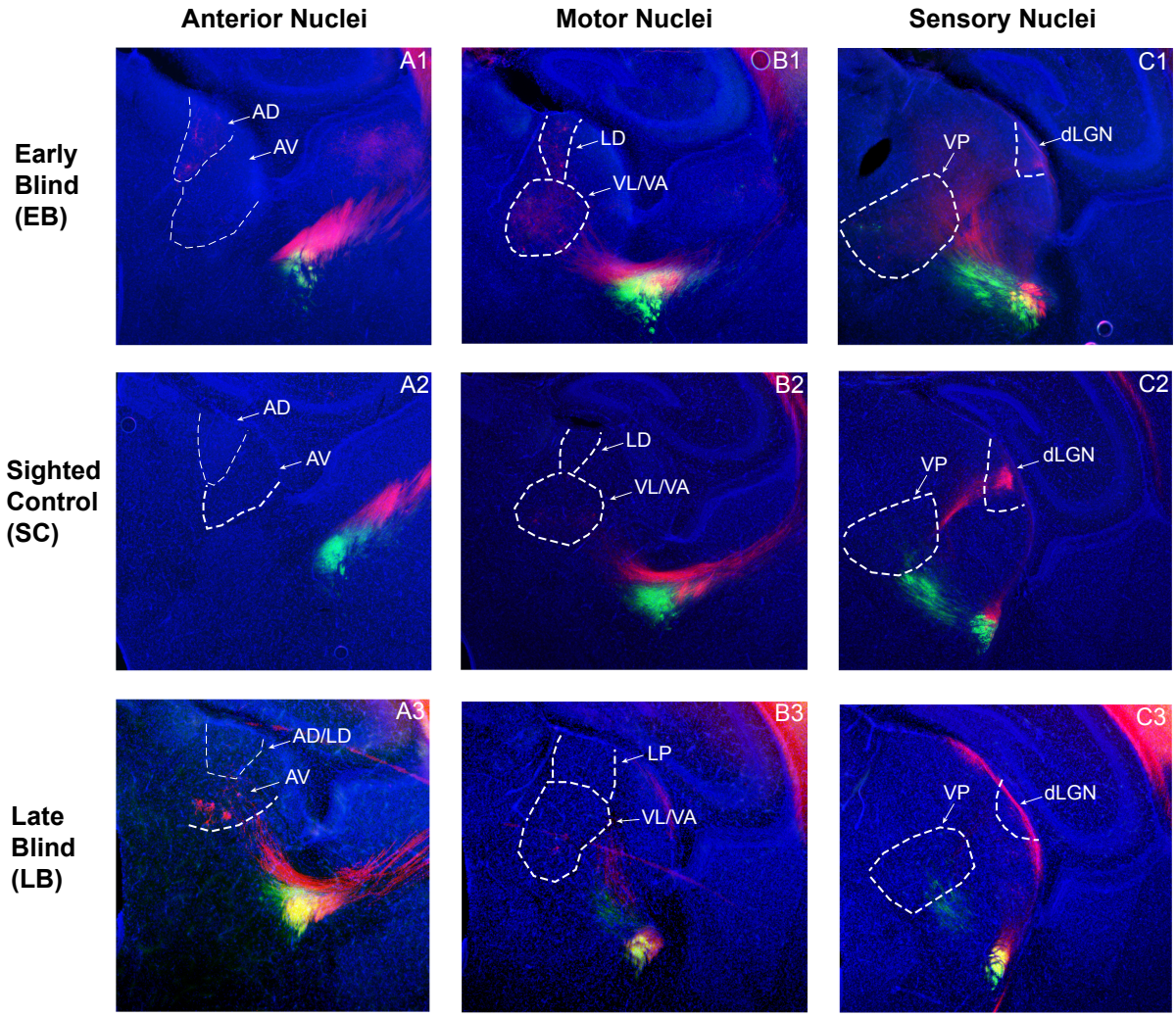

Figure 3. **Primary sensory thalamic tracing at P36. A,B** EB and LB animals display ectopic labeling of red DiI-traced cells stemming from V1 injections within the anterior and motor nuclei. **C,** EB animals also show ectopic label in the ventral posterior nucleus. Images oriented dorsal (D) up, lateral (L) right. Scale bar, 500 um.

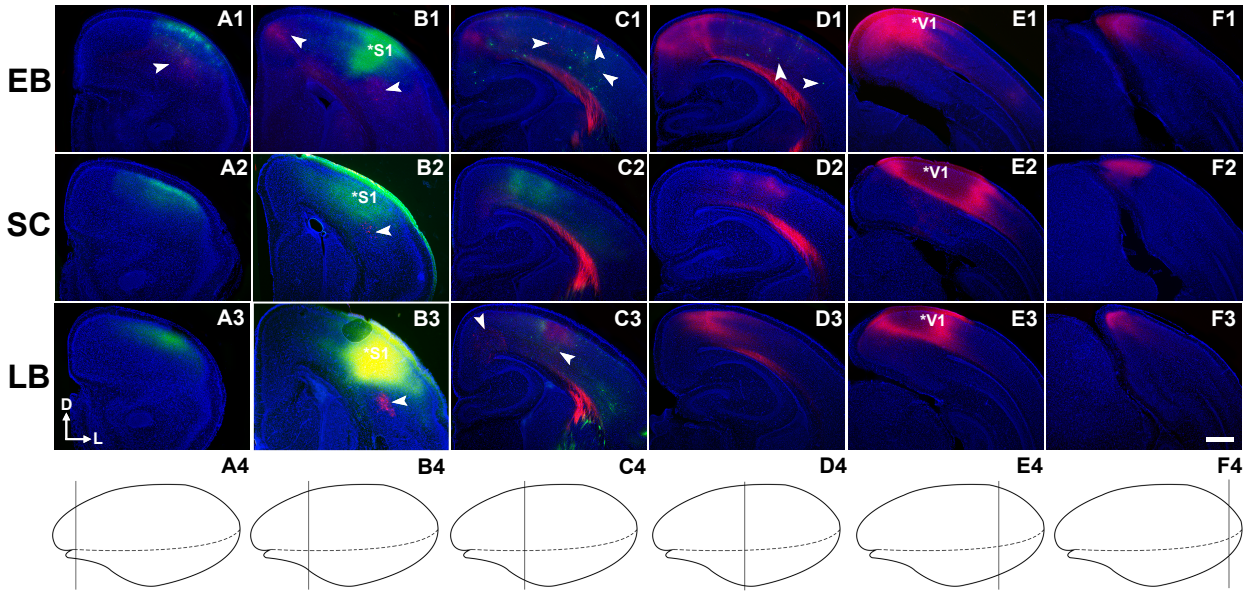

Figure 4. Cortical tracing of S1 and V1 at P36. Rostral-to-caudal series of coronally cut sections in P36 EB (A1-F1), control (A2-F2), and LB (A3-F3) opossum brains which were injected with DiA in S1 (*S, B1-3) and DiI in V1 (*V, E1-3). Rostral-to-caudal level of coronal sections are indicated by vertical lines depicted in cortical hemisphere drawings in A4-F4. EB animals display a wide increase in overall projection zones of both S1 and V1 compared to controls, as indicated by red-labeled cells in rostral portions of cortex not seen in controls (white arrows, A1-C1) and green labeled cells in caudal positions not seen in controls (white arrows, D1). In comparison, LB animals display an overall reduction in the severity of this phenotype but do show an overall increase in V1 projection zone, as seen by rostral red-labeled cells in cortex (white arrows, B3-C3). Images oriented dorsal (D) up, lateral (L) right. Scale bar, 500 um.

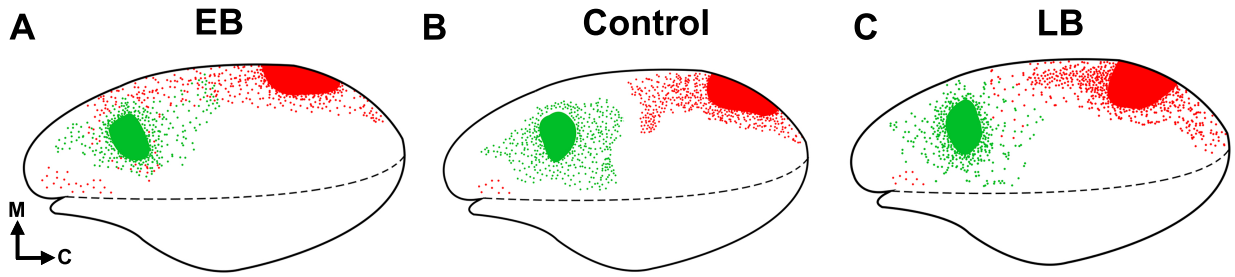

Figure 5. 2D 'flattened' reconstructions of dye tracing experiments. Coronal section data transformed and plotted on 2D 'flattened' single hemisphere templates for overall projection zone visualization. EB animals display marked increases in projection zones of both S1 and V1 injections patterns compared to sighted controls (SC). In contrast, LB animals show only a rostral shift in V1 projection zone compared to controls. Reconstructions oriented medial (M) up, caudal (C) right. Scale bar, 1 mm.

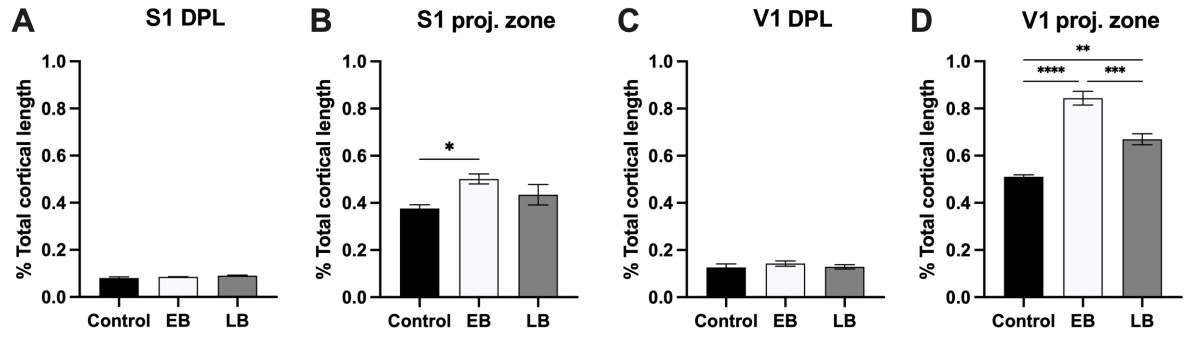

Figure 6. Dye tracing quantification. A, S1 dye placement location (DPL) quantification. No differences are seen in overall spread of S1 injections amongst any group. **B,** EB animals show a statistically significant increase in S1 projection zone compared to controls. **C,** No differences are seen in overall spread of V1 injections amongst any group. **D,** EB and LB animals both show increased projection zones stemming from V1 injections compared to controls. However, LB animals show a reduction in the severity of this difference as indicated by the significant

decrease in V1 projection zone compared to EB animals. * *P* <0.05, ** *P* <0.01, *** *P* <0.001, **** *P* <0.0001. Control: *n* =5 ; EB: *n* = 6; LB: *n* = 5.

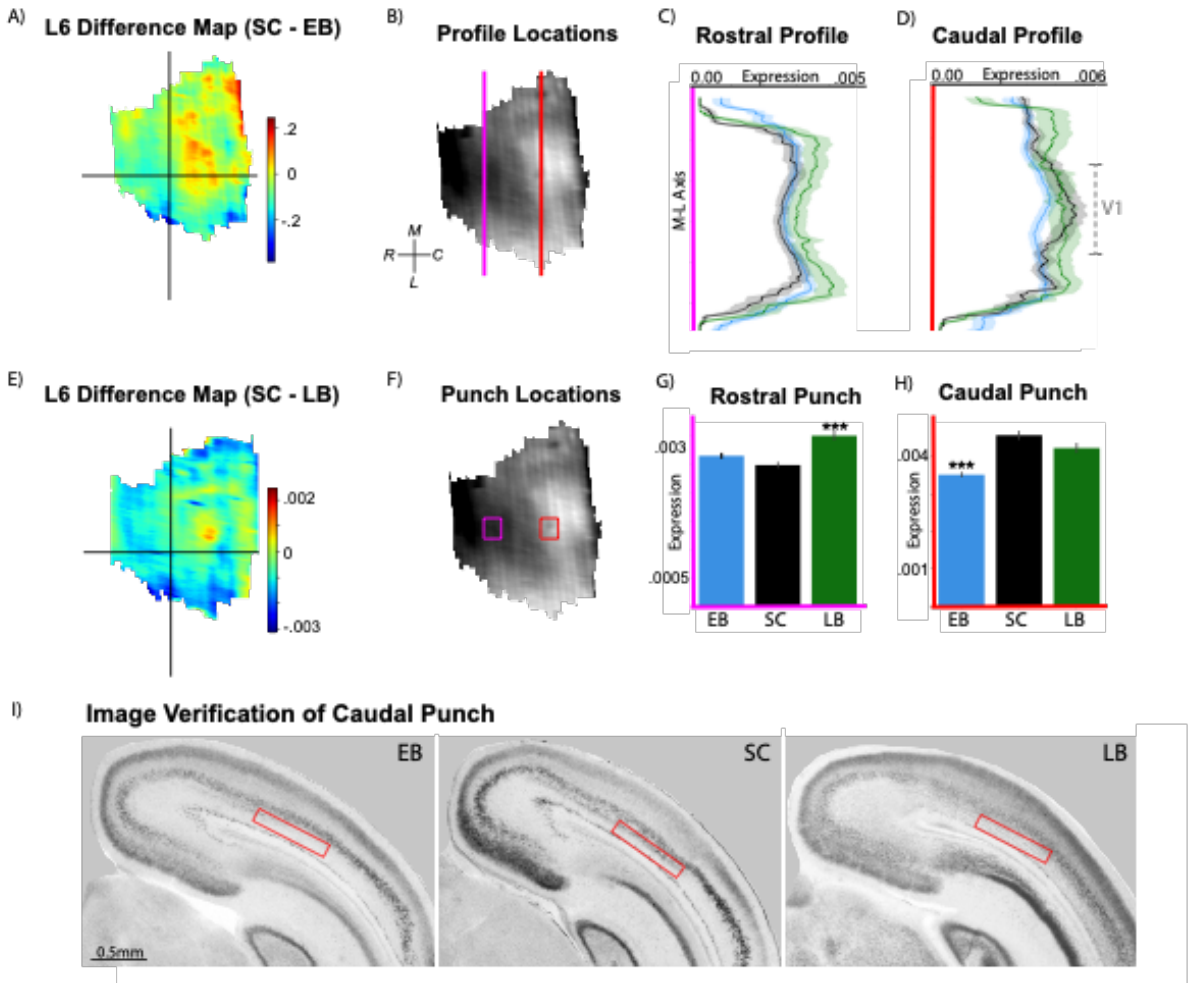

Figure 7. Differences in Layer 6 Id2 expression between blind and sighted opossums. A) Id2 expression difference map created from cortex-wide layer 6 Id2 expression in early blind and sighted opossums. The early blind (EB) map was subtracted from the sighted control map (SC). Yellow and red areas indicate higher expression of Id2 in sighted controls.
Red areas indicate regions of interest. (B) Average Layer 6 Id2 sighted control expression map showing the locations for the visual cortex profiles (red line) and digital micropunch

(red box). Locations were determined from areas of high difference in (A). (C) Line graphs show medial-lateral average expression in EB (blue), LB (green), and SC (black) opossums. The Y-axis corresponds to the location picture in (B). The X-axis denotes expression level. Note that Id2 expression is high in layer 6 of LB and SC opossums, but decreases in EB opossums. (D) Bar graphs showing average level of expression in caudolateral visual cortex shown in the red box in (B). Early and late blind opossums have significantly less Id2 expression than sighted controls ($p < .001$). (E) Coronal sectionsof EB, LB, and SC oppossums hybridized for Id2. This serves as image verification of the location used to quantify expression level in (D). The red box corresponds to the spatial location shown in (B) and quantified in (D). Note that layer 6 expression is absent in EB animals, and low in LB animals compared to sighted controls.

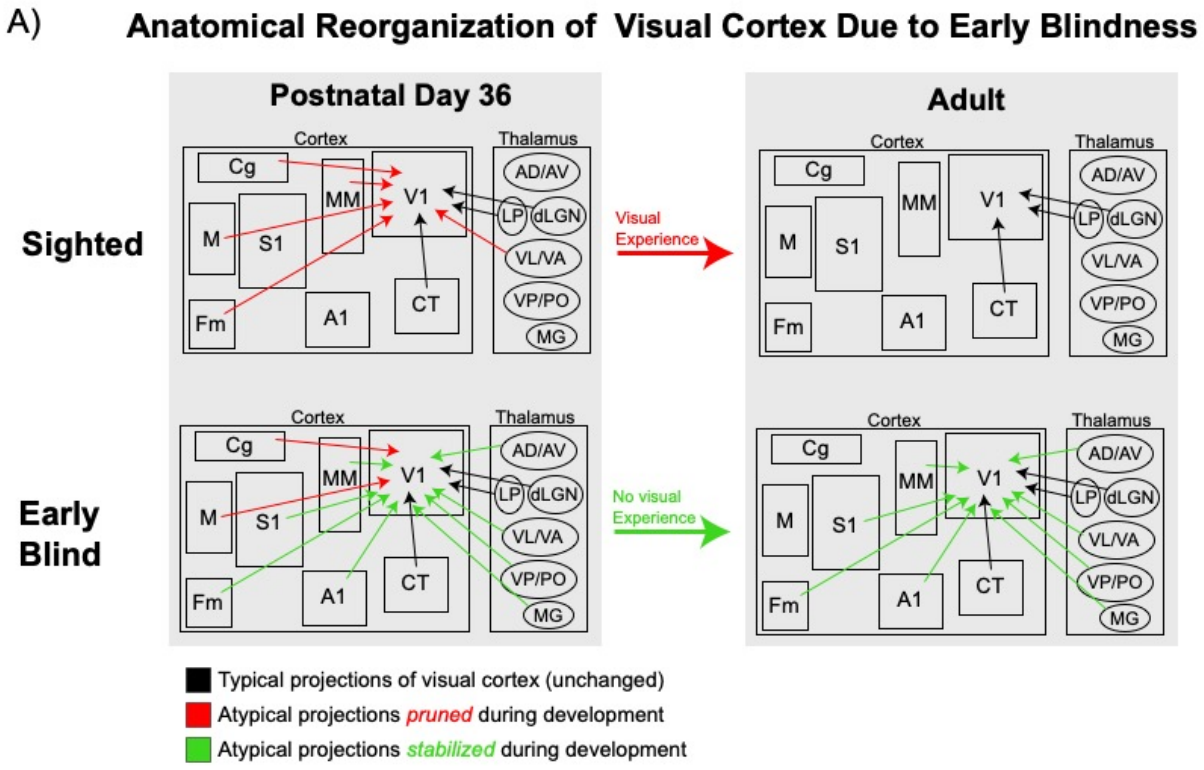

Figure 8. Summary diagram. A) connection diagrams showing changes in thalamocortical and corticocortical connections in sighted and blind opossums from P36 (left) to adulthood (right). At P36, early blind opossums already show a different phenotype compared to sighted controls (top vs bottom row). By adulthood, connections are pruned in sighted animals, but remain unchanged in blind opossums. Data was pooled from the current study and Karlen and Krubitzer 2009.

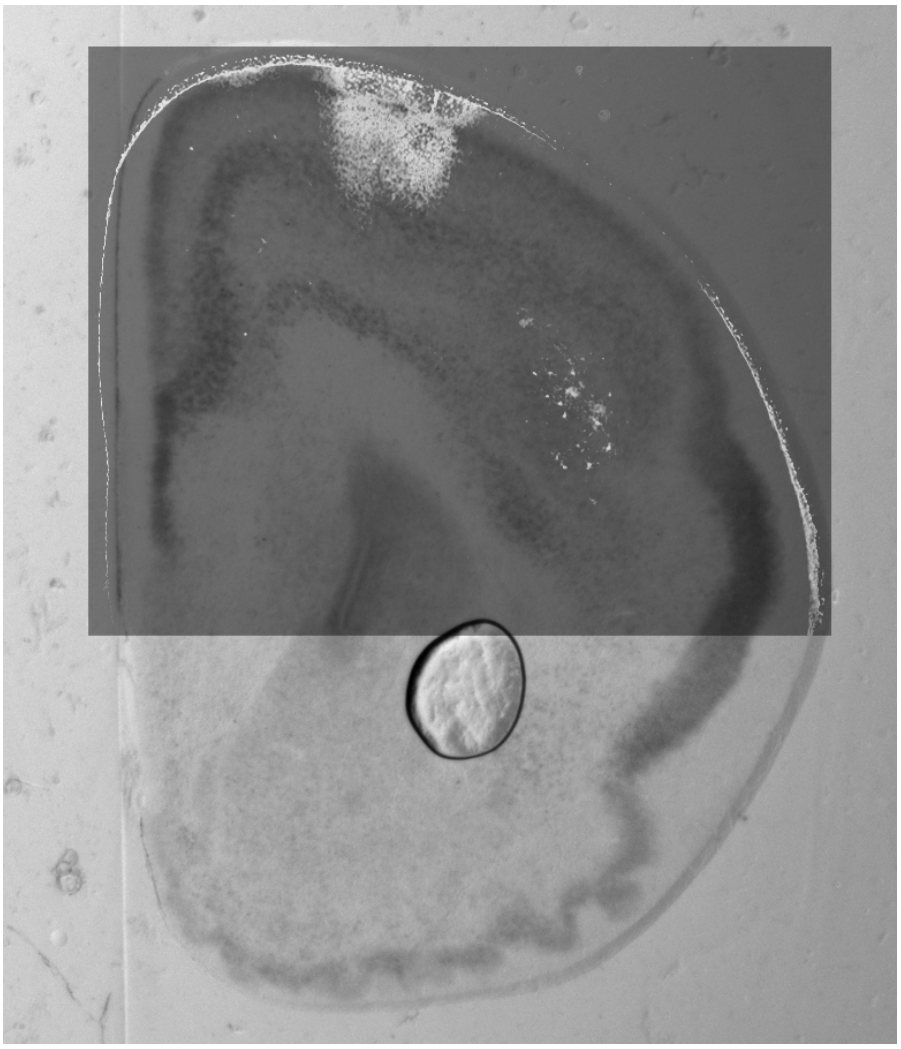

Figure S1. Overlay of DiI label from visual cortex on coronal section of Id2-hybridized tissue. Note the cells (white dots to lateral aspect of cortex) overlap with the darkly stained frontal “F” region.

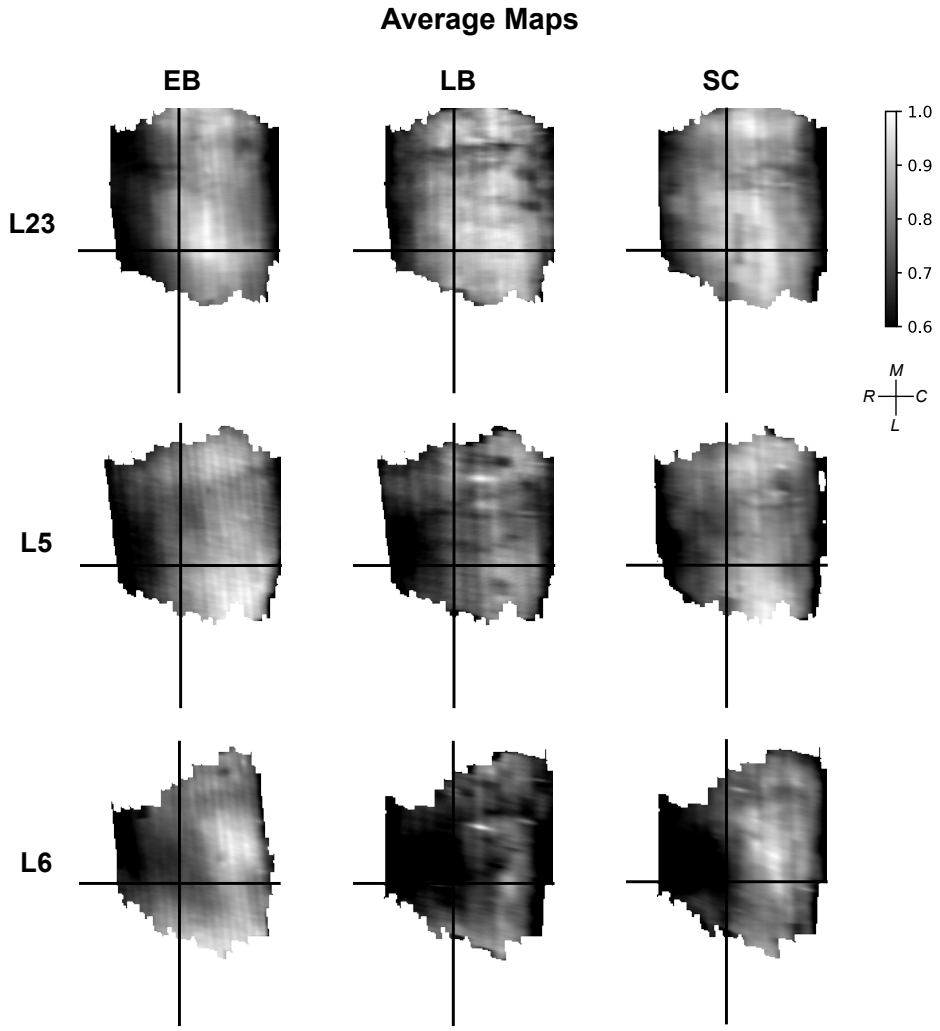

Figure S2. Average expression heatmaps by condition showing whole cortex layer-specific Id2 expression. Rows show layers chosen for analysis while columns denote condition. White regions denote areas of high expression while dark grey denotes low expression. For all data shown, rostral is to the left (R). Note the high expression in caudal cortex for layer 6 maps, elucidating the average boundary of visual cortex for each condition. Abbreviations (EB: early blind, SC: sighted control, LB: late blind).

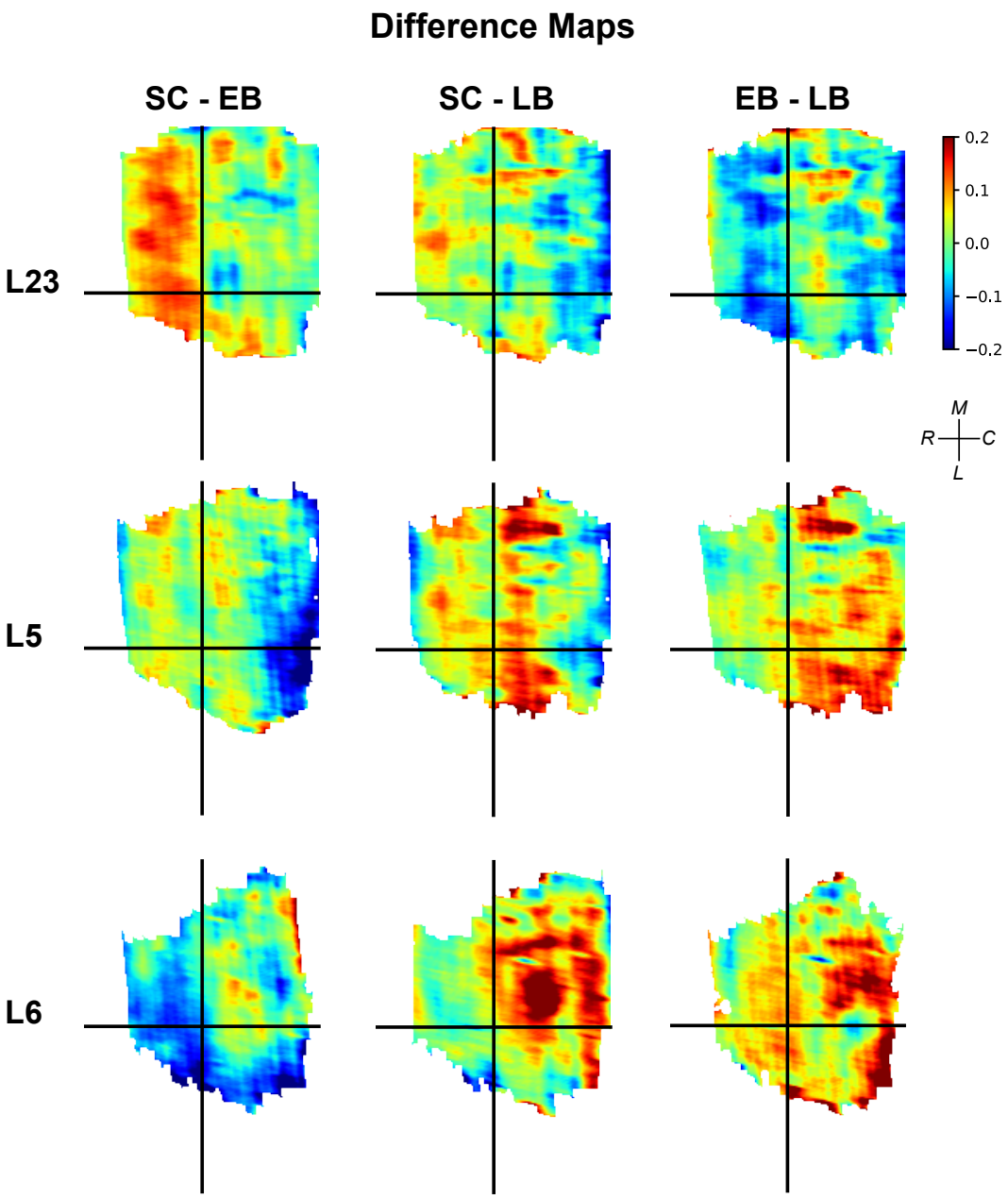

Figure S3. Layer specific id2 difference heatmaps generated by subtracting maps from figure S2.

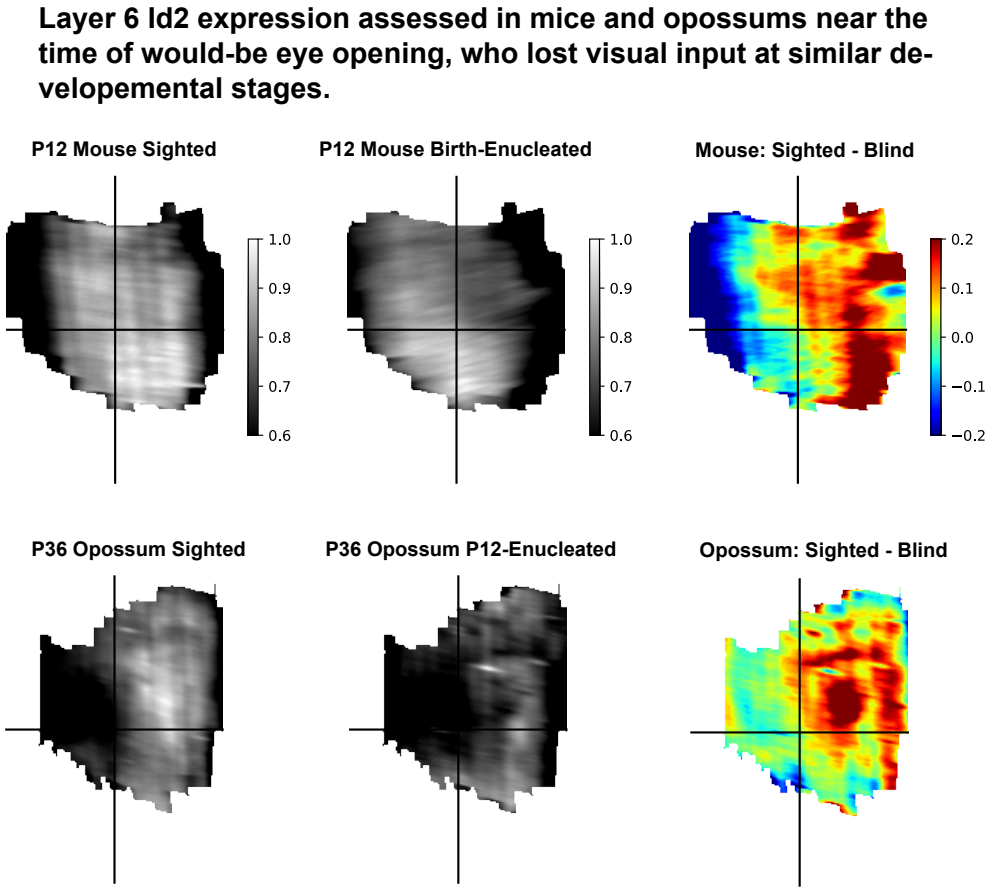

Figure S4. Id2 Layer 6 difference maps of mice and possums enucleated at similar developmental time points (after TCA innervation) and assessed near the time of eye opening. Data was collected from dye et al 2012 and re-analyzed using the stalefish program. Note the similarity in the reduction of id2 expression in both blind mice and opossums, showing a similar effect of vision loss across species.

Chapter 4.

At the time of this dissertation, the following manuscript entitled "**Comparing cortex-wide gene expression patterns between two rodent species in a common reference frame**," is currently in revision at *P.N.A.S*, and thus is presented in the format of the journal.

Supplementary information for this article can be found at:
https://www.biorxiv.org/content/10.1101/2021.07.28.454203v1

Citation:
Englund, M., James, S. S., Bottom, R., Huffman, K. J., Wilson, S. P., & Krubitzer, L. A. (2021). Comparing cortex-wide gene expression patterns between species in a common reference frame. *bioRxiv*.

Comparing cortex-wide gene expression patterns between two rodent species in a common reference frame.

Authors: Mackenzie Englund[1]†, Sebastian S. James[2]†, Riley Bottom[3], Kelly J. Huffman[3], Stuart P. Wilson[2]‡, Leah A. Krubitzer[1]*‡

Affiliations:

[1] Department of Psychology, University of California Davis; 1 Shields Ave, Davis, CA, 95616, US.

[2] Department of Psychology, University of Sheffield; Sheffield S10 2TN, UK.

[3] Department of Psychology, University of California Riverside; 900 University Ave, Riverside, CA, 92521, US.

*Corresponding author. Email: lakrubitzer@ucdavis.edu

† These authors contributed equally to this work

‡ These authors contributed equally to this work

Abstract: Advances in sequencing techniques have made comparative studies of gene expression a current focus for understanding evolutionary and developmental processes. However, insights into the spatial expression of genes have been limited by a lack of robust methodology. To overcome this obstacle, we developed methods for quantifying and comparing tissue-wide spatial patterns of gene expression within and across species. Here we compare cortex-wide expression of *Id2* and *RZRβ* mRNA in early postnatal mice and voles. We show that neocortical patterns of *Id2* expression are moderately conserved between species, but that the degree of conservation varies by cortical layer and area. By comparison, patterns of *RZRβ* expression are highly conserved in somatosensory areas, and more variable between species in visual and auditory areas. We propose that these differences reflect the independent evolution of brains, bodies and sensory systems in the 35 million years since their last common ancestor.

Almost everything we know about the human brain comes from comparative studies of other animals: from genes involved in cortical development to system-level networks that generate complex behaviours. Comparative studies of living species provide a robust means by which to understand unknown forms, like humans, and even extinct forms like our early mammalian ancestors. Importantly, these types of studies are critical for identifying features of brain organization that are conserved between species and those that may have been derived in different lineages. They also allow us to determine how developmental programs and timing schedules may vary across species, and better understand how phenotypic diversity can be generated over shorter and longer timescales. Finally, by making valid comparisons across species, we can begin to understand how complexity emerges in different nervous systems, the rules of brain construction, and the constraints imposed on developing and evolving nervous systems.

Despite the importance of comparative studies in biology, most comparisons of anatomically reconstructed data are subjective, and most gene sequencing studies neglect the actual spatial patterns of gene expression across a structure, focusing instead on cell-type expression (1–3). Moreover, many current methods for making comparisons fail to capture the three-dimensional nature of the brain, which is composed of asymmetrical structures that can vary markedly in relative shape, size, and location across species and between developmental time-points. Despite the 3D nature of the brain, most studies collapse data into two dimensions driven largely by the plane of section at which the brain is cut.

As such, neurobiologists are faced with two challenges. First, attempting to understand 3D structures by analyzing 2D images is inherently problematic because the loss of spatial information is unavoidable, especially in curved structures (4). 2D analysis often involves pre-specifying regions of interest (ROI's) to quantify the presence of labelled cells or mRNA

expression after in-situ hybridization (ISH), narrowing the focus and potentially missing overall differences. A second challenge, which arises when making comparisons between structures in different species and/or at different developmental time-points, or between different experimental conditions, is determining the extent to which 2D spatial patterning might be invariant to basic transformations in the size and shape of the 3D structure. To this end, it is important for comparisons to be made with respect to a common anatomical reference frame.

In the current study, we overcame these challenges by developing a set of algorithms for brain slice registration in 3D, and for incorporating ISH data into a common reference frame to enable point-by-point comparisons between species or experimental conditions. These tools, which we refer to collectively as *Stalefish*, *The Spatial Analysis of Fluorescent (and non-fluorescent) In-Situ Hybridization*, allowed for the laminar and spatial patterns of expression of genes involved in cortical development to be quantified and compared in two species of age matched rodents. Our analysis of *Id2* and *RZRβ* cortical expression patterns in early postnatal mouse and vole brains reveals both a strong layer-specific conservation of the patterning of these genes, as well as area-specific differences that shed new light on the ontogeny and phylogeny of neocortical arealization.

Reconstructing whole-brain patterns of gene expression from processed tissue.

In mice (*Mus musculus)* and prairie voles (*Microtus ochrogaster*), direct layer- and area-specific comparisons were made between the cortex-wide expression patterns of two genes important for cortical development: *Id2* (Inhibitor of DNA-binding 2), and *RZRβ* (RAR-related orphan receptor beta) (5–9). Using a novel algorithm for slice registration developed as part of the *Stalefish* methodology, we could for the first time visualize and quantify cortex-wide layer-specific patterns of gene expression in 3D, and determine the extent to which these patterns are conserved across species or derived in a particular lineage. To illustrate how layer-specific

cortical in-situ hyridization (ISH) data can be reconstructed from coronal sections, the *Stalefish* curve drawing tool was used to process an entire hemisphere of a postnatal day zero (P0) vole brain (Fig. 1A) hybridized for *Id2* (Fig. 1, B-E). The *Stalefish* 3D viewer tool was then used to show the 3D-reconstructed expression pattern in the superficial layers (Fig. 1, F-G). Finally, the *Stalefish* digital flattening tool was used to project the data into a new 2D plane for subsequent analysis. In this plane, the piriform cortex became clearly demarcated as an area of high expression, and the shapes and positions of several other areas of high and low expression in the neonatal vole cortex were revealed to correspond well with descriptions of cortical field boundaries later observed in adult voles (10) (Fig. 1H), confirming the proposed role of this gene as an 'area marker' for putative neocortical fields. The *Stalefish* methodology was further validated by comparing reconstructions of our mouse data to reconstructions that we made using similar data obtained from the Allen Mouse Brain Atlas (11,12) (fig. S1).

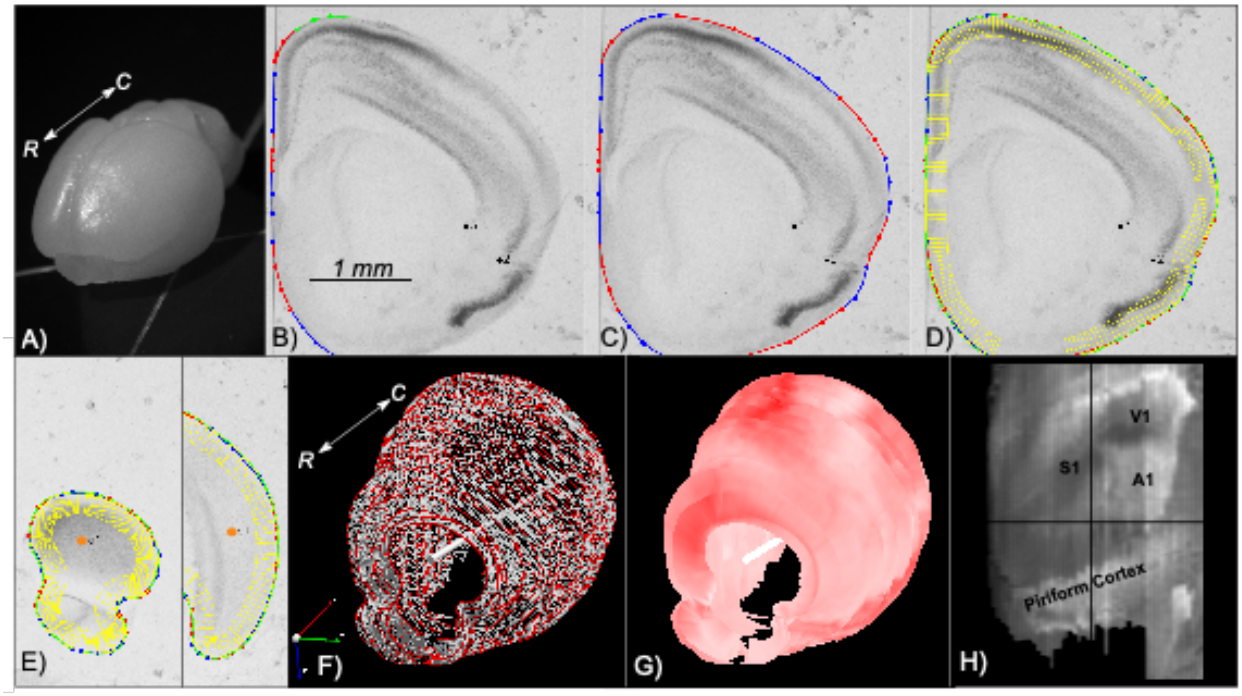

Fig. 1. Stalefish Workflow. (A) Rostral view of an unfixed vole brain. The rostral-caudal axis is shown (white arrow). (B-E) Screenshots from *Stalefish* of coronal sections of *Id2*-hybridized vole

tissue showing the curve drawing method. Dark regions indicate a higher incidence of *Id2* mRNA. (B) Marked locations around the perimeter of the brain. The perimeter points are collected into small sets of 4 or 5 points at a time. The green points are the newest set of perimeter locations and will become the next 'blue' set (the red and blue colors are simply a guide for the user). The number of points in each section determines the order of the Bezier curve which will be fitted to that section. The black dots numbered 2 and 3 show landmark placement location for alignment. (C) Once the perimeter points have been laid out, a piecewise fit is found for the points by modifying the individual Bezier curves to ensure that the curve gradient is continuous at the joints. (D) The green line shows the final fit. Evenly spaced normal vectors extended down from the fit line give sampling boxes in yellow. For each sampling box, the user can access the mean luminance, along with all of the per-pixel values and the position within the sampling box. (E) An axis mark (orange dot, drawn larger for illustrative purpose) on the first and last slice define a user-defined 'brain axis' used for alignment. (F) *Stalefish* output using sfview. Curve points are shown as red spheres. By connecting the spheres to make a mesh, a surface is generated. The white bar shows the user-defined brain axis, derived from the two axis marks placed on the brain slices. The rostral-caudal axis is shown (white arrow). (G) The mean luminance of the sampling boxes can then be indicated on the smoothed surface to give a 3D reconstruction of the gene expression map. Here, we used a monochrome colormap for which full-saturation red corresponds to the maximum *Id2* expression signal. (H) Digitally-flattened and reference-frame transformed 3D surface map (from B-G) using sfview. Abbreviations: rostral (R), caudal (C), millimeter (mm), primary somatosensory cortex (S1), primary visual cortex (V1), primary auditory cortex (A1).

Conservation of cortex-wide gene expression across species.

Id2 is a key transcription factor in neurodevelopment that regulates cellular differentiation and neurite outgrowth (13–16). We quantified the degree of conservation of cortex-wide patterns of *Id2* expression between prairie voles and mice and found that the laminar and areal patterns of *Id2* expression are highly conserved across species. We first hybridized neonatal vole (n = 7) and mouse (n = 3) brain tissue for *Id2* in animals matched for developmental stage. *Id2* was expressed in all cortical layers except layer 4 in both species, similar to findings from previous studies (17). *Stalefish* was used to fit curves on each *Id2*-hybridized section of the series at depths from the neocortical surface that correspond to layer 2/3, layer 5, and layer 6, and to digitally unwrap and flatten the 3D reconstructed expression patterns. Using the positions of external anatomical landmark locations commonly identifiable in all brains, a linear transformation was computed for mapping the flattened reconstruction of each brain to the coordinate system of an arbitrary reference brain from the comparison set, allowing cortex-wide expression patterns from multiple brains to be compared point-by-point in a common reference frame (See *Methods*).

Following these transformations, we quantified the similarity of cortex-wide patterns of *Id2* expression by applying Pearson correlation analyses to the point-by-point matched expression levels between maps, excluding any points not present in every pattern submitted for a given set of comparisons. Correlation coefficients were calculated for each pair of expression patterns and comparisons were made with respect to cortical layer, and within and across species (Fig. 2, A and B). To our knowledge, this is the first time that cortex-wide patterns have ever been quantitatively compared across layers and species. Within-species comparisons demonstrated that layer 2/3 expression maps were highly correlated (Vole: $r_{avg}(6) = .523 \pm .105$, Mouse: $r_{avg}(3) = .854 \pm .031$), as were layer 5 and layer 6 maps (Layer 5: Vole: $r_{avg}(6) = .605 \pm .077$, Mouse: $r_{avg}(3) = .873 \pm .015$) (Layer 6: Vole: $r_{avg}(6) = .748 \pm .047$, Mouse: $r_{avg}(3) = .644 \pm .041$).

Examining expression maps across layers within a species revealed that layer 2/3 expression was weakly correlated with layer 5 (Vole: $r_{avg}(16) = .159 \pm .141$, Mouse: $r_{avg}(9) = .318 \pm .078$), and layer 5 expression was weakly correlated with layer 6 expression (Vole: $r_{avg}(16) = .169 \pm .078$, Mouse: $r_{avg}(9) = .303 \pm .075$). Conversely, as expected by the lack of expression in layer 2/3 of primary somatosensory (S1) and primary visual (V1) cortex, and high expression in layer 6 of these areas, layer 2/3 expression was negatively correlated with layer 6 expression in both mice and voles (Vole: $r_{avg}(16) = -.208 \pm .149$, Mouse: $r_{avg}(9) = -.241 \pm .073$). As depicted in Figure 2A and 2B, the directions of these layer-specific correlations were remarkably well conserved across species. However, when comparing the degree of within-layer correlation across species, mice exhibited significantly higher correlations on 5 out of the 6 comparisons ($p_{Layer\ 2/3} = .014$, $p_{Layer\ 5} = .014$, $p_{Layer\ 6} = .047$, $p_{Layer\ 2/3\ vs\ 5} = .007$, $p_{Layer\ 2/3\ vs\ 6} = .466$, $p_{Layer\ 5\ vs\ 6} = .001$), suggesting that spatial patterns of expression of *Id2* amongst neonatal mice varied less than amongst neonatal voles. Between species, layer 2/3 *Id2* expression in mice (n = 3) and voles (n = 4) was positively correlated ($r_{avg}(12) = .523 \pm .109$) (Fig. 2C), as were layer 5 and layer 6 expression maps (Layer 5: $r_{avg}(12) = .482 \pm .112$, Layer 6: $r_{avg}(12) = .234 \pm .084$). Taken together, the similarities in direction and magnitude of the above correlational data provide the first ever direct and quantitative evidence that mice and voles have conserved laminar expression profiles of *Id2* during early postnatal brain development. These findings add support for our hypothesis that the spatial pattern of *Id2* expression across the entire neocortex is conserved on a by-layer basis.

Following our analysis of *Id2* expression by layer, we sought to determine if expression of Id2 in specific regions of the neocortex was conserved across species (Fig. 2, D-L). While previous work has suggested that high *Id2* expression overlaps roughly with sensory areas (16,18–20), our data show that extremely precise regions of high and low expression of *Id2* correspond with the shapes of putative cortical areas in each layer, and how this correspondence varies

between species. Specifically, in both species there was a marked absence of *Id2* expression in layer 2/3 in the putative primary visual (V1) and primary somatosensory cortex (S1), while *Id2* expression was highly expressed in layer 2/3 of the putative primary auditory cortex (A1) (Figure 2D/E/F). Layer 5 *Id2* expression in both mice and voles was strongest in A1 and in the caudal portion of the medial wall (Fig. 2, G, H, I). In layer 6, *Id2* was highly expressed in all of the putative primary sensory areas (S1, V1, A1), in both voles and mice, although putative cortical areas were more clearly defined in voles (Fig. 2, J, K, L).

Next, we observed that expression maps appeared more similar between species in the caudal compared to rostral half of the neocortex. To quantify this observation, and to demonstrate the usefulness of the transformed data for comparing expression levels in specific regions of interest, we created 200μM thick expression profiles of the different layers in the caudal portion of the neocortex (Fig. 2, F, I, J). Profiles spanned medial to lateral, encompassing portions of the medial wall, visual, and auditory cortex (red line in Fig. 2 E, H, K). The average expression profiles in voles (blue trace) and mice (orange trace) were highly correlated for layer 2/3 ($r(10) = .860$), with both species exhibiting high expression at the medial wall, a substantial decrease in expression in putative V1, and a rise in expression in putative A1 (Fig. 2F). The layer 5 profiles showed three clear peaks of expression in both species, corresponding to the medial wall, putative V1, and putative A1, and were also strongly correlated ($r(10) = .714$) (Fig. 2I). Lastly, the *Id2* expression profiles of layer 6 were also highly correlated between mice and voles ($r(10) = .97$), with bootstrapped 95% confidence intervals overlapping for nearly the entire medial-lateral length of the section, including a decrease in expression between visual and auditory cortical areas (Fig. 2L, black arrow).

To adjust for the possibility of inflated or spurious correlations, we normalized expression levels between species by differencing the data along the medial-lateral axis, using percentage

change to the previous value instead of absolute magnitude. This cautious approach corrected for differences that may still exist between species even after mean-centering (fig. S2). Correlations of percentage change showed weaker, but still strong correlations between species across cortical layers (fig. S2, right). Posterior layer 2/3 *Id2* expression profiles remained positively correlated between voles and mice ($r_{\%\ change}(10) = .57$). Similarly, layer 5 and 6 *Id2* expression remained significantly correlated (Layer 5: $r_{\%\ change}(10) = .697$), Layer 6: $r_{\%\ change}(10) = .414$). Thus, after controlling for changes in absolute magnitude, expression profile data from caudal cortex confirms that *Id2* expression is tightly conserved on a layer-by-layer basis between mice and voles at early stages of cortical development.

Taken together, between-species correlations show that the spatial pattern and level of *Id2* is moderately conserved across the neocortex in mice and voles, but the extent of conservation varies by layer and area. Notably, while whole-map correlations between species ranged from high to moderate between layers, expression profiles of caudal cortex encompassing visual and auditory cortex specifically, were tightly correlated, suggesting that *Id2* expression in caudal areas is highly conserved. However, the above data also shows that key differences exist between species in layer 6 and rostral neocortex, where the weakest correlations were present. These differences may be due to the fact that laboratory mice are highly inbred and not reflective of their natural counterparts, or they may represent species specializations and changes in developmental trajectories that have emerged in the 35 million years of independent evolution that mice and voles have undergone (21).

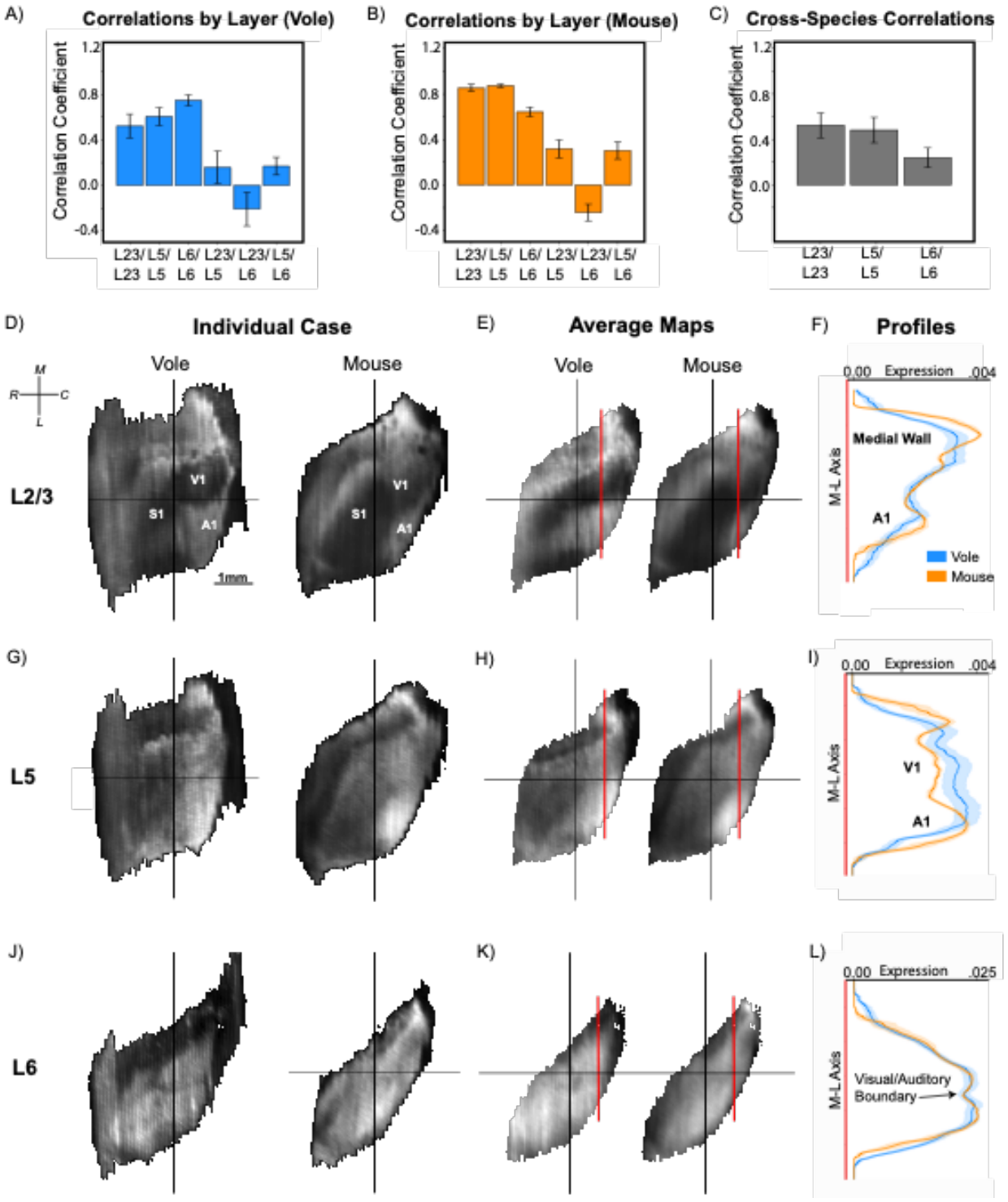

Fig. 2. The spatial pattern of *Id2* expression is conserved on a layer-by-layer and area basis. (A & B) Bar graphs of average correlation coefficients between individuals within-species shown as mean with standard deviation across cortical layers. There is little within-species

variation of *Id2* expression by layer, and both voles (n=6) and mice (n=3) show similarities in degree and direction of correlations across layers. (C) Bar graph of average correlation coefficient of *Id2* expression maps between species by cortical layer. (D,G,J) Digitally flattened maps (individual example cases) of Id2 expression in different layers reconstructed from coronal sections in a vole (left) and mouse (right) by *Stalefish*. Cases are displayed post-transform and aligned to a common axis. The x and y axes denote spatial coordinates, while expression level is represented as pixel-value at a given coordinate (black = lowest, white = highest). (E, H, K) Average maps of each species by layer. Average maps are displayed as only the locations which overlapped between species post-transform (rostral left, medial up). Vertical red lines show the location at which medial-to-lateral expression profiles were sampled and analyzed (line graphs on the far right). (F, I, L) Line graphs show the 200μM average medial-to-lateral expression profiles between voles (blue) and mice (orange) for a given layer at a specific rostral-caudal depth (red lines in F/I/L). Data is presented as mean with bootstrapped 95% confidence intervals. The x-axis denotes signal level (after mean-centering) and the y-axis denotes the medial-lateral axis from the subiculum to the rhinal fissure. Abbreviations: Layer 2/3 (L23), Layer 5 (L5), Layer 6 (L6), rostral (R), caudal (C), medial (M), lateral (L), millimeter (mm), primary somatosensory cortex (S1), primary visual cortex (V1), primary auditory cortex (A1)

Divergent areas of cortical gene expression across species.

After finding that *Id2* was conserved between mice and voles across cortical layers, we sought to quantify the extent to which area-specific patterns of expression for *RZRβ*, a long-studied primary sensory area marker, diverge. We hybridized neonatal vole and mouse brain tissue for *RZRβ*, whose high layer 4 expression is heavily influenced by input from thalamic sensory nuclei (9,22). Because *RZRβ* is highly expressed in this layer, and sparse in other layers at early stages of development, we restricted our analysis to layer 4 (Fig. 3, A-D) (23). We analyzed serial 100μM sections of tissue, and again reconstructed the data in 3D, digitally

unwrapped and flattened the expression patterns, and projected individual patterns into a common reference frame to enable point-by-point comparisons. We then calculated correlations between the transformed RZRβ expression patterns within and across species (Fig. 3A). Vole *RZRβ* expression patterns were highly correlated across individuals ($r_{avg}(21) = .742 \pm .110$). Remarkably, not only were mouse *RZRβ* maps highly correlated with one another (and significantly more so than with voles: $p = .009$), but the amount of individual variation was near zero ($r_{avg}(3) = .858 \pm .006$). As with *Id2*, cortex-wide *RZRβ* expression patterns were well correlated between species ($r_{avg}(21) = .534 \pm .083$). These results were expected given the evolutionary and life history of these rodent species, and tightly regulated thalamocortical development, which influences *RZRβ* expression. However, the moderate (not strong) correlation in expression between species indicates also that differences have emerged in each lineage.

Because *RZRβ* was found to be expressed in layer 4 in both species and at similar levels, we hypothesized that species differ in terms of the identity of the putative cortical area in which *RZRβ* is expressed, rather than in terms of cortical layer. To begin to address where these differences may have emerged, we compared reconstructed neonatal *RZRβ* cortical expression maps to flattened cortical sections of adult animals stained for myelin, which show clear delineations of cortical field boundaries. We found that *RZRβ* expression in the early postnatal brains revealed the putative cortical areas that were later delineated by myelin stains in adult neocortex (Fig. 3, B and D) (24,25). Specifically, reconstructed *RZRβ* expression patterns clearly demarcated the cortical field boundaries of putative S1, A1 and V1 in the prairie vole (Fig. 3B). While expression patterns for neonatal mice revealed a clearly defined primary somatosensory cortex (Fig. 3D), they did not reveal the putative A1 and V1 to the same extent. In both species, the sub-regions representing the map of the entire body could be identified from the expression patterns in putative S1 (26,27). To our surprise, the second

somatosensory/parietal ventral area (S2/PV) was also delineated in both species. Both mice and voles also displayed *RZRβ* expression in V1, but this expression was more clearly defined in prairie voles. Furthermore, across all vole cases (n = 7), *RZRβ* expression patterns displayed a distinct boundary between the primary and the second visual areas (V1 and V2). To our knowledge, evidence for distinct higher order (HO) cortical fields has not previously been demonstrated at such an early stage in development, and this result suggests that thalamocortical interactions or early arealization gradients may play a stronger role in patterning HO areas than has been previously thought (28). However, we also note that mice lacked a clear delineation between these visual areas and displayed an absence of *RZRβ* expression in putative A1.

We next quantified the magnitude of these species differences by taking digital micro-punches of regions of interest, whose location was determined post-hoc, i.e., after examining cortex-wide difference maps. These maps were created by subtracting the average mouse expression map from the average vole expression map (data not shown). We selected micro-punch regions of interest corresponding to peaks in expression of putative S1, S2/PV, V1, V2, and A1 (Fig. 3, E-H). We then compared the average post-differencing signal value around each expression peak, finding no significant difference in the change in peak expression between species in S1 (anterior barrel cortex) (Fig. 3F; pink box) or S2/PV (Fig. 3F; green box) (S1: R^2_{adj} = .023, F(2) = 1.458, p = 0.255, S2/PV: R^2_{adj} = -.019, F(2) = .636, p = 0.267). While less apparent when observing average or difference maps, we also found no significant difference in the average percentage-change in expression level between species in V1 (Fig. 3H; purple box) (R^2_{adj} = .091, F(2) = 2.961, p = 0.442), which means that for this portion of V1, voles and mice showed similar changes in levels of expression. On the other hand, neonatal voles had significantly higher changes in *RZRβ* expression in V2 than neonatal mice (Fig. 3H; red box) (R^2_{adj} = .315, F(2) = 9.977, p < 0.001). Neonatal voles also showed increased *RZRβ* expression at the spatial

location for A1 (R^2_{adj} = .382, F(2) = 9.037, p = 0.013) (data not shown). Thus, comparison of digital micro-punches from putative cortical fields across species suggests that layer 4 *RZRβ* expression is tightly conserved for some areas (S1, S2/PV, V1), and not others (V2, A1). Together with the correlational data, we interpret these results as evidence that spatial expression patterns and signal levels of *RZRβ* expression are conserved across the somatosensory cortices of mice and prairie voles, but that the patterns and levels of *RZRβ* expression in visual and auditory areas vary between species. Similar to *Id2*, these differences may be products of independent evolution and associated with species specific behaviors mediated by these different sensory systems, or to changes in mice due to inbreeding.

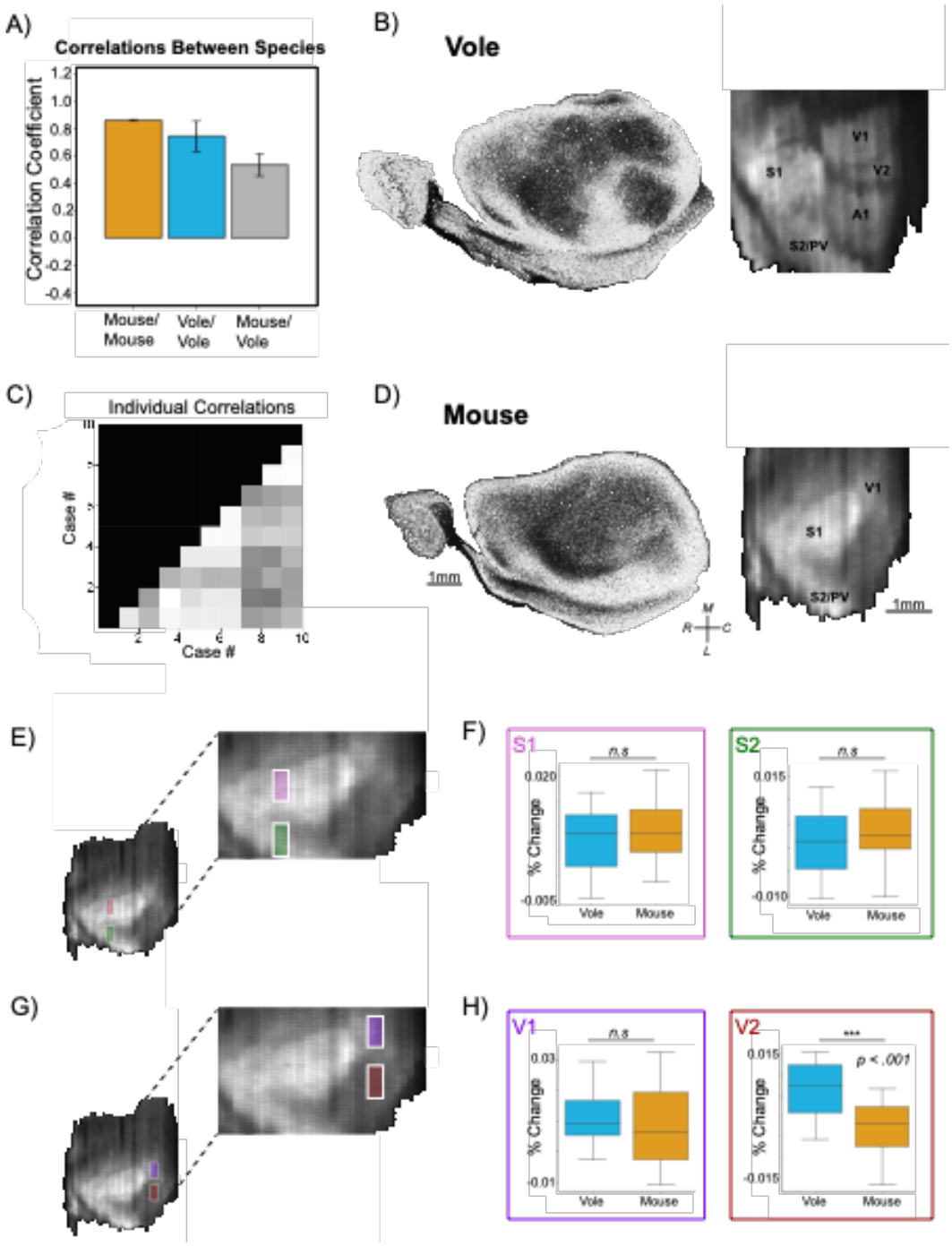

Fig. 3. *RZRβ* expression shows divergent patterns for visual and auditory areas between species. (A/C) Bar graph (A) of average correlation coefficients of whole-cortex layer 4 *RZRβ* maps within and across species (vole: n=8, mouse: n=3) shown as mean with standard deviation. Note the low variation between individual mouse maps. Correlation matrix (C) showing correlations between individual cases (White = 0, Dark Grey = 1). (B/D; Left) Flattened

cortical sections stained for myelin in an adult vole (B; top) and mouse (D; bottom) showing cortical field boundaries. (B/D; Right) Example cases of digitally flattened *RZRβ* maps reconstructed by Stalefish from coronally-sectioned tissue in a vole (top) and mouse (bottom). The medial wall was cropped in these reconstructions to align data with myelin stains. The pattern of *RZRβ* in layer 4 appears to be coincident with the boundaries of cortical fields in both species. Expression level is represented as pixel-value at a given coordinate (black = lowest, white = highest). (E) Example of a mouse *RZRβ* reconstructed expression map showing the location and relative size of digital micro-punches from S1 (pink) and S2/PV (green). 200μM by 500μM digital micro-punches are drawn to scale on flattened expression maps (post-transform). (F) Box plots of digital micro-punches taken from locations in S1 (pink) and S2/PV (green). In this case, the Y-axis denotes average percent-change (not raw signal level); x-axis denotes species. Box size represents quartiles 1 and 3 with median. Whiskers are set as 2 times the interquartile range. (G) Example of a mouse *RZRβ* expression map showing the location of digital micro-punches from V1 (purple) and V2 (red). (H) Box plots of digital micro-punches taken from V1 (purple) and V2 (red) with the same parameters as F. Abbreviations: Primary Visual Cortex (V1). Secondary Visual Cortex (V2). Primary Somatosensory Cortex (S1). Secondary Somatosensory Cortex (S2). Parietal Ventral Area (PV). Not significant, $p > 0.05$ (n.s). $p < .001$ (***).

Conclusions

Our results indicate that cortex-wide *Id2* expression patterns of early postnatal brains are conserved between voles and mice in a layer-dependent manner, ranging from moderately (Layer 6) to highly (Layers 2/3 and 5) conserved. However, in caudal neocortex, all layers yielded strong correlations, suggesting that species-specific expression of *Id2* is greater in rostral areas. In contrast, patterns of *RZRβ* expression are highly conserved in somatosensory areas and more variable between species in visual and auditory areas. While it is possible that these differences are due to the fact that laboratory mice are highly inbred and thus may have derived patterns of expression compared to other rodents, we believe the observed differences reflect the independent evolution of brains, bodies and life histories of voles and mice, whose ancestors diverged some 35 million years ago (21). For example, voles are crepuscular with seasonal changes in activity periods while mice are nocturnal; these differences may have a large impact on visual cortex development, organization, and function. On the other hand, both mice and voles have an elaborate barrel cortex and actively engage in whisking behaviors as a central component of exploration (26,29,30). However, their respective social structures and early life parental care differ markedly. Prairie voles are monogamous and biparental, live in extended family groups and have a complex acoustic communication system (31,32). Mice, on the other hand, are promiscuous, alloparental, and colonial, with a more limited repertoire of vocal communication. While differences in early life experience have been shown to alter cortical organization and gene expression in both mice and voles (23), it is unlikely that the differences in cortical organization that we observed are purely experience-driven because our data is from neonatal animals, who have limited exposure to external environmental stimuli. Instead, we posit that the observed variation is due to evolutionary changes to sensory arrays, body morphology and the neurodevelopmental program, which serves as a scaffold for the respective social and physical environment that voles and mice experience in early postnatal life

and beyond. These differences in lifestyle and use of their sensory systems likely co-evolved with alterations in sensory areas of the neocortex, orchestrated by transcription factors such as *Id2* and *RZRβ,* which are associated with the formation and transcriptional identity of cortical layers and areas during neurodevelopment (9,14–16,33).

In sum, our study highlights the usefulness of *Stalefish* for analyzing whole brain regions, for observing overall patterns, and for allowing the scientist to then focus on ROI's in search of the factors that drive strong and weak correlations, i.e., the factors underlying species similarities and differences. Specifically, the *Stalefish* tools enabled us to observe that *RZRβ* is expressed in higher-order cortical areas such as S2/PV and V2. This discovery would not have been possible with traditional analysis.

It would be of great interest to catalogue the emergence of these higher order areas along with how patterns of expression of other genes involved in cortical development change across the first two postnatal weeks, to study species or experimental differences in developmental trajectories in quantitative terms and at the level of entire neural structures. The *Stalefish* algorithms and software tools are readily applicable for the analyses of multiple species over multiple postnatal days, to elucidate where and when developmental processes are conserved or have diverged in evolution. Further, they allow for the study of how variation emerges across development and across species. Lastly, while we used *Stalefish* to show how spatial patterns of *Id2* and *RZRβ* are conserved in the cortex, these tools can easily be applied to study laminar expression profiles (fig. S3), or other brain structures whose spatial patterns of gene expression have eluded quantitative study for decades, such as the hippocampus and dorsal thalamus (fig. S4 and S5). While we present the first data using this new methodology in this study, we believe that neuroscientists will be able to utilize *Stalefish* to quantify spatial patterns of gene expression (or histological markers) in a variety of brains of different shapes, sizes and levels of

complexity, and be able to build on this approach to address longstanding evolutionary and developmental questions, generating novel comparisons and deriving unique insights that may otherwise have remained elusive.

References

1. Bayraktar OA, Bartels T, Holmqvist S, Kleshchevnikov V, Martirosyan A, Polioudakis D, et al. Astrocyte layers in the mammalian cerebral cortex revealed by a single-cell in situ transcriptomic map. Nat Neurosci. 2020 Apr;23(4):500–9.
2. Hirokawa J, Watakabe A, Ohsawa S, Yamamori T. Analysis of Area-Specific Expression Patterns of RORbeta, ER81 and Nurr1 mRNAs in Rat Neocortex by Double In Situ Hybridization and Cortical Box Method. PLOS ONE. 2008 Sep 25;3(9):e3266.
3. Zhu Q, Shah S, Dries R, Cai L, Yuan G-C. Identification of spatially associated subpopulations by combining scRNAseq and sequential fluorescence in situ hybridization data. Nat Biotechnol. 2018 Dec;36(12):1183–90.
4. Crombach A, Cicin-Sain D, Wotton KR, Jaeger J. Medium-Throughput Processing of Whole Mount In Situ Hybridisation Experiments into Gene Expression Domains. PLOS ONE. 2012 Sep 28;7(9):e46658.
5. Cadwell CR, Bhaduri A, Mostajo-Radji MA, Keefe MG, Nowakowski TJ. Development and Arealization of the Cerebral Cortex. Neuron. 2019 Sep 25;103(6):980–1004.
6. Cholfin JA, Rubenstein JLR. Frontal cortex subdivision patterning is coordinately regulated by Fgf8, Fgf17, and Emx2. Journal of Comparative Neurology. 2008;509(2):144–55.
7. Clark EA, Rutlin M, Capano L, Aviles S, Saadon JR, Taneja P, et al. Cortical RORβ is required for layer 4 transcriptional identity and barrel integrity. Dulac C, West AE, Sestan N, editors. eLife. 2020 Aug 27;9:e52370.
8. Fukuchi-Shimogori T, Grove EA. Neocortex Patterning by the Secreted Signaling Molecule FGF8. Science. 2001 Nov 2;294(5544):1071–4.
9. Jabaudon D, Shnider SJ, Tischfield DJ, Galazo MJ, Macklis JD. RORβ induces barrel-like neuronal clusters in the developing neocortex. Cereb Cortex. 2012 May;22(5):996–1006.
10. Seelke AMH, Yuan S-M, Perkeybile AM, Krubitzer LA, Bales KL. Early experiences can alter the size of cortical fields in prairie voles (Microtus ochrogaster). Environ Epigenet. 2016 Aug;2(3).
11. Lein ES, Hawrylycz MJ, Ao N, Ayres M, Bensinger A, Bernard A, et al. Genome-wide atlas of gene expression in the adult mouse brain. Nature. 2007 Jan;445(7124):168–76.
12. Ng L, Bernard A, Lau C, Overly CC, Dong H-W, Kuan C, et al. An anatomic gene expression atlas of the adult mouse brain. Nat Neurosci. 2009 Mar;12(3):356–62.
13. Huang Z, Liu J, Jin J, Chen Q, Shields LBE, Zhang Y-P, et al. Inhibitor of DNA binding 2 promotes axonal growth through upregulation of Neurogenin2. Experimental Neurology. 2019 Oct 1;320:112966.
14. Lasorella A, Stegmüller J, Guardavaccaro D, Liu G, Carro MS, Rothschild G, et al. Degradation of Id2 by the anaphase-promoting complex couples cell cycle exit and axonal growth. Nature. 2006 Jul 27;442(7101):471–4.
15. Park HJ, Hong M, Bronson RT, Israel MA, Frankel WN, Yun K. Elevated Id2 expression results in precocious neural stem cell depletion and abnormal brain development. Stem Cells. 2013 May;31(5):1010–21.

16. Rubenstein JLR, Rakic P. Genetic Control of Cortical Development. Cerebral Cortex. 1999 Sep 1;9(6):521–3.
17. Kitajima K, Takahashi R, Yokota Y. Localization of Id2 mRNA in the adult mouse brain. Brain Research. 2006 Feb 16;1073–1074:93–102.
18. Armentano M, Chou S-J, Srubek Tomassy G, Leingärtner A, O'Leary DDM, Studer M. COUP-TFI regulates the balance of cortical patterning between frontal/motor and sensory areas. Nat Neurosci. 2007 Oct;10(10):1277–86.
19. Dye CA, El Shawa H, Huffman KJ. A Lifespan Analysis of Intraneocortical Connections and Gene Expression in the Mouse II. Cerebral Cortex. 2011 Jun 1;21(6):1331–50.
20. Sur M, Rubenstein JLR. Patterning and Plasticity of the Cerebral Cortex. Science. 2005 Nov 4;310(5749):805–10.
21. Swanson MT, Oliveros CH, Esselstyn JA. A phylogenomic rodent tree reveals the repeated evolution of masseter architectures. Proceedings of the Royal Society B: Biological Sciences. 2019 May 15;286(1902):20190672.
22. Chou S-J, Babot Z, Leingärtner A, Studer M, Nakagawa Y, O'Leary DDM. Geniculocortical Input Drives Genetic Distinctions Between Primary and Higher-Order Visual Areas. Science. 2013 Jun 7;340(6137):1239–42.
23. Bottom RT, Krubitzer LA, Huffman KJ. Early postnatal gene expression in the developing neocortex of prairie voles (Microtus ochrogaster) is related to parental rearing style. Journal of Comparative Neurology. 2020;528(17):3008–22.
24. Campi KL, Bales KL, Grunewald R, Krubitzer L. Connections of Auditory and Visual Cortex in the Prairie Vole (Microtus ochrogaster): Evidence for Multisensory Processing in Primary Sensory Areas. Cerebral Cortex. 2010 Jan 1;20(1):89–108.
25. Krubitzer L, Campi KL, Cooke DF. All Rodents Are Not the Same: A Modern Synthesis of Cortical Organization. BBE. 2011;78(1):51–93.
26. Campi KL, Karlen SJ, Bales KL, Krubitzer L. Organization of sensory neocortex in prairie voles (Microtus ochrogaster). Journal of Comparative Neurology. 2007;502(3):414–26.
27. Zembrzycki A, Chou S-J, Ashery-Padan R, Stoykova A, O'Leary DDM. Sensory cortex limits cortical maps and drives top-down plasticity in thalamocortical circuits. Nat Neurosci. 2013 Aug;16(8):1060–7.
28. Zembrzycki A, Stocker AM, Leingärtner A, Sahara S, Chou S-J, Kalatsky V, et al. Genetic mechanisms control the linear scaling between related cortical primary and higher order sensory areas. Chao MV, editor. eLife. 2015 Dec 24;4:e11416.
29. Mitchinson B, Grant RA, Arkley K, Rankov V, Perkon I, Prescott TJ. Active vibrissal sensing in rodents and marsupials. Philos Trans R Soc Lond B Biol Sci. 2011 Nov 12;366(1581):3037–48.
30. Grant RA, Haidarliu S, Kennerley NJ, Prescott TJ. The evolution of active vibrissal sensing in mammals: evidence from vibrissal musculature and function in the marsupial opossum Monodelphis domestica. Journal of Experimental Biology. 2013 Sep 15;216(18):3483–94.
31. Beery AK, Christensen JD, Lee NS, Blandino KL. Specificity in Sociality: Mice and Prairie Voles Exhibit Different Patterns of Peer Affiliation. Front Behav Neurosci [Internet]. 2018 [cited 2021 Aug 6];0. Available from: https://www.frontiersin.org/articles/10.3389/fnbeh.2018.00050/full
32. Stewart AM, Lewis GF, Yee JR, Kenkel WM, Davila MI, Sue Carter C, et al. Acoustic features of prairie vole (Microtus ochrogaster) ultrasonic vocalizations covary with heart rate. Physiol Behav. 2015 Jan;138:94–100.
33. Oishi K, Aramaki M, Nakajima K. Mutually repressive interaction between Brn1/2 and Rorb contributes to the establishment of neocortical layer 2/3 and layer 4. PNAS. 2016 Mar 22;113(12):3371–6.

Acknowledgments: Thank you to Dr. Andrew Fox, Dr. Andrew Halley, and Jordan Crivelli-Decker for initial comments on conceptualization of the software.

Funding:

National Institute of Neurological Disorders and Stroke grant 1 F31 NS115242-01 (ME)

McDonnell Foundation grant 220020516 (LK, SJ, SW)

Author contributions:

Conceptualization: ME, SJ

Methodology: ME, SJ

Investigation: ME, SJ, RB, SW

Funding acquisition: LK, SW

Supervision: LK, SW

Writing – original draft: ME, LK

Writing – review & editing: ME, LK, SW, SJ, KH, RB

Competing interests: Authors declare that they have no competing interests.

Data and materials availability: All data are available in the main text or the supplementary materials, and at https://github.com/ABRG-Models/Stalefish.

Supplementary Materials

Materials and Methods

Supplementary Text

Figs. S1 to S14

Tables S1 to S3

Movies S1

General Conclusions

In the above dissertation I provided behavioral and anatomical data in blind and sighted short-tailed opossums, and a comparison of in-situ hybridization in mice and voles. The first three chapters of this dissertation show how alterations in sensory input can cause drastic changes to brain and behavior within the lifetime of an individual, without changes the genetic code. Alternatively, the cross-species work in mice and voles illustrates the types of changes that are the result of changes in the genetic code. Together, these chapters show the types of changes to the neocortex that are possible with and without differences in genetic code. First, I showed that available sensory input (whiskers or vision) determines motor performance and strategy in short-tailed opossums. I showed that the early loss of vision, prior to the onset of spontaneous activity, leads to enhanced performance on the tactilely mediated, ladder-rung walking task. Furthermore, I used the python-based DeepLabCut pose-estimation package to show that limb kinematics change drastically when the whiskers are trimmed in either sighted or blind opossums. Both blind and sighted possums take a conservative approach to ladder crossing without whiskers. This work provided data on cross-modal behavioral plasticity, and how the whiskers guide forelimb motion in whisking mammals. One limitation of this study however, was that we did not directly relate whisking to forelimb motion, and thus only a correlation can be drawn between the presence of whiskers and forelimb movement. Second, I provided lipophilic dye tracing data on developing opossums who lost visual input at varying developmental stages. I showed that early vision loss results in a reorganization of thalamocortical and cortical connections near the time of eye opening (postnatal day 36). Late vision loss, on the other hand, results in mostly a reorganization of cortical connections. Thus, the level of reorganization was found to be dependent on the stage at which vision was lost. Furthermore, the data from this study suggests that long-range cortical connections to V1 exist in sighted and blind animals at P36 but are pruned by adulthood. Intermediate ages will assess the specific neurodevelopmental events that surround these pruning/stabilization events. This research

provides the first evidence of whether cross-modal connections (observed in many different animal models) are the result of a growth of new connections or a lack of pruning. While our results show that cross-modal reorganization is due to a lack of pruning, the lack of multiple age groups used for analysis limits our findings (see Chapter 3; summary figure). Indeed, a limitation of this entire dissertation is that multiple developmental timepoints were not used to study how changes between experimental condition or species arise. Instead, the single time points chosen for analysis provide only a snapshot of how differences in the developmental program due to experience or genetics unfold over time.

Regardless, in chapter 3 I also provided a discussion on the possible anatomical identity of what visual cortex is reorganized into due to the early loss of vision. Although preliminary, both the anatomical connections and in-situ hybridization results suggest that visual cortex is reorganized to resemble the adjacent multimodal area (MM). Electrophysiological data will be needed to confirm this finding. This is critical to the field, as decades of research across species has shown that the early loss of vision results in a cross-modal reorganization of visual cortex. But what exactly visual cortex is reorganized into has remained elusive. Many studies have suggested that it takes on the role of a spatial area which processes somatosensory and auditory information (see Chapter 3 discussion). Whether this makes rV1 a new cortical field, or if it takes on the identity of surrounding areas is still unknown. As stated in the introduction, we must define cortical fields based on electrophysiology, connections, and cytoarchitecture. Ongoing studies in the Krubitzer lab will provide a definitive answer to this by providing a functional component. Yet I believe another way to answer this question is by studying the ontogeny of cortical fields (as done in chapter 3). This method of study allows us to determine how cortical fields are formed during development and defined by the input they receive. Cross-species work in this field moves to answer questions of why different species have different numbers of cortical fields.

As a last chapter, I provided a new technique which allows researchers to analyze in-situ hybridization rapidly, and project brains of varying sizes and shapes into a common reference frame. While I provided one example of how this technique can be used, comparing the expression patterns of two genes in mice and voles, there are many other applications. Regardless, the cross-species data showed that expression of *Id2* and *RZRb* is conserved across neocortical layers, but that RZRb expression differs between mice and voles in what specific areas it is expressed. I posit that these represent differences in developmental trajectories. We are currently acquiring/analyzing data which answers this question. Again, the lack of multiple developmental timepoints is a major limitation of our work. Altogether, the data in this dissertation works to address cortical phenotypic diversity within and across species. Over time, evolution has tinkered with the developmental program to create phenotypic diversity (see Chapter 1). While the cortical developmental program is a rigid cascade of events, the eventual outcome is a neocortex capable of high degrees of within-lifetime plasticity, allowing mammals to adapt to the environments they are born into. Data from this dissertation (Chapters 1-3) shows the possible extent of this plasticity and suggests a mechanism by which it may occur (pruning differences in development). Thus, as rigid as the developmental cascade is, part of neocortical plasticity occurs via the lack of specificity in the program – or at least this is the case for axon guidance. That is, while exuberance is built into the developmental program, differential pruning between individuals due to varied experience is allowed and results in within-species phenotypic diversity. While the experimental manipulation is drastic in Monodelphis (a complete removal of visual input), it represents the extreme end of the spectrum of what is possible when sensory inputs are altered within a species. In sum, cortical phenotypic diversity can be generated via direct alterations in the genetic program (cross-species) or from interactions between the organism and environment that act on flexible aspects of neurodevelopment (within-species). Together, these mechanisms create immense phenotypic diversity within the mammalian clade.